

# THE PROCEEDINGS OF THE PHYSICAL SOCIETY

## Section A

VOL. 62, PART 11

1 November 1949

No. 359 A

## CONTENTS

	PAGE
Prof. W. HEITLER and Prof. L. JÁNOSSY. On the Size-Frequency Distribution of Penetrating Showers . . . . .	669
Dr. A. DUPERIER. The Meson Intensity at the Surface of the Earth and the Temperature at the Production Level . . . . .	684
Mr. C. B. VAN WYK. On the Decay of $\tau$ -Mesons . . . . .	697
Miss J. JACOBS. Excited Electronic Levels in Conjugated Molecules—III: Energy States of Naphthalene . . . . .	710
Dr. H. G. WOLFARD and Dr. W. G. PARKER. A New Technique for the Spectroscopic Examination of Flames at Normal Pressures . . . . .	722
Dr. G. F. J. GARLICK and Mr. A. F. GIBSON. Dielectric Changes in Phosphors containing more than One Activator . . . . .	731
Prof. A. RUBINOWICZ. Eigenfunctions following from Sommerfeld's Polynomial Method . . . . .	736
Letters to the Editor:	
Mr. B. V. THOSAR. Origin of Low-Energy Electron Lines in the $\beta$ -spectrum of $^{198}\text{Au}$ . . . . .	739
Mr. B. EISLER and Dr. R. F. BARROW. The Ultra-Violet Absorption Spectrum of $\text{SnO}$ . . . . .	740
Mr. W. H. HALL. X-Ray Line Broadening in Metals . . . . .	741
Dr. R. STREET and Mr. J. C. WOOLLEY. Magnetic Viscosity in Mn-Zn Ferrite . . . . .	743
Reviews of Books . . . . .	745
Corrigendum . . . . .	746
Contents for Section B . . . . .	747
Abstracts for Section B . . . . .	747

Price to non-members 10s. net, by post 6d. extra. Annual subscription: £5 5s.

Composite subscription for both Sections A and B : £9 9s.

Published by

THE PHYSICAL SOCIETY

1 Lowther Gardens, Prince Consort Road, London S.W.7



## PROCEEDINGS OF THE PHYSICAL SOCIETY

The *Proceedings* is now published monthly in two Sections.

### ADVISORY BOARD

*Chairman:* The President of the Physical Society (S. CHAPMAN, M.A., D.Sc., F.R.S.).

E. N. da C. ANDRADE, Ph.D., D.Sc., F.R.S.  
Sir EDWARD APPLETON, G.B.E., K.C.B., D.Sc.,  
F.R.S.

L. F. BATES, Ph.D., D.Sc.

P. M. S. BLACKETT, M.A., F.R.S.

Sir LAWRENCE BRAGG, O.B.E., M.A., Sc.D.,  
D.Sc., F.R.S.

Sir JAMES CHADWICK, D.Sc., Ph.D., F.R.S.

LORD CHERWELL OF OXFORD, M.A., Ph.D.,  
F.R.S.

Sir JOHN COCKCROFT, C.B.E., M.A., Ph.D.,  
F.R.S.

Sir CHARLES DARWIN, K.B.E., M.C., M.A.,  
Sc.D., F.R.S.

N. FEATHER, Ph.D., F.R.S.

G. I. FINCH, M.B.E., D.Sc., F.R.S.

D. R. HARTREE, M.A., Ph.D., F.R.S.

N. F. MOTT, M.A., F.R.S.

M. L. OLIPHANT, Ph.D., D.Sc., F.R.S.

F. E. SIMON, C.B.E., M.A., D.Phil., F.R.S.

T. SMITH, M.A., F.R.S.

Sir GEORGE THOMSON, M.A., D.Sc., F.R.S.

Papers for publication in the *Proceedings* should be addressed to the Hon. Papers Secretary,  
Dr. H. H. HOPKINS, at the Office of the Physical Society, 1 Lowther Gardens, Prince  
Consort Road, London S.W.7. Telephone: KENSington 0048, 0049.

Detailed Instructions to Authors were included in the February 1948 issue of  
the *Proceedings*; separate copies can be obtained from the Secretary-Editor.

## THE PHYSICAL SOCIETY

### MEMBERSHIP

Membership of the Society is open to all who are interested in Physics.

**FELLOWSHIP.**—A candidate for election to Fellowship must, as a rule, be recommended  
by three Fellows, to two of whom he is known personally.

**STUDENT MEMBERSHIP.**—A candidate for election to Student Membership must be  
between 18 and 26 years of age and must be recommended from personal knowledge  
by a Fellow.

Fellows and Student Members may attend all meetings of the Society, and are  
entitled to receive some of the Society's publications free and others at much reduced  
rates.

Books and periodicals may be read in the Society's Library, and a limited number  
of books may be borrowed on application to the Honorary Librarian.

### SUBSCRIPTIONS

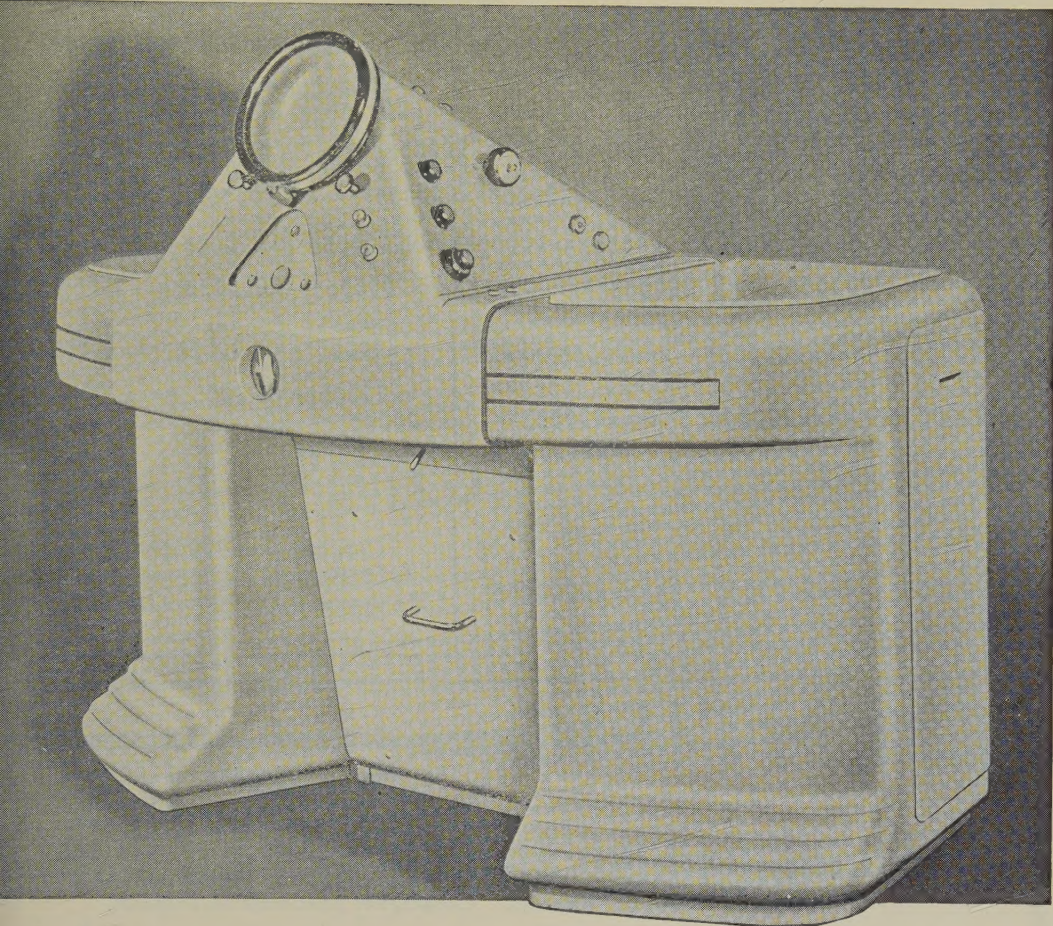
Fellows pay an Entrance Fee of £1 1s. and an Annual Subscription of £3 3s.  
Student Members pay only an Annual Subscription of 15s.

Fellows and Student Members may become members of the specialist Groups of  
the Society (Colour, Optical, Low Temperature, Acoustics) without additional sub-  
scription.

*Further information may be obtained from the Secretary-Editor at the Offices of the Society,  
1 LOWTHER GARDENS, PRINCE CONSORT ROAD, LONDON S.W. 7*



# the PHILIPS Electron Microscope



**A**CCCELERATION of voltage maximum 100 kV ★ Magnification range continuously variable between 1,000 and 60,000 diameters ★ Photographic enlargement up to 150,000 diameters ★ Stereo-micrographs obtainable ★ Special self-sealing airlock for specimen holder ★ Film camera for obtaining micro-graphs.

Focusing device and quick electronic alignment ★ Apertures adjustable and removable for cleaning without dismantling ★ Large final image screen of 8-in. diameter Microscope tube not sensitive to vibrations ★ No special foundations required ★ Suitable to work in any climate and at any altitude.



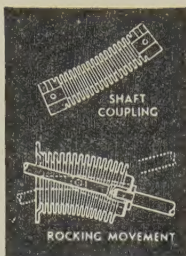
## PHILIPS ELECTRICAL

LIMITED



## PLEASE tell us of OTHER applications

Drayton 'Hydroflex' Metal Bellows are an essential component part in Automatic coolant regulation . . . Movement for pressure change . . . Packless gland to seal spindle in high vacua . . . Reservoir to accept liquid expansion . . . Dashpot or delay device . . . Barometric measurement or control . . . Pressurised couplings where vibration or movement is present . . . Dust seal to prevent ingress of dirt . . . pressure reducing



valves . . . Hydraulic transmission . . . Distance thermostatic control . . . Low torque flexible coupling . . . Pressure sealed rocking movement . . . Pressurised rotating shaft seals . . . Aircraft pressurised cabin control . . . Refrigeration expansion valves . . . Thermostatic Steam Traps . . . Pressure amplifiers . . . Differential pressure measurements . . . Thermostatic operation of louvre or damper.

### for HYDRAULICALLY FORMED

Seamless, one-piece, metal bellows combining the properties of a compression spring able to withstand repeated flexing, a packless gland and a container which can be hermetically sealed. Made by a process unique in this country, they are tough, resilient, with a uniformity of life, performance and reliability in operation unobtainable by any other method.

## Drayton METAL BELLOWES

Write for List No. V800-1 DRAYTON REGULATOR & INSTRUMENT CO. LTD.,  
WEST DRAYTON, MIDDLESEX. West Drayton 2611 B.8

## PROCEEDINGS OF THE PHYSICAL SOCIETY

### ADVERTISEMENT RATES

The *Proceedings* are divided into two parts, A and B. The charge for insertion is £18 for a full page in either Section A or Section B, £30 for a full page for insertion of the same advertisement in both Sections. The corresponding charges for part pages are:

$\frac{1}{2}$ page	£9 5 0	£15 10 0
$\frac{1}{4}$ page	£4 15 0	£8 0 0
$\frac{1}{8}$ page	£2 10 0	£4 5 0

Discount is 20% for a series of six similar insertions and 10% for a series of three.

The printed area of the page is  $8\frac{1}{2}'' \times 5\frac{1}{2}''$ , and the screen number is 120.

Copy should be received at the Offices of the Physical Society six weeks before the date of publication of the *Proceedings*.

# SCIENTIFIC BOOKS

Messrs. H. K. LEWIS can supply from stock or to order any book on the Physical and Chemical Sciences. Catalogues post-free on request.

FOREIGN DEPARTMENT: Select stock. Books not in stock obtained under Board of Trade licence.

SECOND-HAND SCIENTIFIC BOOKS. 140 GOWER STREET.

An extensive stock of books in all branches of Pure and Applied Science may be seen in this department. Large and small collections bought. Back volumes of Scientific Journals.

## SCIENTIFIC LENDING LIBRARY

Annual subscription from One Guinea. Details of terms and prospectus free on request.

THE LIBRARY CATALOGUE revised to December 1943, containing a classified index of authors and subjects: to subscribers 12s. 6d. net, to non-subscribers 25s. net, postage 9d. Supplement from 1944 to December 1946. To subscribers 2s. 6d. net; to non-subscribers 5s. net; postage 4d.

Bi-monthly List of Additions, free on application.

Telephone: EUSton 4282

Telegrams: "Publicavit,  
Westcent, London"

## H. K. LEWIS & Co. Ltd.

136 GOWER STREET, LONDON, W.C.

Business hours: 9 a.m. to 5 p.m., Saturdays to 1 p.m.

## MONOCULAR &amp; BINOCULAR RESEARCH MICROSCOPES

The Hall Mark of a



Precision Built Microscope

IN BUYING A

## PRIOR MICROSCOPE

YOU PURCHASE AN INSTRUMENT  
BUILT TO THE HIGHEST STANDARDS OF

OPTICAL &amp; MECHANICAL PRECISION

Enquiries Invited

Early Delivery

Catalogue on Request

## W. R. PRIOR &amp; Co. LTD.

13 NORTHGATE END,  
BISHOP'S STORTFORD, HERTS.  
Telephone 43728A DEVONSHIRE STREET,  
LONDON, W.1.  
Telephone: WELbeck 4695

LABORATORY MICROSCOPES

LOWER POWER BINOCULAR MICROSCOPES

## MICROCHEMICAL BALANCES

*We are able to arrange good delivery  
of Bunge Microchemical Balances—  
load 30 gm., sensitivity 0.001 mgm.,  
projection reading—subject to the granting  
of import licence by the Board of Trade.*

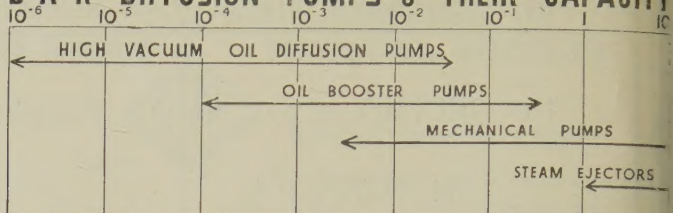
## GRIFFIN and TATLOCK Ltd

*Established as Scientific Instrument Makers in 1826*

LONDON	MANCHESTER	GLASGOW	EDINBURGH
Kemble St., W.C.2	19, Cheetham Hill Rd., 4	45, Renfrew St., C.2	7, Teviot Place, 1
BIRMINGHAM: STANDLEY BELCHER & MASON LTD., Church Street, 3			

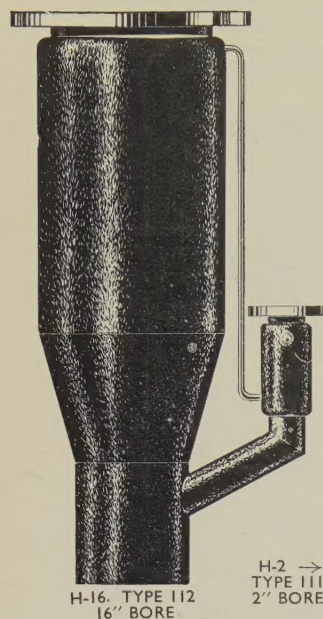


## B.A.R. DIFFUSION PUMPS &amp; THEIR CAPACITY



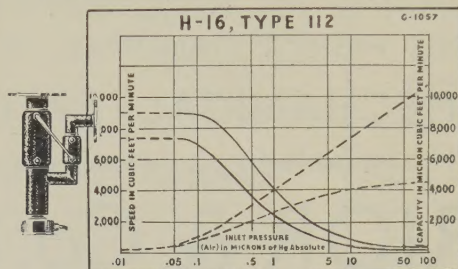
B.A.R. all-metal high-capacity diffusion pumps range from 2-in. inlet to 16-in. inlet. The H-2, Type III, smallest of the range, is suitable for cryostat, vacuum furnace, laboratory electronic tube and coating work on a laboratory scale. It can be joined to glass systems easily. Delivery from stock. The H-16, Type II2, largest of the range

combines great capacity at high vacuum with ability to work against high fore-pressures—an unusual feature. Recommended for industrial applications such as distillation, production coating, and vacuum furnace work. Delivery of H-2, H-6 and H-16 pumps from stock. Full operation data about B.A.R. pumps is available upon request and a demonstration merely awaits your request.



H-16, TYPE II2  
16" BORE

H-2 →  
TYPE III  
2" BORE



# BRITISH AMERICAN RESEARCH LTD

DESIGNERS AND MANUFACTURERS OF HIGH VACUUM GAUGES · VALVES · SEALS  
DIFFUSION PUMPS · STILLS · FURNACES · COATING EQUIPMENT AND DEHYDRATION PLANT  
BLOCK E2 · HILLINGTON NORTH · GLASGOW S.W.

## VACUUM-CELL PHOTOMETER, type MN

Measures and compares—

**ILLUMINATION  
DENSITY  
REFLECTIVITY  
COLOUR**

The amplifier is a.c. mains operated; either 1 or 2 photo-cells may be used.

**Ranges—0.1, 1, 10 millilumens;  
Density 0–4.**

**BALDWIN INSTRUMENT Co. Ltd.,  
DARTFORD, KENT.**

F. C. Robinson & Partners Ltd., 308, Deansgate, Manchester, 3, are our agents for Lancashire, Cheshire & Derbyshire.

# BALDWIN



Telephone : DARTFORD 2989.



# THE PROCEEDINGS OF THE PHYSICAL SOCIETY

## Section A

VOL. 62, PART 11

1 November 1949

No. 359 A

### On the Size-Frequency Distribution of Penetrating Showers

BY W. HEITLER AND L. JÁNOSSY

Dublin Institute for Advanced Studies

*MS. received 30th June 1949*

**ABSTRACT.** We have calculated the relative number of showers containing  $n$  mesons when a fast primary nucleon hits a compound nucleus on the assumption that in a single nucleon-nucleon collision only one meson is produced (pure plural production). The cross section for meson production is assumed to have the form  $\Phi(\epsilon/E) d\epsilon/E$ , where  $E$  is the energy of the primary and  $\epsilon$  the energy lost by it, but the absolute value of  $\Phi$  and its dependence on  $\epsilon/E$  are left open. The fluctuations of the shower size are duly taken into account. For comparison with experiments it is assumed that about half the number of fast shower particles are fast protons as suggested by the positive excess of penetrating shower particles. The theoretical results depend on two constants, the total cross section and some weighted average over the energy distribution  $\Phi(\epsilon/E)$ . Choosing these suitably, the results are in good agreement with the relevant data within the experimental statistical errors, and the agreement extends also to the "large showers" with 20 or so thin tracks. The values of the constants thus determined are physically reasonable. It is concluded that the size-frequency distribution of penetrating showers can be fully understood on the basis of pure plural production, but some—small or large—contribution from multiple processes cannot be excluded.

#### § 1. INTRODUCTION

IN recent papers by Brown, Camerini, Fowler, Heitler, King and Powell (1949) the relative frequency of stars with a given number  $n$  of "thin tracks" is measured. There can be little doubt that these events in the photographic emulsion are identical with the penetrating showers previously found and observed in counter and cloud chamber experiments by Jánossy, Rochester and others. If this is true, then it is also highly probable that we have to deal here with the process of meson-production by fast nucleons (and, indeed, roughly half of the stars are initiated by charged, half by neutral particles) and that at least a considerable fraction of the thin tracks are mesons ( $\pi$ -mesons, presumably, perhaps also  $\tau$ -mesons). Some of the tracks are also likely to be fast protons.

For the interpretation of these events, two widely different hypotheses have been put forward: (i) The occurrence of groups of particles is explained in a natural way as due to a multiple collision of the primary nucleon with *several* of the closely packed nucleons in a compound nucleus, O, C, N or Ag, Br in the photographic plate. We call this process, following J. G. Wilson, plural production. (ii) The groups are assigned to a single elementary process in which the fast



nucleon would produce several mesons in one single collision with a single nuclear nucleon (genuine multiple process). It is assumed here that the emission of several mesons in one act is *more probable* than that of a single meson. The process (ii) would be a type of process for which so far no analogue is known in physics\*, in so far as the emission of the minimum number of particles or quanta (compatible with conservation laws) is always the most probable event. A decision between the two interpretations therefore involves a rather fundamental issue and would be of great importance for the future development of meson theory. In this paper we examine the question whether the data available to date can be understood by the assumption (i) of pure plural production. It will be seen that this is the case quantitatively within the present accuracy of the experimental data, with exception of an irregularity that—possibly—occurs in the experimental distribution curve (cf. §6). But this irregularity is not firmly established.

The agreement also applies to the “large showers.” observed so far (up to 22 particles and, perhaps, even to the one case of 31 particles, cf. §6), and there is no necessity to assume a different type of process for these showers.

It will furthermore be seen that the assumptions one has to make about the cross section for meson production etc. to reach this agreement are physically reasonable and they are in harmony with the known facts about the absorption coefficient of fast nucleons†. They are further compatible with the values given in the theory of meson production put forward by Hamilton, Heitler and Peng in its later version‡, within the rather wide limits set by this theory.

Whilst the facts can be explained by the assumption of pure plural production, the issue is not yet decided. It might be possible to explain the facts also by process (ii) (see, e.g., Heisenberg 1949, also Dallaporta and Clementel 1948), making suitable assumptions about the multiplicities and their energy dependence, but a complete theory that would predict them as more probable than the single emission is not available. Nor can it be stated—even if the explanation of mainly plural processes is accepted—that all of the showers in question are plural. It might well be that a fraction of the showers or part of the multiplicity in a given shower is due to genuine multiple processes.

We shall work out the pluralities of the process in a more phenomenological way without assuming any detailed theory of meson production. We shall only make some very general assumptions about the energy dependence of the cross section etc. It will be seen that then two constants occur, the total cross section and some weighted average over the energy distribution of the emitted mesons. We shall try to fix these constants, as far as is possible, by comparison with the facts.

For a first orientation we shall neglect in this paper any secondary production of mesons by fast recoil nucleons within the same nucleus. This effect may not be negligible when the primary is very fast and tends to make an already big shower still bigger, especially in heavy nuclei. This will have to be taken into account in the discussion of the available material (§6).

\* The emission of several extremely soft photons in any electromagnetic process (which is sometimes quoted as an analogue) hardly bears any resemblance to the high energy multiple processes in question. The former is a purely classical phenomenon, translated into the language of quantum theory.

† Cf. Heitler and Jánossy 1949, quoted in the following as HJ.

‡ For references see Heitler 1949, quoted in the following as HHP.



## § 2. THEORY OF PLURAL PRODUCTION

We wish to calculate the probability for  $n$  mesons to be emitted in a collision of a fast nucleon with a given nucleus. Let  $\Phi(\epsilon, E)d\epsilon$  be the cross section for emission of a meson with an energy loss  $\epsilon$  suffered by the nucleon with initial energy  $E$  in a collision with a single nucleon.  $\epsilon$  includes the recoil energy. Instead of  $\epsilon$  we use  $E' = E - \epsilon$ . In a passage through a nucleus in general several acts of meson emission and discontinuous energy losses will occur. We make the following basic assumptions:

(i) That 
$$\Phi(E', E) dE' = \Phi\left(\frac{E'}{E}\right) \frac{dE'}{E} \quad \dots\dots (1)$$

shall be a function of  $E'/E$  only. This assumption has a high degree of probability for being at least approximately correct. In the first place the analogous law for Bremsstrahlung has the same form, and in the second place the (very crude) theory of HHP leads to the same result. (1) holds, of course, only for sufficiently high energies  $E$ , say above a certain critical energy  $E_c$ .

(ii) The individual acts of emission shall be statistically independent events. This assumption is somewhat doubtful, on account of the large disturbance caused in the nucleus even after the first emission. However, one may argue that the recoil energies produced in each emission act are in most cases small compared with the energy of the primary nucleon. The energy communicated through the recoil to the second nucleon which suffers the second hit from the primary will be even smaller, and since we may treat the nuclear nucleons anyhow as free it will hardly be very wrong to consider them all at rest before they are hit by the primary.

It is convenient to write

$$\Phi\left(\frac{E'}{E}\right) \frac{dE'}{E} = \Phi \cdot \omega\left(\frac{E'}{E}\right) \frac{dE'}{E}, \quad \int_0^E \omega\left(\frac{E'}{E}\right) \frac{dE'}{E} = 1 \quad \dots\dots (2)$$

( $\omega$  differs from the quantity  $w$  used in HJ by the factor  $Nd_A\Phi$ ).  $\Phi$  is the total cross section and is, by (1), a constant. Let  $N$  be the density of nuclear matter. The probability for a total loss of energy from  $E$  to  $E' \equiv E_{n-1}$  in  $n-1$  individual acts of emission, each taking place in the intervals of distance between  $x_1$  and  $x_1 + dx_1, \dots, x_{n-1}$  and  $x_{n-1} + dx_{n-1}$ , is

$$p_{n-1} dE' = \int \dots \int \omega\left(\frac{E_1}{E}\right) \frac{dE_1}{E} \omega\left(\frac{E_2}{E_1}\right) \frac{dE_2}{E_1} \times \dots \times \omega\left(\frac{E_{n-1}}{E_{n-2}}\right) \frac{dE_{n-1}}{E_{n-2}} (\Phi N)^{n-1} \exp(-\Phi N x_n) dx_1 \dots dx_{n-1}, \quad \dots\dots (3)$$

$$(E > E_1 > E_2 \dots > E_{n-1}); \quad E_{n-1} \equiv E' > E_c. \quad \dots\dots (3')$$

The integral is to be extended over all values  $E_1, E_2 \dots E_{n-2}$  ( $E_{n-1}$  is given) satisfying (3'). It is furthermore to be extended over all values of  $x_1, x_2 \dots x_{n-1}$  satisfying

$$0 < x_1 < x_2 < x_3 \dots < x_{n-1} < x_n \text{ say.} \quad \dots\dots (3'')$$

The factor  $\exp(-\Phi N x_n)$  is the probability that within the total distance  $x_n$  no emission act takes place, except in the infinitesimal intervals  $dx_1 \dots dx_{n-1}$  whose total length is, of course, zero compared with  $x_n$ . The reason for denoting the total length by  $x_n$  will become clear below.

We introduce  $y_m = \log(E_{m-1}/E_m), \quad Y = \log(E/E').$



The integration over  $x_1 \dots x_{n-1}$  yields  $x_n^{n-1}/(n-1)!$  because the integration can be performed for each  $x_m$  from 0 to  $x_n$  irrespective of order, and keeping the order (3'') introduces merely the factor  $1/(n-1)!$ . Then (3) becomes

$$\left. \begin{aligned} p_{n-1} dE' &= \int \omega(y_1) \omega(y_2) \dots \omega(y_{n-1}) dy_1 dy_2 \dots dy_{n-2} \\ &\times \frac{dE'}{E'} \exp(-\Phi N x_n) \frac{(\Phi N x_n)^{n-1}}{(n-1)!}, \end{aligned} \right\} \dots \dots (4)$$

$$y_1 + y_2 + y_3 + \dots + y_{n-1} = Y, \quad \dots \dots (4')$$

and the normalization for  $\omega$  becomes

$$\int_0^\infty \omega(y_m) dy_m = 1.$$

The length of path in nuclear matter is, of course, limited, and clearly two cases are possible. (i) When  $n$  emission acts take place the primary nucleon may have lost so much energy that it is no longer capable of further meson emission. This is the case if, in the last emission act, the  $n$ th say, the nucleon loses energy from a value  $E' > E_c$  to some value below  $E_c$ . (ii) The primary nucleon may commit  $n$  emission acts and leave the nucleus still retaining an energy  $> E_c$ . We call the probabilities for these two types of events  $p^{(1)}$  and  $p^{(2)}$  respectively.

We consider first the case where one further collision takes place, the  $n$ th, in which  $E$  drops from  $E'$  to a value  $E''$  below the critical energy  $E_c$ . Below  $E_c$ ,  $\omega$  will steadily decrease and will eventually vanish at the meson threshold. We have no exact information as to how rapid this decrease is, but there are reasons, both experimental and theoretical, for believing that it is fairly rapid. We can idealize the situation by assuming that below  $E_c$  the probability for further meson production can be neglected, but that for the jump from  $E'$  to  $E''$  the cross section has still its full value  $\omega\Phi$ . Evidently this idealization is crude, but since it is made only for the last step the total error cannot be very large, except for small showers with only one or two particles which we shall exclude from the comparison with the experiments. The probability for the last step is

$$\Phi N \int_0^{E_c} \omega \left( \frac{E''}{E'} \right) \frac{dE''}{E'} dx_n.$$

Instead of carrying out the integration over the  $y_m$ 's in (4) we first average over the primary spectrum of the incident nucleons. In HJ it was shown that this remains a power spectrum for any depth in the atmosphere if the spectrum falling on the top of the atmosphere was a power spectrum, and this is very probable. We therefore assume a primary spectrum of the form

$$F(E) dE = \gamma E_c^\gamma \frac{dE}{E^{\gamma+1}}, \quad \gamma \sim 1.5. \quad \dots \dots (5)$$

(5) is normalized so that the total number of nucleons above the critical energy  $E_c$  is unity. Primaries with  $E < E_c$  do not contribute according to our assumptions. Actually (5) is only correct if  $E_c$  is larger than the latitude cut-off energy (for Europe  $3 \times 10^9$  ev.). We have reasons to think that  $E_c$  is of about the same order of magnitude (again the theory of HHP suggests this). Even for energies somewhat below the latitude cut-off (5) is still almost correct at some not too small depth below the top of the atmosphere, say at Jungfraujoch or sea level.



We obtain for the probability of emission of  $n$  mesons with the last emission act taking place in the interval  $dx_n$ :

$$p_n^{(1)} dx_n = \gamma E_c^\gamma \int_{E_c}^{\infty} \frac{dE}{E^{\gamma+1}} \int_{E_c}^E p_{n-1} \frac{dE'}{E} \int_0^{E_c} \omega\left(\frac{E''}{E'}\right) \frac{dE''}{E'} \Phi N dx_n. \quad \dots\dots (6)$$

We first carry out the integration over  $E$ , using the variable  $Y = \log(E/E')$ :

$$p_n^{(1)} dx_n = \gamma E_c^\gamma \int_{E_c}^{\infty} \frac{dE'}{E'^{\gamma+2}} \int_0^{\infty} p_{n-1} \exp\{-(\gamma+1)Y\} dY \int_0^{E_c} \omega\left(\frac{E''}{E'}\right) dE'' \Phi N dx_n. \quad \dots\dots (7)$$

The integration over the  $y_m$ 's can now be performed very easily using (4'):

$$\int_0^{\infty} p_{n-1} \exp\{-(\gamma+1)Y\} dY = \frac{(\Phi N x_n)^{n-1}}{(n-1)!} \left\{ \int_0^{\infty} \omega(y_m) \exp\{-(\gamma+1)y_m\} dy_m \right\}^{n-1}.$$

We denote for abbreviation

$$\begin{aligned} \omega_{\gamma+1} &= \int_0^{\infty} \omega(y) \exp\{-(\gamma+1)y\} dy = \int_0^E \omega\left(\frac{E'}{E}\right) \left(\frac{E'}{E}\right)^{\gamma+1} \frac{dE'}{E'} \\ &= \int_0^E \omega\left(\frac{\epsilon}{E}\right) \left(1 - \frac{\epsilon}{E}\right)^{\gamma} \frac{d\epsilon}{E}, \quad \dots\dots (8) \end{aligned}$$

which depends on the elementary distribution  $\omega(\epsilon/E)$  only and is a pure number.

The remaining integrations in (7) yield

$$\begin{aligned} \int_{E_c}^{\infty} \frac{dE'}{E'^{\gamma+2}} \int_0^{E_c} \omega\left(\frac{E''}{E'}\right) dE'' &= \int_0^1 \omega(\xi) d\xi \int_{E_c}^{E_c/\xi} \frac{dE'}{E'^{\gamma+1}} \quad (\xi = E''/E') \\ &= \frac{1}{\gamma} \int_0^1 \omega(\xi) d\xi \frac{1 - \xi^\gamma}{E_c^\gamma} = \frac{1}{\gamma} (1 - \omega_{\gamma+1}) \frac{1}{E_c^\gamma}. \quad \dots\dots (9) \end{aligned}$$

Collecting our formulae, we obtain

$$p_n^{(1)} dx_n = \frac{(\Phi N x_n)^{n-1}}{(n-1)!} \exp(-\Phi N x_n) \omega_{\gamma+1}^{n-1} (1 - \omega_{\gamma+1}) \Phi N dx_n. \quad \dots\dots (10)$$

This has now still to be integrated over  $x_n$ , because the last act of emission (and all previous acts) can take place anywhere between 0 and  $x$ , say, if  $x$  is the total length of path. The probability for no emission to take place between  $x_n$  and  $x$  is unity because the energy is there less than  $E_c$ , and therefore  $x_n$  must not be replaced by  $x$  in the exponential  $\exp(-\Phi N x_n)$ . Thus we have to integrate (10) over  $x_n$  from 0 to  $x$ . Denoting the incomplete  $\Gamma$ -function by

$$\int_0^a \frac{z^{n-1}}{(n-1)!} e^{-z} dz \equiv \Gamma_n(a), \quad \dots\dots (11)$$

$$\text{we get finally} \quad p_n^{(1)} = \Gamma_n(\Phi N x) \omega_{\gamma+1}^{n-1} (1 - \omega_{\gamma+1}). \quad \dots\dots (12)$$

This  $p_n^{(1)}$  is the probability for a nucleon to commit within the distance  $x$  in nuclear matter exactly  $n$  acts of meson emission and afterwards to have an energy less than  $E_c$ .

Next we consider the second case where the nucleon has, within the distance  $x$ , committed  $n$  acts of meson emission but has retained an energy greater than  $E_c$ . This probability  $p_n^{(2)}$ , say, is obtained from (4) directly, replacing  $n-1$  by  $n$ ,  $x_n$  by  $x$ , and averaging over the primary spectrum (5). We obtain immediately

$$p_n^{(2)} = \frac{(\Phi N x)^n}{n!} \exp(-\Phi N x) \omega_{\gamma+1}^n. \quad \dots\dots (13)$$



The total probability for emission of  $n$  mesons within the distance  $x$  is the sum

$$p_n = p_n^{(1)} + p_n^{(2)}. \quad \dots\dots (14)$$

$p_n^{(2)}$  can be split up, for a more symmetrical representation,

$$p_n^{(2)} = \omega_{\gamma+1}^n \{ \Gamma_n(\Phi N x) - \Gamma_{n+1}(\Phi N x) \}, \quad \dots\dots (15)$$

and hence

$$p_n = \omega_{\gamma+1}^{n-1} \Gamma_n(\Phi N x) - \omega_{\gamma+1}^n \Gamma_{n+1}(\Phi N x). \quad \dots\dots (16)$$

The last step in the calculation is now to consider the variation in the length of path  $x$ . If the nuclear diameter is  $d_A$ , the probability for a path length  $x$  is  $2x dx d_A^2$ . This is to be multiplied into (16) and integrated over  $x$  from 0 to  $d_A$ . Changing the order of integration, the integration is elementary and gives (we denote the result by  $P_n$ )

$$\left. \begin{aligned} P_n = \omega_{\gamma+1}^{n-1} \left\{ \Gamma_n(a_A) - \frac{n(n+1)}{z_A^2} \Gamma_{n+2}(a_A) \right\} \\ - \omega_{\gamma+1}^n \left\{ \Gamma_{n+1}(a_A) - \frac{(n+1)(n+2)}{z_A^2} \Gamma_{n+3}(a_A) \right\}, \quad \dots\dots (17) \\ a_A = \Phi N d_A, \quad \omega_{\gamma+1} = \int_0^E \omega \left( \frac{\epsilon}{E} \right) \left( 1 - \frac{\epsilon}{E} \right)^\gamma \frac{d\epsilon}{E}. \end{aligned} \right\}$$

(17) is our final result. As can be seen, it depends on (i) the total cross section  $\Phi$ ; (ii) a weighted average over the energy spectrum of the elementary cross section,  $\omega_{\gamma+1}$ , the weight function being  $(1 - \epsilon/E)^\gamma$ ; (iii) the power  $\gamma$  of the primary spectrum ( $\gamma \sim 1.5$ ); (iv) the atomic weight, through  $d_A$ . For sake of completeness we also give the formula for  $P_0$  ( $n=0$ ), because (17) does not immediately permit the transition to  $n=0$ . One gets

$$P_0 = \frac{2}{a_A^2} \Gamma_2(a_A). \quad \dots\dots (17')$$

It can easily be verified that (17) and (17') are normalized to unity:  $\sum_0^\infty P_n = 1$ .

### § 3. SOME GENERALIZATIONS

It is highly probable that amongst the  $n$  mesons emitted some are neutretos which are not observed directly in either the cloud chamber or the photographic plate. We shall be more interested in the probability,  $P'_\nu$  say, for the emission of  $\nu$  charged mesons than in  $P_n$ . If the probability is known for the particle emitted in an individual emission act to be a neutretto,  $\delta$  say, the probability for  $\nu$  charged mesons to be emitted is derived from  $P_n$  by\*

$$P'_\nu = \sum_{n=\nu}^{n=\infty} \binom{n}{\nu} (1-\delta)^\nu \delta^{n-\nu} P_n. \quad \dots\dots (18)$$

\* We do not distinguish here between proton-proton, proton-neutron, neutron-proton etc. collisions. It is by no means evident, or even probable, that the cross sections for these collisions are all equal and that in all of them the probabilities for the emission of a neutretto are the same fraction. In fact Peng and Morette (1948) arrived, for low energies, at the result that the cross sections are quite different, although the charge-symmetrical theory is used. Nothing is known about this point for the energies in which we are interested. Since, however, any such differences must average out in the end, when both neutrons and protons are considered as "primaries", because there is certainly some symmetry in the proton-neutron system, we may assume that the probabilities of neutretto emission are the same fraction of the total, irrespective of the charge of the nucleon.



The evaluation of this sum is straightforward and gives a formula for  $P'_\nu$  that differs from  $P_n$  essentially in a re-definition of the constants. We get

$$P'_\nu = \chi_{\nu+1} \left\{ \omega'_{\nu+1} \left[ \Gamma_\nu(a'_A) - \frac{\nu(\nu+1)}{a'^2_A} \Gamma_{\nu+2}(a'_A) \right] - \omega'^\nu_{\nu+1} \left[ \Gamma_{\nu+1}(a'_A) - \frac{(\nu+1)(\nu+2)}{a'^2_A} \Gamma_{\nu+3}(a'_A) \right] \right\} \dots\dots (19)$$

with

$$a'_A = \Phi N d_A (1 - \delta \omega_{\nu+1}), \quad \omega'_{\nu+1} = \chi_{\nu+1} \omega_{\nu+1}, \quad \dots\dots (19')$$

$$\chi_{\nu+1} = \frac{1 - \delta}{1 - \delta \omega_{\nu+1}}.$$

Apart from one common factor,  $\chi_{\nu+1}$ , which will be quite close to 1, this means that  $\omega$  is to be replaced by  $\chi\omega$  and  $\Phi$  by  $\Phi(1 - \delta\omega)$ .

For  $P'_0$  one finds

$$P'_0 = 1 - \chi_{\nu+1} + 2\chi_{\nu+1} \frac{\Gamma_2(a'_A)}{a'^2_A} \dots\dots (19'')$$

$\Phi$  is here the total cross section, including that for emission of neutrettos. In the charge symmetrical theory  $\delta$  has probably the value  $\frac{1}{3}$  and, as will be seen in § 4, the value of  $\omega_{\nu+1}$  is between 0.5 and 1, probably  $\frac{2}{3}$  or so.  $\chi_{\nu+1}$  is then close to 1. Likewise  $a'_A$  is only slightly reduced. Since the values of  $\Phi$  and  $\omega_{\nu+1}$  are anyhow not accurately known, we shall work below with formula (17) and evaluate it for a range of values  $\Phi$  and  $\omega_{\nu+1}$ . Since we shall renormalize our results to the total number of showers observed, the constant factor  $\chi$  drops out.

A second generalization concerns the contribution of fast recoil protons. The experiments on the positive excess of shower particles suggest that as many as half the number of shower particles are protons (Rochester 1949). This is not surprising. We expect indeed that one fast recoil nucleon is produced for each meson produced. On the average half of these will however be neutrons. Since neutrettos are also accompanied by recoil nucleons we expect for four charged mesons three fast recoil protons. This figure may be further increased since the strong interaction of the recoil nucleons with the nucleus gives rise not only to a general heating up of the nucleus but also to a few further fast ejected nucleons. Evidently the mechanism of the production of recoil particles is very complicated, much more so than for the mesons, which can be expected to leave the nucleus unhindered (the most that could happen to a meson is a nuclear scattering). Instead of using some model for the ejection of fast protons we adopt a more phenomenological procedure.

Since in the experiments only the total number of fast particles is measured (so far), we would prefer to have the probabilities for a total of  $N$  particles, mesons + protons, rather than those for a given number of mesons. Obviously a certain statistical correlation may exist connecting the number of mesons with the number of protons. (In the first place one recoil nucleon is produced for each nucleon.) If that correlation were quite strict, each meson would be accompanied by one proton, and we should merely need to divide the experimental total number of particles by two to obtain the number of mesons. This is one way of comparing the experiments with the theory (cf. § 6), but it is certainly an exaggeration.



Alternatively we may assume that the fast protons are statistically independent of the mesons. We assume then that each observed particle has a probability  $\xi$ , say, of being a meson and  $1-\xi$  of being a proton, independently of how many particles there are. The experiments indicate  $\xi \sim \frac{1}{2}$ . We have already the probabilities  $P'_\nu$  for a given number of charged mesons. And we ask, what are then the probabilities  $P''_N$  for a given total of particles to be ejected? This procedure may give too wide a spread of the number of protons relative to that of mesons.  $P''_N$  can be calculated as follows:

Supposing  $P''_N$  were known, on the hypothesis of statistical independence, then the  $P'_\nu$ 's would be determined by

$$P'_\nu = \sum_{N \geq \nu} \binom{N}{\nu} P''_N \xi^\nu (1-\xi)^{N-\nu}. \quad \dots\dots (20)$$

To give the answer to our question, we have to solve (20) for the  $P''_N$ 's\*.

(20) can be solved for the  $P''_N$ 's. The solution, as can easily be verified, is

$$P''_N = \sum_{\mu \geq N} \binom{\mu}{N} (-1)^{N-\mu} P'_\mu \frac{1}{\xi^\mu (1-\xi)^{N-\mu}}. \quad \dots\dots (21)$$

It is remarkable that, although for a given  $N$  the number of mesons is certainly less than or equal to  $N$ ,  $P''_N$  is expressed by the  $P'_\mu$ 's with  $\mu \geq N$ . This shows that there can be no arbitrariness in the  $P'_\mu$ 's. (21) has the same form as (18). We get then the explicit expression for  $P''_N$  again by a modification of the constants:

$$P''_N = \chi'_{\gamma+1} \left\{ \omega''_{\gamma+1} \left[ \Gamma_N(a''_A) - \frac{N(N+1)}{a_A''^2} \Gamma_{N+2}(a''_A) \right] - \omega''_{\gamma+1} \left[ \Gamma_{N+1}(a''_A) - \frac{(N+1)(N+2)}{a_A''^2} \Gamma_{N+3}(a''_A) \right] \right\}, \quad \dots\dots (22)$$

$$a''_A = a'_A \frac{\xi + \omega' - \xi \omega'}{\xi} = a_A \frac{\xi + \omega(1-\delta-\xi)}{\xi},$$

$$\chi' = \frac{1}{\xi + \omega' - \xi \omega'}, \quad \omega'' = \chi' \omega' = \chi' \chi \omega = \frac{(1-\delta)\omega}{\xi + \omega(1-\delta-\xi)}, \quad \dots\dots (22')$$

dropping the index  $\gamma+1$  in  $\omega$  and  $\chi$ . We get for  $P''_N$  again the same formula, only with different values for the constants. Using this formula below, we shall put  $\xi = \frac{1}{2}$ .

#### § 4. THE NUMERICAL VALUES OF $\Phi$ AND $\omega_{\gamma+1}$

Since  $\omega(\epsilon/E)$  is by definition normalized to 1,  $\omega_{\gamma+1}$  must be less than 1. If we tentatively put  $\omega(\epsilon/E) = (\beta+1)^{-1} (1-\epsilon/E)^\beta$  (the true law will probably be well approximated by this with some value of  $\beta$ ), convergence at  $\epsilon = E$  requires  $\beta > -1$ . It is almost certain that  $\beta > 1$  because there is no known law of energy loss in physics that makes high energy losses more probable than small ones. Then  $\omega_{\gamma+1} = (\beta+1)/(\beta+\gamma+1)$ . As was mentioned in HJ, the theory of HHP gives

\* It is far from certain that (20) has always solutions with all  $P''_N$ 's positive, when the  $P'_\nu$ 's are given arbitrarily. In fact the assumption of statistical independence of the  $P'_\nu$ 's and the probability  $\frac{1}{2}$  for being a meson or proton may be self-contradictory. In the present case, when the  $P'_\nu$ 's are given by a formula of the type (19) no difficulty arises.



results close to  $\beta=2^*$ . With  $\gamma=1.5$ , we see that  $\omega_{\gamma+1}$  would be 0.4 for  $\beta=0$ , but this is also improbable. For  $\beta=2$ ,  $\omega_{\gamma+1}=\frac{2}{3}$ . It is quite safe to say that  $\omega_{\gamma+1}$  lies between 0.5 and 1 and, more probably, near 0.6 or 0.7. If neutrettos are included, and if we accept, for instance,  $\omega_{\gamma+1}=\frac{2}{3}$ , we get  $\chi_{\gamma+1}=\frac{6}{7}$  (for  $\delta=\frac{1}{3}$ ) and  $\omega'_{\gamma+1}=\frac{4}{7}$ . If we calculate the total number of particles  $N$ , including protons, we get (with  $\xi=\frac{1}{2}$ )  $\chi'_{\gamma+1}=14/11$  and  $\omega''_{\gamma+1}=\chi'_{\gamma+1}\omega'_{\gamma+1}=8/11=0.73$ . If we exclude neutrettos and accept  $\omega'_{\gamma+1}=\omega_{\gamma+1}=\frac{2}{3}$ , we get  $\chi'_{\gamma+1}=6/5$ ,  $\omega''_{\gamma+1}=\frac{4}{5}=0.8$ . If the low energy mesons mentioned in the footnote immediately preceding exist,  $\omega$ ,  $\omega'$ ,  $\omega''$  are still slightly larger. When comparing the results with the experiments we should therefore choose some fairly small value for  $\omega$ , about 0.6 to 0.7, when only mesons are considered, and some higher value, 0.7 or 0.8, when all particles are considered.

The total cross section  $\Phi$  must be expected to be of the order of a few times  $(\hbar/\mu c)^2$ . From the absorption coefficient of fast (meson-producing) nucleons a relation between  $\Phi$  and  $\omega_{\gamma+1}$  was determined in HJ, namely

$$\Phi(1-\omega_{\gamma+1})=1.15(\hbar/\mu c)^2 \quad (\mu=286m). \quad \dots\dots (23)$$

In  $\Phi$  neutrettos are, of course, included. Putting, for instance,  $\omega_{\gamma+1}=\frac{2}{3}$ , we get

$$\Phi=3.5(\hbar/\mu c)^2.$$

This agrees, as was already mentioned in HJ, with the predictions of the HHP theory, within the limits given by that theory.

The quantity  $Nd_A(\hbar/\mu c)^2$  has the value 0.95 for oxygen and about 1.9 for Ag or Br. Thus we should get, if neutrettos are emitted,  $a_A=3.3$ ,  $a'_A=2.6$  for oxygen, and  $a_A=6.6$ ,  $a'_A=5.2$  for Ag or Br. For the calculation of the total number of particles according to (22) we have  $a''_A=4.1$  for oxygen and 8.2 for Ag, Br. These figures increase further if the low energy mesons mentioned in the footnote below exist (as may well be the case, though not in the exaggerated way mentioned). We have then for oxygen  $\bar{a}_A=6.6$ ,  $\bar{a}'_A=5.2$  for mesons alone,  $\bar{a}''_A=8.2$  for the total number of particles, and for Ag, Br twice these values. In all, we can say that for the calculation of mesons alone some values are to be expected as follows:— $\bar{a}'_A\sim 2.5$ –5 for O or C,  $\sim 5$ –10 for Ag or Br, and for the total number  $\bar{a}''_A\sim 4$ –9 for O or C,  $\sim 8$ –18 for Ag or Br.

Finally we must also remark that in the derivation of the connection (23) the contribution from recoil nucleons to the effective absorption coefficient has been neglected. It is hardly likely that this will amount to much because  $\Phi$  has already about the largest value it can possibly have, namely a few times  $(\hbar/\mu c)^2$ . In fact we have shown in HJ (in "Note added in proof") that this effect is probably small.

\* Actually this theory predicts also the production of mesons with fairly low energies, of the order  $3 \times 10^8$  ev., which do not follow the law (1). Their number is on the average equal to the number of fast mesons, but their contribution to the energy loss is of a smaller order of magnitude. We have not considered these mesons in this paper. This could easily be done if we neglect the energy loss due to these low energy mesons completely (although this is, of course, a gross exaggeration) and add a term to (1) of the form  $\Phi \delta(\epsilon/E) d\epsilon/E$ . It can then easily be seen that the net effect is a slight increase of the constant  $\omega$  to  $(\omega+1)/2$ , i.e. from  $\frac{2}{3}$  to  $\frac{3}{4}$  (if the numbers of slow and fast mesons are equal) and an increase of  $\Phi$  by a factor 2. The distinction between these two energy groups of mesons is, of course, highly artificial, and the true distribution is certainly a smooth transition between both groups, but the consideration shows that nothing changes, apart from a change of constants, if the law (1) is not strictly obeyed, as long as the main contribution to the energy loss follows from (1).



All this serves only as a guide to the values of the constants to be expected; exact values cannot be predicted, but if the experiments can be explained with some values of  $\omega$  and  $a_A$  similar to the above we can say that this is physically reasonable.

### § 5. NUMERICAL RESULTS

We give the numerical results for  $P_N''$  or  $P_n$  according to formula (17) for a variety of values  $a_A$  and  $\omega_{\gamma+1}$ . The formulae (19) and (22) differ from (17) only by a re-definition of the constants, the constant factors  $\chi_{\gamma+1}$  or  $\chi'_{\gamma+1}$  amount merely to a renormalization of all probabilities for  $n \neq 0$  (the cases  $n=0$  are in any case not observed). The range of values for the constants given,  $a_A=2.5-20$ ,  $\omega=0.6-0.9$ , are wide enough to include the cases considered.  $\omega_{\gamma+1}$  is independent of the atomic weight.

The probabilities are normalized to 100, including the case  $n=0$ , but  $P_0$  is in all cases less than 20%.

$P_n$  decreases more or less rapidly with increasing  $n$ . It is remarkable that for small  $n$ ,  $P_n$  varies very slowly with  $a_A$ , i.e. the atomic weight and the total cross section. It is the number of large showers which depends sensitively on  $\Phi$  and  $A$ .

We see that small showers with one or two mesons are far the most frequent. (Here, however, our approximations are very crude.) In light materials the shower size is limited to a maximum of 3-5 mesons (larger numbers being extremely improbable), in Ag, Br the largest showers to be expected (apart from rare exceptions) are 6-10. The total number of particles (including protons) is larger, as the larger values of constants have to be used.

### § 6. COMPARISON WITH EXPERIMENTS AND DISCUSSION

To compare our results with the data, we consider only showers with at least three thin tracks, for the following reason. The small showers are evidently produced by primaries with energies not much above those in the region where the cross section drops more or less rapidly to a negligible value with decreasing energy. Here the approximation made in § 2 is too crude. The same approximation had been made in HJ in the derivation of the power spectrum at all depths. The power spectrum may therefore not hold in this low energy region either (indeed the decreasing energy loss may make these primaries relatively more frequent). We cannot therefore expect that the present calculation gives the number of small showers very satisfactorily.

Of the thin tracks we take it from the positive excess (Rochester 1949) that roughly half are protons, the rest mesons. We do not expect any of the thin tracks to be electrons, although they accompany as a rule the larger showers in cloud-chamber pictures. These however are very probably the decay products of some short-lived type of meson which the photographic plate would not show to originate from the same grain (unless the lifetime were extremely short).

We compare our results with the experimental data in two ways. We first assume that half the number  $n'$  of the observed thin tracks in each shower are protons. We divide then the experimental numbers  $n'$  by 2 and, when  $n$  is odd, attribute half the number of showers to the preceding, half to the subsequent even number.  $n'/2=n$  is then the number of mesons in the shower. Thus we assume first a very strict correlation between the number of mesons and protons, which is probably much too strict. The ratio  $\frac{1}{2}$  for the number of protons is, of course, none too accurately known, and it is not even known if this ratio is independent of the shower size. The figure  $\frac{1}{2}$  refers to comparatively small showers.

Table 1. Relative Frequency (%) of Showers  $P_n$  with  $n$  Mesons\*

$\omega=0.6$											
$\begin{smallmatrix} n \\ a_A \end{smallmatrix}$	1	2	3	4	5	6	7	8	9	10	
2.5	49	21	5.5	1.5	0.4	0.1	0	0	0	0	
3	48	22	8.3	2.6	0.73	0.18	0	0	0	0	
4	46	24	11	4.3	1.5	0.46	0.13	0	0	0	
5	45	25	13	5.7	2.3	0.85	0.28	0.09	0	0	
7	43	25	14	7.3	3.6	1.6	0.70	0.28	0.10	0	
9	42	25	14	8.0	4.3	2.2	1.1	0.50	0.22	0.09	
11	41	25	14	8.2	4.6	2.5	1.3	0.69	0.34	0.16	

$\omega=0.7$														
$\begin{smallmatrix} n \\ a_A \end{smallmatrix}$	1	2	3	4	5	6	7	8	9	10	11-12	13-14	15-16	
3	43	23	10	4.0	1.3	0.36	0.09	0	0	0	0	0	0	
4	40	25	13	6.3	2.6	0.93	0.30	0.09	0	0	0	0	0	
5	38	25	15	8.1	3.9	1.7	0.66	0.24	0.08	0	0	0	0	
7	34	24	16	10	5.8	3.1	1.6	0.74	0.32	0.13	0	0	0	
9	33	23	16	10	6.7	4.1	2.4	1.3	0.67	0.33	0.2	0	0	
11	32	22	15	11	7.0	4.5	2.8	1.7	1.0	0.55	0.3	0	0	
14	31	22	15	11	7.2	4.7	3.2	2.1	1.3	0.85	0.73	0.25	0.07	

$\omega=0.8$														
$\begin{smallmatrix} n \\ a_A \end{smallmatrix}$	1	2	3	4	5	6	7	8	9	10	11-12	13-14	$\geq 15$	
3	37	24	13	5.5	2.1	0.67	0.19	0	0	0	0	0	0	
4	33	25	16	8.6	4.1	1.7	0.64	0.22	0.07	0	0	0	0	
5	30	24	17	11	6.0	3.0	1.4	0.56	0.21	0.07	0	0	0	
7	26	21	17	12	8.4	5.3	3.1	1.7	0.84	0.39	0.3	0	0	
9	23	19	16	12	9.2	6.6	4.4	2.8	1.7	1.0	0.9	0.3	0	
11	22	18	15	12	9.2	7.0	5.1	3.6	2.4	1.6	1.6	0.6	—	
14	22	18	14	11	8.9	7.0	5.4	4.0	3.0	2.2	2.5	1.1	0.58	
17	21	18	13	11	8.7	6.9	5.3	4.2	3.2	2.4	3.2	1.6	1.2	
20	21	17	13	11	8.5	6.9	5.3	4.2	3.3	2.5	3.4	1.9	1.9	

$\omega=0.9$																
$\begin{smallmatrix} n \\ a_A \end{smallmatrix}$	1	2	3	4	5	6	7	8	9	10	11-12	13-14	15-16	17-18	$\geq 19$	
3	31	24	15	7.3	3.1	1.2	0.4	0.11	0	0	0	0	0	0	0	
4	26	23	17	11	6.0	2.9	1.2	0.46	0.16	0	0	0	0	0	0	
5	22	21	18	13	8.5	4.9	2.5	1.2	0.50	0.20	0	0	0	0	0	
7	17	17	16	14	11	8.1	5.5	3.4	1.9	1.0	0.6	0	0	0	0	
9	14	14	14	13	11	9.4	7.4	5.4	3.8	2.4	2.3	0.4	0	9	0	
11	13	13	12	11	10	9.2	7.9	6.4	5.0	3.7	4.4	1.6	0.4	0	0	
14	12	11	10.5	10	9.2	8.2	7.5	6.5	5.4	5.0	6.9	3.9	1.9	0.75	0.37	
17	11	10.5	9.5	9.2	8.5	7.5	6.9	6.1	5.6	4.8	7.8	5.3	3.3	1.8	1.3	
20	11	10	9.3	8.4	8.0	7.1	6.5	5.7	5.4	4.6	7.8	5.8	4.1	2.7	3.0	

\* or mesons plus protons, cf. text.



However, as our parameters  $\omega$  and  $a_A$  are not determined accurately either, a constant change in this ratio will only change the parameters. For the discussion of large showers, however, the possibility has to be kept in mind that the fraction of protons may be quite different. For the second comparison with experiments we assume a large measure of statistical independence of mesons and protons and use formula (22) to calculate the relative frequencies of the total numbers of particles  $N$ .

The chemical composition of the plate is such that there are 1.04 light atoms C, O, N to one heavy atom Ag or Br. We need not distinguish between C, O, N nor between Ag and Br, as the nuclear diameters of these atoms are not very different. Thus we multiply the theoretical figures of Table 1 for some rather small value of  $a_A$  by 1.04, add the figures for about twice the value of  $a_A$ , and renormalize the total number of showers so as to agree with the actual experimental figures. On account of the renormalization of the theoretical  $P_n$ 's any common factor  $\chi_{\gamma+1}$  as it occurs in (19) or (22) is irrelevant.

Table 2. Experimental and Theoretical Distribution of Shower Sizes (Mesons)

$n$	Experi- mental*	Theoretical		
		$a=3$ and 7 $\omega=0.7$	$a=4$ and 9 $\omega=0.6$	$a=4$ and 9 $\omega=0.7$
2	89	77	83 (41)	70 (37)
3	31.5	42	42 (19)	42 (19)
4	12	23	22 (7.3)	24 (9.6)
5	17	11.5	9.6 (2.5)	13.5 (3.8)
6	9.5	5.6	4.4 (0.8)	7.3 (1.4)
7	0.5	2.7	1.9 (0.2)	3.8 (0.4)
8	0.5	1.2	0.8 (0)	1.9 (0.1)
9	1.5	0.5	0.4 (0)	1.0 (0)
$\geq 10$	1.0	0.3	0.15 (0)	0.75 (0)

\* Results of Powell and collaborators at Bristol.

The figures in brackets show the contribution from light atoms C, O, N.

Since the size-frequency distribution of showers does not seem to vary much with altitude, we may add the results of Powell and his collaborators for Jungfraujoch and balloon heights. Similar data have also been collected in the photographic plate by Rochester and Page. Furthermore, Fretter (1949) has obtained a distribution from cloud-chamber measurements. But, as Fretter himself points out, some particles may be lost for geometrical reasons and also, perhaps, by absorption in the rather thick lead plates, and, indeed, his distribution is more concentrated on smaller showers than the photographic plate results. We therefore base our comparison on the photographic plate results alone. The first comparison with the theory is then given in Table 2 for a few relevant values of the parameters.

The agreement is seen to be very good indeed. The actual values of these parameters could be determined more definitely from the number of large showers if more statistical data were available. The number of small showers ( $n=2-5$ ) is given well by almost any choice of the parameters. It is to be noticed in particular that the large showers, containing a total of 17, 18, 22 particles, are also well accounted for. The theory gives for the total number to be expected with  $n \geq 7$  ( $\omega=0.6$ ,  $a_A=4$  and 9) the value 3.3, whereas a total of 3.5 has been observed.

The number of showers with  $n=1$  would, if calculated in the same way, be smaller than the experimental figure. As mentioned before, we believe that this may be due to the crude approximations made in this energy region as well as to a departure from the power law at lower energies. It may even be that some of these have nothing to do with mesons at all but are merely the effect of the scattering of fairly slow (i.e.  $\sim 10^9$  ev.) protons or neutrons by protons.

We now carry out the same comparison with experiments but calculating the total number of particles and assuming a large amount of statistical independence of meson and proton emission, thus using the constants  $\omega''$ ,  $a''_A$ . These can be compared directly with the experimental figures. We use the latter for  $n \geq 3$ ; this means that we are using more material on small showers than in the former comparison, because there only half of the showers  $n=3$  were attributed to two mesons. According to § 3 we should use now larger values for  $\omega$  and  $a''$ , roughly  $\omega'' = \omega' \{2/(1 + \omega)\}$ ,  $a'' = a'(1 + \omega')$ , but of course, with the assumption of statistical independence, we must expect to have to use somewhat different values.

Table 3. Experimental and Theoretical Distribution of Shower Sizes  
 $N$  = total number of particles

$N$	Experi- mental*	Theoretical	
		$a''=7$ and 14 $\omega=0.8$	$a''=9$ and 20 $\omega=0.8$
3	61	55 (30)	48 (27)
4	44	41 (21)	38 (21)
5	29	31 (15)	30 (15)
6	14	22 (9.5)	22 (11)
7	6	15 (5.5)	16 (7.6)
8	5	10 (3.0)	11.5 (4.6)
9	8	6.8 (1.5)	8.2 (2.9)
10	9	4.7 (0.7)	5.7 (1.7)
11	8	} 5.0 (0.5)	} 7.1 (1.5)
12	5		
13	1		
14	0	} 2.0 (0)	} 3.6 (0.6)
15-16	0		
$\geq 17$	3	} 1.0 (0)	} 3.2 (0)

\* Results of Powell and collaborators at Bristol.

The figures in brackets show the contribution from light atoms C, O, N.

The agreement is almost equally good, and it is certainly not justifiable to draw any conclusions about a correlation of proton and meson numbers. Since the numerical evaluation of our formula is rather laborious (partly owing to the lack of suitable tables of the incomplete  $\Gamma$ -function) we have not attempted to secure the "best fit" by slightly varying the constants. The accuracy of the present data makes this hardly worth while. The experimental distribution shows a minimum at  $N=7, 8$  (also in Table 2 at  $n=4$ ). The present material is compatible with the assumption that this is a statistical fluctuation and this has to be assumed if we wish to account for the whole distribution. (If this minimum should turn out to be real, a special explanation must be sought, possibly on lines different from those suggested here.) What appears to be certain, however, is that the experimental distribution shows a break in the slope at  $N=7, 8$ .



This is reproduced in the theory—not quite as pronounced as in the experiments—and is due to the rapid falling off of the contribution from light elements so that only the contribution from Ag, Br is left, with its much longer tail.

Also in this comparison there is no reason to conclude that the large showers of 20 particles or so are extraordinary. One shower with 31 thin tracks has been found by Cosyns, Dilworth, Occhialini, Schönberg\* and Vermasen, and the probability for this would, of course, be very small for any reasonable values of  $\omega$  and  $a_4$ . However, even in this case we feel it unwarranted to interpret this shower by a different process, for the following reasons.

Amongst the recoil nucleons which accompany every act of meson production some may be sufficiently fast to produce themselves further mesons and secondary nucleons. These secondary processes have been neglected throughout this paper. The effect would resemble a mild cascade, only probably much less pronounced than in the well-known electron case. The recoil nucleons will also produce further nucleons by nucleon-nucleon scattering if their energy is not high enough to produce mesons. All this tends to make an already large shower still bigger, and the effect is naturally more pronounced in Ag and Br than in C, O, N. If these secondary effects give a substantial contribution, the tail end of our distribution curves would have to be drawn out much longer, and if the effect is important, the values of our constants are smaller than Tables 2 and 3 suggest and, instead, the larger showers owe their large size to some extent to the cascade effect.† Pending an investigation, we feel it unjustified to interpret even the shower with 31 particles as a novel phenomenon.

An indication of the existence of a cascade effect can perhaps be seen in the following fact. As was pointed out to us by Professor Powell, the experiments show that showers with eight or more thin tracks are nearly all produced in Ag, Br (as follows from the number of heavy tracks) and less than one-seventh of these showers are produced in C, O, N (possibly even none). The figures in brackets in Table 3 show that, according to the present calculations, about a quarter or a fifth is still due to light elements. This can be understood if the cascade effect is important; our constants would be smaller and, considering the primary effects only, the distribution would fall off more rapidly than in Tables 2 and 3. Instead, the shower size is increased considerably, and mainly so in Ag, Br by the cascade effects. The fact that large showers are predominantly produced in heavy elements only provides a strong argument for the plural character of the process. If the process were purely multiple, the size of the nucleus should be immaterial.

The conclusions that must be drawn from these results are clear: the statistical data on the size-frequency distribution of penetrating showers can well be accounted for by the assumption of pure plural production (with the possible exception of the minimum). This applies also to the largest showers observed. There is no evidence so far for the existence of any other process such as a genuine multiple process. The values for the total cross section for meson production and other constants which have to be used to represent the experimental data are all reasonable on general physical grounds.

\* We are indebted to Dr. Schönberg for sending us this photograph.

† An interesting cloud-chamber picture has been described (private communication) by Lovati, Mura, Salvini and Tagliaferri: two particles emerging from a penetrating shower create a second penetrating shower in a second lead plate. This means that at least one recoil nucleon has sufficient energy to create a second penetrating shower. It seems that this event is not infrequent. If this can happen in two nuclei in succession, it surely must happen within the same nucleus also.

On the other hand, there is no proof that multiple processes do not occur in appreciable numbers. With a suitably invented dependence of the multiplicity on the primary energy it may be possible to explain the whole of the frequency distribution equally well. It is even more difficult to exclude the possibility that some of the showers, or part of the multiplicity in a given shower, are due to genuine multiple processes. If, for example, the average multiplicity in an individual nucleon-nucleon encounter were 2 or 3, the larger showers would be mixed, partly plural, partly multiple, and the treatment would be much the same as our treatment of the proton contribution. The distribution curve would hardly be much different from the one obtained here (with suitable readjustments of the constants).

The following arguments seem to point in the direction of—at least largely—plural production: the maximum shower size (i.e. excepting comparatively rare fluctuations) agrees roughly with the number of nucleons arranged along the diameter of an Ag or Br nucleus. If the process were purely multiple, the average multiplicity would have to be a similar number, which would be somewhat accidental. Purely multiple processes are difficult to reconcile with the large cross section that follows from the observed absorption coefficient, and so some plurality must surely exist. Finally, as was already mentioned, large showers with eight or more thin tracks occur nearly always in Ag, Br but rarely in C, O, N, and there would be no reason for this correlation were the processes all multiple; this correlation is even stronger than we have reason to expect.

All this tends to show only that the processes are probably to a large extent plural. In order to decide whether multiple processes contribute at all, and if so to what extent, further experiments are needed. The best would be experiments in hydrogen but, failing this, observations on the average shower size in different elements *made separately* would give strong indications. In C, O, N the shower sizes would be roughly half the size of those in Ag, Br if the process is all plural, even less than half if the cascade effects contribute, but the same if the process is all multiple.

#### ACKNOWLEDGMENTS

We are very much indebted to Prof. Powell for communicating to us all the Bristol data before publication and for interesting discussions during his stay in Dublin; to Dr. Rochester for sending us Miss Page's material and for advice regarding the probable ratio of the proton contribution; to Dr. Schönberg for sending us the photograph of a shower with 31 thin tracks; to Dr. Fretter for his manuscript on the cloud-chamber statistics, and finally to Miss M. Houston for computing Table 1 for us.

#### REFERENCES

- BROWN, R. H., CAMERINI, U., FOWLER, P. H., HEITLER, H., KING, D. T., and POWELL, C. F., 1949, *Phil. Mag.*, **40**, 862.  
 DALLAPORTA, N., and CLEMENTEL, E., 1948, *Nuovo Cim.*, **4**, 235, 298.  
 FRETTER, W. B., 1949, *Phys. Rev.*, in the press.  
 HEISENBERG, W., 1949, *Z. Phys.*, **126**, 569.  
 HEITLER, W., 1949, *Rev. Mod. Phys.*, **21**, 113 (compare also THOMSON, G. P., 1949, *Phil. Mag.*, **40**, 589).  
 HEITLER, W., and JÁNOSSY, I., 1949, *Proc. Phys. Soc. A*, **62**, 374.  
 PENG, H. W., and MORETTE, C., 1948, *Proc. R. Irish Acad. A*, **51**, 17, 217.  
 ROCHESTER, G. D., 1949, *Rev. Mod. Phys.*, **21**, 20.  
 THOMSON, G. P., 1949, *Phil. Mag.*, **40**, 589.



# The Meson Intensity at the Surface of the Earth and the Temperature at the Production Level

By A. DUPERIER

Turner and Newall Research Fellow of the University of Manchester

*Communicated by P. M. S. Blackett; MS. received 30th March 1949, and in amended form 11th July 1949*

**ABSTRACT.** Meson intensity has been recorded by using a triple-coincidence arrangement with a lead absorber 25 cm. thick between the counters. The comparison of daily mean values with the height of a number of pressure-levels has led us to take into consideration the temperature of the air layer between 200 and 100 mb. The results show that this temperature appears to be a factor closely controlling the meson intensity at the surface of the earth; the intensity increases with increasing temperature at the rate of 0.12% per °C.

Other factors in determining the intensity are the mass of air and the height of the 100 mb. level over the station. The corresponding coefficients of absorption and decay prove to be comparable with those obtained from other measurements for mesons of the same momentum. It has also been found that the coexistence of the three effects permits explanation of the variability exhibited by the barometric coefficient when evaluated from short periods of observations.

These results may therefore be taken as evidence that the bulk of mesons is produced at the height of 100 mb.

If the positive effect of temperature is interpreted as the result of processes of decay and interactions with air nuclei of  $\pi$ -mesons at the production level, then the coefficient 0.12% per °C. leads to a value of  $4.9 \times 10^{-8}$  sec. for the upper limit of the mean life of  $\pi$ -mesons.

## §1. INTRODUCTION

THE results of the comparison of the cosmic-ray intensity, as measured by means of a counter arrangement without using absorbers, with the height of different pressure-levels have been reported in a former paper (Duperier 1944). For this comparison the variation of intensity from day to day was assumed to be given by the regression equation

$$\delta I = \mu \delta B + \mu' \delta H, \quad \dots\dots(1)$$

where  $I$  is the intensity in percentages of the mean,  $B$  the barograph reading at the station and  $\mu$  the true absorption coefficient,  $H$  the height of the pressure-level and  $\mu'$  the probability of meson decay per unit length of path. The partial correlation  $r_{IH \cdot B}$ , or correlation of  $I$  with  $H$  at constant  $B$ , was then obtained by following standard methods of multiple correlation analysis without necessity for reducing the cosmic-ray data beforehand.

Since these results were published, some other observers have made similar studies, but the results obtained are difficult to interpret on account of the procedure followed. Benedetto (1946) has compared the meson intensity at the ground with the height of different pressure-levels, but after reducing the data by applying the so-called barometric coefficient  $\beta$ . This is the coefficient which results from assuming that meson intensity is a function of atmospheric pressure only. It is given by  $\beta = \delta I / \delta B$ . But if  $I$  is in reality represented by equation (1)

then, by substituting, we have  $\beta = \mu + \mu' \delta H / \delta B$ . This expression shows that  $\beta$  by being a function of  $\delta H / \delta B$  will vary with the weather, since the factor  $\delta H / \delta B$  depends on the change in atmospheric temperature accompanying the change in pressure  $\delta B$ . It is therefore clear that the data after being reduced by applying  $\beta$  will appear to be related in one way or another to the height of a certain pressure-level according to the meteorological conditions during the period of observations.

Millican and Loughridge (1948) have compared the intensity of mesons with the temperature of the air mass underlying different pressure-levels, but as they have also reduced the data first by using  $\beta$  the results are again uncertain for the same reason.

It will be seen from the present paper that there is another mechanism, in addition to that expressed by the above expression, which also causes the coefficient  $\beta$  to depend on the weather.

An account is given in this paper of a new study, similar to that made formerly, but using now a lead absorber of 25 cm. thickness between the counter-trays. The comparison of the meson intensity with the height of a number of pressure-levels has led us to take into consideration the temperature of the air layer lying between 200 and 100 mb. The rather unexpected result is found that this temperature appears to be a factor closely controlling the meson intensity at ground-level; the latter intensity is found to increase with the temperature of the layer.

## §2. MEASUREMENTS AND METEOROLOGICAL DATA

The meson intensity has been measured by using a counter arrangement consisting of three trays of counters of three units each. The effective length and the diameter of the tubes were about 60 cm. and 5 cm. respectively. The upper and intermediate trays were directly above each other and separated from the lower tray by a block of lead of 25 cm. thickness. This lead was supported on a steel platform 1 cm. thick. The counting rate was about 7,400 triple coincidences per hour, and was recorded photographically every hour.

The following five periods of observations have been analysed separately :

- (1) 1-4, 7-11 Jan. 1948 (9 days),
- (2) 21 Jan.-9 Feb. 1948 (20 days),
- (3) 12-29 Feb. 1948 (18 days),
- (4) 27 June-3 July, 5-24 July 1948 (27 days),
- (5) 5-10 Nov., 12 Nov.-8 Dec. 1948 (33 days).

During the first three periods the apparatus was installed on the top floor at the Imperial College of Science and during the last two on the top floor at the Birkbeck College, London.

For the analysis, the hourly numbers of coincidences as well as the barograph readings at the station have been averaged in groups of 24 hours centred for convenience at 0030 G.M.T. The barograph was daily compared with a barometer of mercury.

The upper-air data have been extracted from the Daily Weather Report of the Meteorological Office, London, using the radio-sonde observations made every day at 03, 09, 15, 21 hours at Larkhill (about 100 km. to the south-west of London) and at Downham Market (about 75 km. to the north-east). Thus the height of a given pressure-level which corresponds to each 24-hour group is the mean of eight different determinations. This procedure has been considered



necessary in order to minimize the meteorological errors arising from the radio-sonde itself and from rapidly changing weather conditions. The comparison of the means of the four determinations for each day at the two stations has shown however that these means are very closely related. Even in the case of the 100 mb. level the correlation, then appearing at its lowest, has a value not less than 0.70.

When the radio-sonde balloons do not reach the upper levels the missing data have been obtained by interpolation after considering the data from the nearest ascent and the simultaneous ascent at the other station. The error so introduced in the average value for the corresponding 24-hour group is negligible. No level higher than 100 mb. has been considered because the number of balloons reaching these levels is much reduced.

### §3. ANALYSIS OF THE DATA

To begin with, the assumption has again been made that the variation of meson intensity from day to day is a function, and a function only, of the variation in the mass of air over the station and the change in height of the pressure-level at which

Table 1

Period 1; $r_{IB} = -0.96$					Period 2; $r_{IB} = -0.93$				
Pressure-level (mb.)	$r_{IH}$	$r_{BH}$	$r_{IH \cdot B}$	$r_{IB \cdot H}$	Pressure-level (mb.)	$r_{IH}$	$r_{BH}$	$r_{IH \cdot B}$	$r_{IB \cdot H}$
100	-0.75	0.66	-0.52	-0.94	100	-0.81	0.74	-0.49	-0.85
200	-0.95	0.87	-0.84	-0.86	200	-0.97	0.89	-0.82	-0.59
500	-0.97	0.92	-0.77	-0.72	500	-0.98	0.94	-0.84	-0.22
900	-0.98	0.99	-0.65	+0.27	900	-0.94	1.00	-0.52	+0.38

Period 3; $r_{IB} = -0.69$					Period 4; $r_{IB} = -0.69$				
Pressure-level (mb.)	$r_{IH}$	$r_{BH}$	$r_{IH \cdot B}$	$r_{IB \cdot H}$	Pressure-level (mb.)	$r_{IH}$	$r_{BH}$	$r_{IH \cdot B}$	$r_{IB \cdot H}$
100	-0.49	0.04	-0.63	-0.76	100	-0.16	0.01	-0.25	-0.70
200	-0.75	0.26	-0.81	-0.77	200	-0.49	0.17	-0.52	-0.71
500	-0.85	0.39	-0.87	-0.73	500	-0.74	0.60	-0.56	-0.47
900	-0.83	0.89	-0.67	+0.20	900	-0.74	0.99	-0.43	+0.27

Period 5; $r_{IB} = -0.87$				
Pressure-level (mb.)	$r_{IH}$	$r_{BH}$	$r_{IH \cdot B}$	$r_{IB \cdot H}$
100	-0.55	0.24	-0.72	-0.85
200	-0.85	0.64	-0.77	-0.81
500	-0.94	0.84	-0.78	-0.45
900	-0.92	0.94	-0.60	-0.02

mesons originate, that is to say, it is again assumed that equation (1) is valid. Then by comparing the partial correlation coefficients  $r_{IH \cdot B}$  and  $r_{IB \cdot H}$  for different pressure-levels it will be possible to see whether the assumption is justified and if so to obtain the pressure-level at which the bulk of mesons is formed.

Table 1 gives the values which have been obtained for these correlations together with those for  $r_{IB}$ ,  $r_{IH}$  and  $r_{HB}$  (total correlations) for each period.

To facilitate the comparison, the values in the last two columns of the table have been plotted in Figures 1 and 2. It can be seen that in spite of the low values of some coefficients, the change of  $r_{IH \cdot B}$  with the pressure level, as well as the change of  $r_{IB \cdot H}$  is practically the same in all the five cases. The significance of

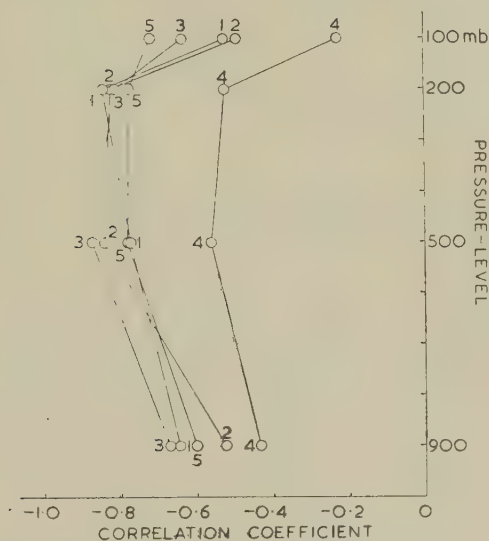


Figure 1. Correlation of meson intensity with height of different pressure-levels at constant ground pressure.

In Figures 1-3 the figures near the points represent the period of observations to which the points correspond.

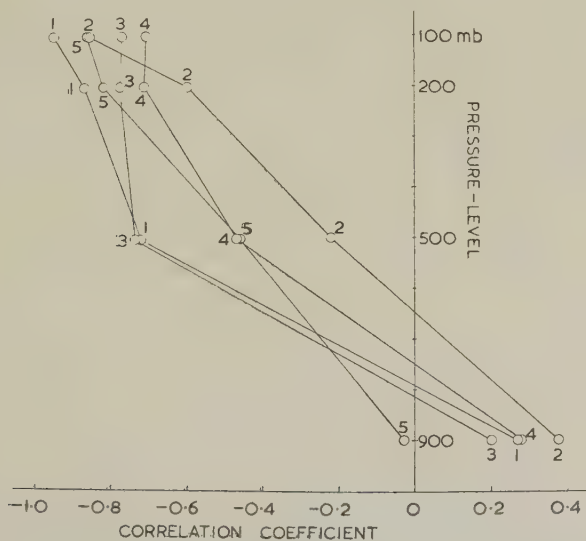


Figure 2. Correlation of meson intensity with ground pressure at constant height of pressure-level for different pressure levels.

both changes could not therefore be questioned, but the fact that  $r_{IB \cdot H}$  increases continually with height while  $r_{IH \cdot B}$  increases only up to about 500 mb., with a very pronounced decrease from 200 to 100 mb., seems to indicate that the variation of meson intensity at ground level is not accounted for entirely by equation (1).



If this had been the case we should have expected the two correlations to have reached their maximum at about the same level, that for which equation (1) would have been valid. Another factor, therefore, must be involved. We will assume that this factor is the density of the air in the proximity of a given pressure-level. For a given pressure-level  $P$  we will consider the mean density of the layer between  $P$  and  $P+100$  mb. Instead of the actual density, it will be convenient to make use of the temperature of the layer, this being inversely proportional to the density. We therefore assume that the variation of meson intensity from day to day at the ground is represented by the regression equation

$$\delta I = \mu \delta B + \mu' \delta H + \alpha \delta T, \quad \dots\dots(2)$$

where the two first terms on the right-hand side have the same meaning as before and  $T$  is the mean temperature of the layer between  $P$ , the chosen pressure-level, and  $P+100$ .

The partial correlations of  $I$  with this particular temperature which have been found by using the third period of observations are given as an example in Table 2. The Table gives also the total correlations between the different variables (with omission of those already given in Table 1) which are necessary to obtain  $r_{IT \cdot BH}$ .

Table 2

Pressure-level (mb.)	$r_{BT}$	$r_{HT}$	$r_{IT}$	$r_{IT \cdot BH}$
100	-0.38	-0.56	+0.80	+0.68
200	-0.28	-0.96	+0.74	+0.01
500	+0.11	+0.92	-0.67	+0.07

As the Table shows, the total correlations  $r_{IT}$  for the two lower pressure-levels are purely accidental, since they both disappear when the other two variables are eliminated. Instead, the correlation for the highest pressure-level remains with its value only slightly reduced after the elimination of  $B$  and  $H$ .

The same result has been obtained for the 100 mb. level with the data for the other four periods. This is shown in Table 3 where the results from period 3 have been inserted to facilitate comparison.

Table 3

Period	$r_{BT}$	$r_{HT}$	$r_{IT}$	$r_{IT \cdot BH}$
1	-0.87	-0.56	0.92	0.75
2	-0.70	-0.30	0.75	0.77
3	-0.38	-0.56	0.80	0.68
4	-0.25	-0.67	0.64	0.74
5	-0.70	-0.58	0.88	0.63

The fact that all the five periods give the same high value for  $r_{IT \cdot BH}$  makes the reality of this correlation unquestionable. Even when taken separately, each value proves to be statistically significant. Following Fisher's method, the probability that correlations of this magnitude should arise from random sampling of uncorrelated observations is about 0.02 in the case of the first period, and less than 0.01 in the case of the others.

In addition, this correlation allows us to explain the rather remarkable change with pressure-level of the correlations  $r_{I \cdot H \cdot B}$  illustrated in Figure 1. If  $I$  is closely related to  $T$  we have to expect that the correlations of  $I$  with  $H$  will be similar to those of  $T$  with  $H$ . In Figure 3 has been plotted the correlations  $r_{TH}$  which have

been obtained by using the upper-air data for two of the observation periods and for the same pressure-levels as in Figure 1. It may be noticed that the change with pressure-level in Figure 3 is entirely similar to the change in Figure 1.

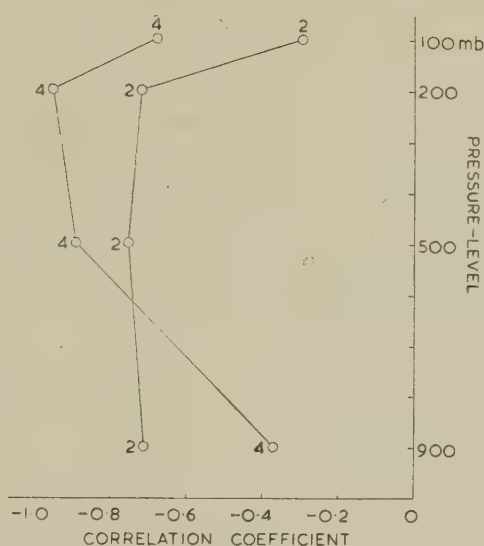


Figure 3. Correlation of the temperature of the 200-100 mb. layer with the height of different pressure-levels.

The conclusion must therefore be that the temperature of the air layer between 200 and 100 mb., or its equivalent, the density, is a controlling factor for the intensity of the penetrating component of cosmic rays at sea-level, this intensity being the greater the higher the temperature of the layer. (According to meteorological observations the mean height of this layer is about 14 km. and its average depth 4.2 km. At mean and high latitudes it lies in the lower stratosphere; in the equatorial belt it is just below the tropopause.)

For the partial correlation of meson intensity with the height of the 100 mb. level and with ground pressure, the following values have been obtained :

Table 4

Period	$r_{IB-HT}$	$r_{IH-BT}$
1	-0.84	-0.74
2	-0.58	-0.79
3	-0.72	-0.33
4	-0.71	+0.28
5	-0.82	-0.49

It can be seen that with the exception of  $r_{IH-BT}$  for the fourth period, all the values are physically of the right sign and sufficiently high to make also these two correlations significant. The exceptional value +0.28 may be partly due to the slight variation of  $H$  during the fourth period, which could accentuate the importance of the meteorological errors. As shown by Table 6, it is just for this period that the standard deviation of  $H$  is at its lowest. In any case, however, if the five periods are taken together, the correlation  $r_{IH-BT}$  proves to be negative and statistically significant, with a level of significance of 0.01.



When the multiple correlation  $r_{I-BHT}$ , or correlation between the two members of equation (2), is considered, the following values are obtained :

Table 5

Period	1	2	3	4	5
$r_{I-BHT}$	0.99	0.98	0.91	0.88	0.96

Equation (2) appears, therefore, to be justified when the pressure-level of 100 mb. is taken.

Figure 4, corresponding to the two first periods of observations, illustrates the daily course of meson intensity and the three meteorological variables.

The coefficients of the equation as well as their probable errors can be determined by using the relevant correlations together with the standard deviations  $\sigma$  of each of the variables. These are given in Table 6, and average values have been obtained as follows :

$$\begin{aligned}\mu &= -(1.05 \pm 0.16)\% \text{ per cm.Hg, or } -(0.77 \pm 0.12) \times 10^{-3} \text{ cm}^2/\text{gm.} \\ \mu' &= -(3.90 \pm 1.10)\% \text{ per km.} \\ \alpha &= +(0.123 \pm 0.024)\% \text{ per } ^\circ \text{C.}\end{aligned}$$

Table 6

Period	$\sigma_I(\%)$	$\sigma_B(\text{cm.Hg})$	$\sigma_H(\text{m.})$	$\sigma_T(^{\circ} \text{C.})$
1	1.33	0.62	73	4.48
2	1.68	0.86	129	4.44
3	0.67	0.39	63	3.82
4	0.64	0.44	48	3.54
5	1.75	0.66	83	4.50

To check these coefficients in the absence of comparable determinations only indirect methods seem to be possible.

#### *Coefficient of mass absorption.*

For the coefficient  $\mu$  we can use the results of measurements of the absorption curve in water. According to Ehmert (1937), the absorption coefficient in water down to a depth of 45 metres is given by  $\mu = 1.56/h$  where  $h$  is the depth in gm.  $\text{cm}^2$ . To use this formula in the present case the range of mesons in air and lead as compared with the range in water must be considered. By using the Bethe-Bloch formula and applying the Fermi correction, Neher and Stever (1940) have found that the range in air is the same as that in water for mesons of rather more than  $10^9$  ev. energy. From the theoretical results of Rossi and Greisen (1941) it may be seen that the range in lead is about 1.6 times greater than in water for mesons of  $10^9$  ev. energy. When vertical incidence only is considered, the mass of water equivalent to the mean barograph reading during our observations (757.5 mm.Hg) together with the thickness of the lead block, steel platform, roof and counter-box, then appears to be  $1,530 \text{ g/cm}^2$ , which would lead to a coefficient

$$1.56/1,530 \simeq 1.0 \times 10^{-3} \text{ cm}^2/\text{g.}$$

Had, however, the aperture angles of the apparatus been taken into account ( $18^\circ \times 63^\circ$  to the vertical) this value would have been a little smaller. The two coefficients are, therefore, quite comparable.

*Decay coefficient.*

As mentioned before,  $\mu'$  represents the probability of meson decay per unit length of path. The average value  $-3.90\%/km.$  has been obtained after rejecting period 4 because the correlation of  $I$  with  $H$  was positive for this period. The mean range before decay would be  $L = (25.6 \pm 7.2) km.$ , which permits evaluation of the mean life of ordinary mesons.

The cut-off momentum of the apparatus corresponding to about 28 cm. of lead equivalent is estimated to be  $4.5 \times 10^8 \text{ ev/c.}$  From this value and by using Jánossy's expression for the average momentum of the mesons along their path down to sea-level (Jánossy 1948), we obtain  $p = 3.5 \times 10^9 \text{ ev/c.}$  As for the mass,

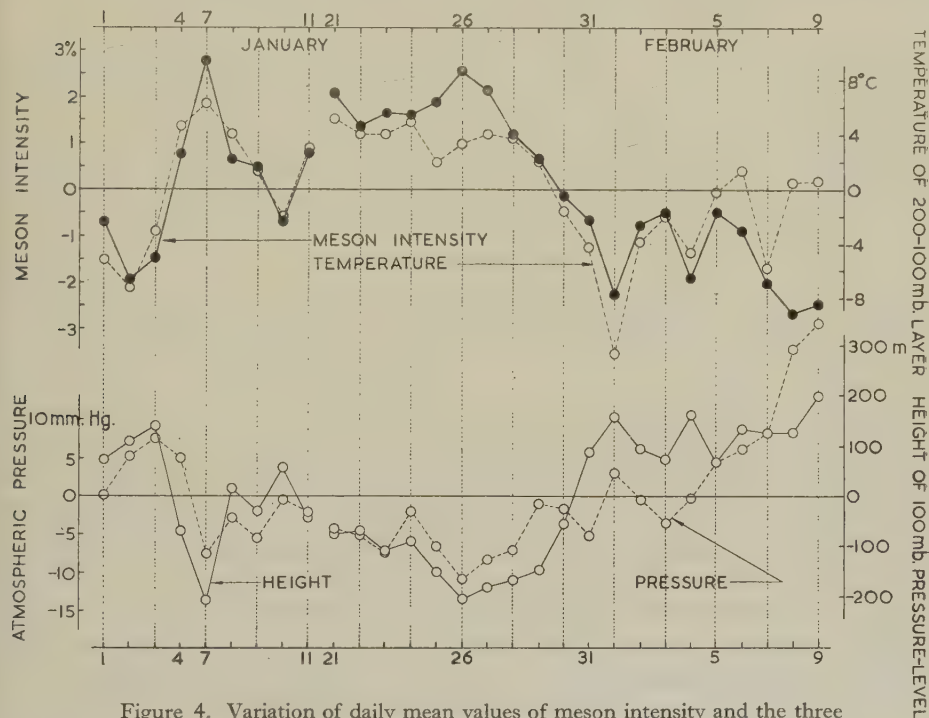


Figure 4. Variation of daily mean values of meson intensity and the three atmospheric variables.

we can take some  $200 m_e$ , the former measurements suggesting an average of  $180 m_e$  while more recent determinations by means both of photographic emulsions and cloud chamber observations give about  $215 m_e$ . Thus from  $L = p\tau_0/m$  we have for the mean life  $(2.49 \pm 0.70) \mu\text{sec.}$ , a value which is also comparable with the value  $2.15 \mu\text{sec.}$  given by Nereson and Rossi (1943) which is generally accepted.

If the multi-directional character of the radiation recorded by the apparatus had been taken into account, it is clear from equation (2) that  $\mu'$  would have been a little smaller, or  $L$  greater, as  $\delta H$  increases with the secant of the zenith angle. The value for  $\tau_0$ , however, would have been but little affected since the average momentum then to be used would have also been greater.

*Positive temperature effect.*

The possible meaning of  $\alpha$  will be discussed in the last section. It may however be noted at this stage that the increase of the cosmic-ray intensity with the temperature of the 200-100 mb. layer (third term of (2)) is not incompatible with the



decrease of intensity with increase of the temperature of the atmosphere as a whole. The latter results from the rising of the meson-producing level caused by the thermal expansion of the atmosphere, and is represented by the second term of equation (2). Thus we must suppose that two separate processes are taking place in the 200–100 mb. layer, one of which leads to an increase and one a decrease of cosmic-ray intensity at sea level with rising temperature of the layer. The latter negative effect is almost certainly due to the decay of  $\mu$ -mesons, and of course also occurs throughout the atmosphere down to the ground. It will be shown that the former positive effect is probably due to the decay of a short-lived intermediate product, probably in fact to  $\pi$ -mesons.

#### § 4. VARIABILITY OF THE BAROMETRIC COEFFICIENT

Further support to the above results is given by the fact that equation (2) also provides an explanation of the variability of the so-called barometric coefficient.

This is the coefficient which results from ascribing the whole variation of cosmic-ray intensity to the variation only of atmospheric pressure. It is given by the regression equation

$$\delta I = \beta \delta B = r_{IB} \cdot \delta B \cdot \sigma_I / \sigma_B \quad \dots\dots (3)$$

It is well known that  $\beta$ , when determined from observations covering only short periods, say 20 days, shows not infrequently a variability much greater than would be expected from the accuracy of the measurements. In the results obtained by Lindholm (1944) differences up to 100% and more occur among the average values for different periods. In the same way we have great discrepancies among the values given by different observers. To quote only a few : 3.1%/cm.Hg with a shield of 36 cm.Pb (Barnóthy and Forro), 1.1% with 20 cm.Pb (Messerschmidt), 1.6% with 12 cm.Pb (Compton and Turner), all quoted by Rossi (1939); 3.4% with 20.5 cm.Pb and 1.5 with 30 cm.Pb (Smith and Gast, quoted by Millican and Loughridge 1948).

This variability is much reduced when long periods are considered. The results obtained by Hogg (1947) from a period covering more than five years show that the whole range of the variation of monthly mean values is only 33% of the mean for the whole period.

Our results give another example of the variability of  $\beta$ . From the relevant data given in previous tables the following values can be directly obtained as indicated by expression (3) :

Table 7

Period	$\beta$ (%/cm.Hg)	$r_{BH}$	$r_{BT}$
1	$-(2.06 \pm 0.22)$	0.66	-0.87
2	$-(1.82 \pm 0.17)$	0.74	-0.70
5	$-(2.33 \pm 0.37)$	0.24	-0.70
Mean	$-(2.22 \pm 0.16)$		
3	$-(1.16 \pm 0.30)$	0.04	-0.38
4	$-(1.00 \pm 0.21)$	0.01	-0.25
Mean	$-(1.07 \pm 0.16)$		

It may be seen that the first three values are about twice as great as the last two. Now if the second term of equation (2) is substituted for  $\delta I$  in (3) we have

$$\beta = \mu + \mu' \delta H / \delta B + \alpha \delta T / \delta B, \quad \dots\dots (4)$$

which shows that  $\beta$ , by depending on the variations  $\delta H$  and  $\delta T$  accompanying the variation of pressure  $\delta B$ , will change with the meteorological conditions during the period. From the correlations given in Table 7 it can be seen that the values of  $\delta H / \delta B$  and  $\delta T / \delta B$  for the first three periods would not only be relatively high but of the right sign to make all the three terms on the right-hand side of (4) negative, thus explaining the high value for  $\beta$ . In fact the values of the second and third terms for these periods are  $-0.36\%$  and  $-0.61\%/\text{cm.Hg}$  respectively.

On the other hand, for the last two periods  $\delta H / \delta B$  is nearly zero, and  $\delta T / \delta B$  is very small, with the result that  $\beta$  is only slightly greater than the coefficient of mass absorption.

It may be noticed that had the term  $\alpha \delta T / \delta B$  been ignored it would not have been possible to account entirely for such a change in the barometric coefficient.

The fact that the values of  $r_{BT}$  are all negative and those of  $r_{BH}$  positive is in accordance with the meteorological result that the stratosphere tends to be warmer over cyclones and colder over anticyclones, whereas most of the troposphere is colder when the pressure is low and warmer with high pressure. On account of this tendency, it is to be expected that over long periods the barometric coefficient will be numerically greater than the coefficient of mass absorption; the observations confirm this.

## § 5. CONCLUSIONS

The above results show that the variation of meson intensity from day to day at the surface of the earth is due to fluctuations in air mass and in the height of the 100 mb. level and in the temperature in its proximity. They may therefore be taken as further evidence that the bulk of mesons is formed at or little above this level.

From a study of the results obtained in different parts of the world of the effects of ground temperature on cosmic-ray intensity, we had already come to the same conclusion regarding the height of meson production (Duperier 1948). It was then suggested that the gradual increase of intensity up to the height of 27 mb. as found by Schein, Jesse and Wollan might be due to primary protons passing through the apparatus. Recently Pomerantz (1949), by investigating the variation of cosmic-ray intensity with altitude in a series of free-balloon flights by using different amounts of absorber between the counters, has been able to evaluate the relative intensity of the electron and proton-plus-meson components. He has found that the maximum of the proton-plus-meson curve occurs at the 80 mb. level while that of the electron component appears to be located a little lower at about 104 mb. These results by Pomerantz seem to suggest that a maximum of the meson component alone must occur somewhere between these two levels, which should be in agreement with our result.

## § 6. INTERPRETATION OF THE POSITIVE EFFECT OF TEMPERATURE

If, as is suggested, the penetrating component is formed by the actions of primary cosmic rays on nuclei of air, the positive effect of temperature in the proximity of the production level appears to indicate that the number of mesons



at the surface of the earth increases as the density of nuclei in that region decreases. This result although apparently anomalous may be explained, at least qualitatively, if we accept the suggestion made by Lattes, Occhialini and Powell (1947) that the greater number of the mesons observed at sea level are the result of decay of  $\pi$ -mesons. Following their view we shall assume that  $\pi$ -mesons originate in the actions of primary rays on nuclei of air and that thereafter they may either be captured by other nuclei with which they collide or disintegrate into  $\mu$ -mesons and presumably a neutral particle. The probability of capture would be the greater the shorter the mean free path of the  $\pi$ -meson for a nuclear collision and the longer its life-time. If  $R$  is the mean free path in gm cm<sup>2</sup> before a collision takes place and if  $L$  is the range before decay in centimetres, the probability of capture would be given by  $L/(R/\rho)$  where  $\rho$  is the density of air. If  $L/(R/\rho)$  is small, the probability of not being captured, that is the probability of decay of the  $\pi$ -meson, would therefore be  $P = 1 - L\rho/R$ . The temperature coefficient would therefore be

$$\alpha = \frac{\delta P}{\delta T} = - \frac{L}{R} \frac{\delta \rho}{\delta T}, \quad \dots\dots(5)$$

which agrees in sign with the experimental effect.

For a quantitative check we can proceed to estimate the life-time of the  $\pi$ -meson and compare the results with other experiments.

If  $m$  is the mass per unit area and  $h$  the depth of the 200–100 mb. layer,

$$\rho \simeq \frac{m}{h} \quad \text{and} \quad \frac{\delta \rho}{\delta T} \simeq - \frac{m}{h^2} \frac{\delta h}{\delta T}.$$

From meteorological data

$$h \simeq 4.2 \text{ km.}, \quad \delta h/\delta T \simeq 20.5 \text{ m/}^\circ \text{C.}, \quad \text{and} \quad m = 102 \text{ gm.}$$

Consequently

$$\alpha = 1.2 \times 10^{-6} \times L/R. \quad \dots\dots(6)$$

As it appears that it is the temperature of the 200–100 mb. layer only that has an appreciable effect on the meson intensity at sea level, it is to be assumed that the process of decay and capture of the heavy meson occurs mainly on this layer, thus indicating that the mean free path of the heavy meson is of the order of magnitude of the depth of this layer. We might, therefore, take  $R$  to be of the order of 100 gm/cm<sup>2</sup>.

Owing to the very small value of the vertical gradient of temperature in the stratosphere it might be expected, however, that the results obtained in this paper would have been but little altered if a thinner layer starting down at the 100 mb. level had been considered. This has been tested by using the first and the second periods of observations for the 150–100 mb. layer; the results obtained show that the correlation of meson intensity with the temperature of this layer and the coefficient  $\alpha$  are both practically the same as in the case of the 200–100 mb. layer. In fact, they appear to be a little higher, but the difference is not statistically significant. The value 100 gm/cm<sup>2</sup> for the mean free path of the heavy meson might therefore be taken as an upper limit.

For the average energy of the ordinary meson at the production level we may use  $5 \times 10^9$  ev. (derived from Blackett's spectrum at sea level and assuming a total energy loss in air of  $2 \times 10^9$  ev.). Allowing for the energy taken by the

neutral particle originating in the  $\pi$ -disintegration we have  $E_\pi \simeq 10^{10}$  ev. If finally we take for the mass  $286 m_e$  and substitute 0.12% for  $\alpha$  we obtain from (6)  $\tau_\pi \leq 4.9 \times 10^{-8}$  sec.

This is consistent with the results from other experiments. Camerini, Muirhead, Powell, and Ritson (1948) have obtained  $6 \times 10^{-9}$  sec. by comparing the relative number of  $\pi$ - and  $\mu$ -particles in the upward stream of mesons near the ground. Richardson (1948) has given, from other experiments,  $1.1 \times 10^{-8}$  sec. for the mean life of negative  $\pi$ -mesons. Finally, Greisen (1948), by using the results of measurements at great depths underground, has claimed the value  $6 \times 10^{-8}$  sec.

Another consideration can be made which leads to further support for this interpretation. According to (5) the positive effect of temperature, being proportional to  $L$ , should increase with the energy of the particles. Records of the cosmic radiation under 40 metres of water by Rau (1939) show that the intensity had a maximum in June and a minimum in January, the difference between these extreme values being about 4%. As the average energy under 40 metres of water is about five times greater than at the surface, we should expect for the temperature effect at this depth  $5 \times 0.12 = 0.60\%$ /°C. approximately.

Now, from the Ramanathan diagram for the vertical distribution of temperature of the atmosphere as modified by Gregg (1931) and by Palmen (1934), the change in temperature at 100 mb. from winter to summer in mean latitudes can be estimated at some 5 or 10°C. Using Rau's results this would give for  $\alpha$  some 0.8 or 0.4% per °C., which is quite consistent with the predicted value from the result at the surface.

However, the existence of heavier mesons, as observed by different workers, makes it doubtful if the process of meson formation is as simple as has been visualized. In particular, the recent report by Brown *et al.* (1949) of a meson of  $900 m_e$  which in disintegrating gives rise to  $\pi$ -mesons would seem to suggest that this heavier particle may be partially, at any rate, responsible for the effect of density at the production level.

\* \* \* \* \*

In the experiments referred to in § 1, when no absorber was used so that the total radiation was recorded, it was found that the variations of intensity at sea level were well accounted for by the fluctuations of pressure and by the height of the 100 mb. level, that is, the effect of the temperature of the 200–100 mb. layer passed unnoticed. Owing to the smaller value of the average energy of the mesons and to the presence of the electronic component due to the lack of the absorber, it is possible that the greater effects of decay and absorption in this case may have contributed to mask the effect of temperature of the 200–100 mb. layer which, in addition, appears to decrease as the energy of the mesons decreases.

Another possibility is the following. If the electrons of the soft component at sea level are partly the product of meson decay in the lower part of the atmosphere, then it is to be expected that the variations of intensity due to the vertical motion of the 100 mb. level will be partly offset by the electrons resulting from the disintegration of mesons. The fact that these variations appear to be well correlated with the variations in height of the 100 mb. level seems therefore to indicate that something happens or tends to happen in the opposite direction



that compensates for the increase or decrease of the electron component. As mentioned above, the thermal change in the troposphere which accompanies a change of pressure tends to be opposite to that in the stratosphere. When the 100 mb. level rises owing to the warming of the troposphere the number of mesons decreases not only because of the rise in height but also because the 200–100 mb. layer becomes colder. The latter decrease would compensate for the increase in the number of electrons, thus making the intensity appear well correlated with the height of the 100 mb. level.

The former results with the total radiation might therefore be regarded as not inconsistent with the results as given in this paper.

#### ACKNOWLEDGMENTS

The author wishes to express gratitude to Professor J. D. Bernal for providing facilities for this work to be carried out in the Physics Department, Birkbeck College, University of London, and to Professor P. M. S. Blackett for his interest and advice.

#### REFERENCES

- BENEDETTO, F. A., 1946, *Phys. Rev.*, **70**, 817.  
 BROWN, R., CAMERINI, U., FOWLER, P. H., MUIRHEAD, H., POWELL, C. F., and RITSON, D. M., *Nature, Lond.*, **163**, 82.  
 CAMERINI, U., MUIRHEAD, H., POWELL, C. F., and RITSON, D. M., 1948, *Nature, Lond.*, **162**, 433.  
 DUPERIER, A., 1944, *Terr. Magn. Atmos. Elect.*, **49**, 1; 1948, *Proc. Phys. Soc.*, **61**, 34.  
 EHMERT, A., 1937, *Z. Phys.*, **106**, 751.  
 GREGG, W. R., 1931, *Bull. Nat. Res. Coun. of the Nat. Acad. Sci., Wash.*, No. 79, 125.  
 GREISEN, K. I., 1948, *Phys. Rev.*, **73**, 521.  
 HOGG, A. R., 1947, *Proc. Roy. Soc. A*, **192**, 128.  
 JÁNOSSY, J., 1948, *Cosmic Rays* (Oxford: University Press).  
 LATTES, C. M. G., OCCHIALINI, G. P. S., and POWELL, C. F., 1947, *Nature, Lond.*, **160**, 486.  
 LINDHOLM, F., 1944, *Ark. Mat., Astr. Fys.*, **30 A**, No. 13.  
 MILLICAN, F. M., and LOUGHRIDGE, D. H., 1948, *Phys. Rev.*, **74**, 66.  
 NEHER, and STEVER, 1940, *Phys. Rev.*, **58**, 766.  
 NERESON, N., and ROSSI, B., 1943, *Phys. Rev.*, **64**, 199.  
 PALMEN, L., 1934, *Met. Z.*, **51**, 17.  
 POMERANTZ, M. A., 1949, *Phys. Rev.*, **75**, 69.  
 RAU, W., 1939, *Z. Phys.*, **114**, 265.  
 RICHARDSON, J. R., 1948, *Phys. Rev.*, **74**, 1720.  
 ROSSI, B., 1939, *Rev. Mod. Phys.*, **11**, 296.  
 ROSSI, B., and GREISEN, K. I., 1941, *Rev. Mod. Phys.*, **13**, 240.

## On the Decay of $\tau$ -Mesons

BY C. B. VAN WYK\*

Department of Mathematical Physics, University of Birmingham

*Communicated by R. E. Peierls; MS. received 19th April 1949*

**ABSTRACT.** The production of  $\tau$ -mesons (mass about 900 electron masses) by cosmic rays in rather thin layers of air in the upper atmosphere seems to indicate that the nucleon  $\tau$ -meson coupling constant is not very small. The Berkeley experiments show that this is also true for the nucleon- $\pi$ -meson coupling constant. Consequently the decay of a charged  $\tau$ -meson into a photon and a charged  $\pi$ -meson by means of virtual creation and annihilation of nucleons ought to be fairly probable. In this paper this decay process, with the emission of one photon, is studied for the various types of  $\tau$ - and  $\pi$ -mesons. Unless both mesons have zero spin, the matrix elements, and therefore the lifetimes, are found to be of the same order of magnitude, and the  $\tau$ -meson turns out to be too short-lived to be observed photographically.

If both mesons have zero spin the emission of only one photon is forbidden. The detailed discussion of higher order decay processes in this case is reserved for a later paper.

### §1. INTRODUCTION

THE decay of a charged meson into a lighter meson and a photon by means of virtual creation and annihilation of nucleons was discussed by Finkelstein (1947). He carried out a perturbation calculation using as the interaction energy between meson and nucleon fields only that part of the total interaction Hamiltonian which contains the derivatives of the meson wave functions. Assuming both kinds of meson fields to interact reasonably strongly with nucleons—as is the case for the Schwinger mixture of nuclear forces—and taking the mass of the final meson as 177 electron masses, he found a lifetime of about  $10^{-18}$  sec. for a vector meson at rest decaying into a pseudoscalar meson and a photon.

It will be shown that if that part of the total interaction Hamiltonian not containing derivatives of the meson wave functions were used as interaction energy in the calculation referred to above, the position would be improved considerably. With the same parameters the lifetime then becomes  $10^{-12}$  sec. However, it is now certain that the lightest meson ( $\mu$ -meson) of a mass about 200 electron masses is not strongly coupled with nucleons so that a  $\pi$ -meson ( $\sim 300$  electron masses) decaying in the way described by Finkelstein would have a very long lifetime, and may therefore decay in some other way. But in connection with the discovery of a meson having a mass of about 900 electron masses (Powell *et al.* 1949), Oppenheimer† has pointed out that the production of these mesons in fairly thin layers of air leads one to expect it to have a strong coupling with nucleons. In that case Finkelstein's calculations would predict a lifetime too short to be compatible with the observation of tracks of these particles in the photographic plate.

\* Now at the University of Natal.

† Unpublished, remark made at Physics Conference at Birmingham in September 1948.

*Note added in proof.* Through private communication the author learned from Professor Powell and Dr. B. Peters that at present there is no reliable evidence for the existence of short-lived mesons of mass around 900 electron masses. However, this does not affect the validity of this discussion of the possible properties of such particles.



The purpose of the present investigation is to see whether this result is dependent on the character of the mesons which are taking part in the decay process and on the type of the coupling.

If both the initial and final mesons have spin zero, the emission of *one* photon is forbidden by the conservation of angular momentum. In this case the lifetime will be determined by a process of higher order which will be discussed in a subsequent paper.

In all other cases the difference between coupling terms with or without derivatives of the meson field variables, to which reference has been made, is less important here since the dependence expresses itself through a power of  $\mu_0/M$  where  $\mu_0$  is the rest energy of the initial meson and  $M$  that of the nucleon. Since this ratio is about  $\frac{1}{2}$  for  $\tau$ -mesons, this factor is not very important.

Apart from this dependence it will be shown that in all cases the lifetime is very short compared to  $10^{-12}$  sec. so that the difficulty pointed out by Oppenheimer would remain.

Unless both  $\tau$ - and  $\pi$ -mesons have spin zero, one would have to conclude either that the present formalism is not adequate, or that the generation of  $\tau$ -mesons must be due to a process quite different from that usually assumed.

## §2. NUCLEON-MESON INTERACTION TERMS

In the perturbation calculation only interaction terms linear in the coupling constants will be used. For charged scalar mesons this term in the Hamiltonian is (Kemmer 1938)

$$(4\pi)^{\frac{1}{2}} \int \Phi^* \{g\beta + f/\kappa [\partial/\partial x_0 + \alpha \cdot \nabla]\} \{\tau_{PN}U + \tau_{NP}U^*\} \Phi d^3x,$$

where  $g$  and  $f$  are constants with the dimension of charge and  $\kappa = mc/\hbar = \mu/\hbar c$ ;  $m$  = meson mass;  $\Phi$  is the nucleon wave function;  $U$  is the meson wave function;  $\alpha$ ,  $\beta$  are the Dirac matrices;  $\tau_{PN}$  and  $\tau_{NP}$  are operators creating a proton and a neutron respectively.

Imagine the system to be enclosed in a cubic box, side length  $L$ . Introduce the expansions

$$\Phi = L^{-3/2} \sum_l \sum_{r=1,2} \left[ \begin{matrix} v_+^r(l) \\ u_+^r(l) \end{matrix} \right] a^r(l) \exp \{i(lx - l_0 x_0)\} + \begin{matrix} v_-^{r*}(l) \\ u_-^{r*}(l) \end{matrix} \left\} b^r(l) \exp \{-i(lx - l_0 x_0)\} \right],$$

$$U = (\hbar c L^{-3})^{\frac{1}{2}} \sum_k (2k_0)^{-\frac{1}{2}} U_+(k) \exp \{i(kx - k_0 x_0)\},$$

where the upper line refers to the neutron component, and the lower line to the proton component, of the nucleon wave function and where  $v$ ,  $u$ ,  $U(k)$  are the occupation operators for neutrons, protons and mesons respectively (the signs refer to charge in case of protons and mesons and magnetic moment in the case of a neutron).  $a^r(l)$  and  $b^r(l)$  are spinors with the property

$$\begin{aligned} \{(\alpha l) + \beta K\} a(l) &= l_0 a(l), \\ \{(\alpha l) - \beta K\} b(l) &= l_0 b(l), \end{aligned}$$

where  $l_0 = +(l^2 + K^2)^{\frac{1}{2}}$ ,  $K = M/\hbar c$ ,  $M$  = nucleon rest energy. The matrix element then becomes

$$(2\pi/L^3 \epsilon)^{\frac{1}{2}} \hbar c u^*(Q) \{g\beta + i\rho(f/\mu)[- \epsilon + (\alpha p)]\} u(P),$$

where  $\rho = 1$  for absorption of a meson,  
 $= -1$  for emission of a meson,

$u(Q)$  can be either  $a(Q)$  or  $b(Q)$ ;  $\epsilon = k_0 \hbar c$ ;  $p = k \hbar c$ ;  $\epsilon^2 = p^2 + \mu^2$ .

For the pseudoscalar case the corresponding expressions are

$$(4\pi)^{\frac{1}{2}} \int \Phi^* \{ig\beta\gamma_5 + (f/\kappa)[\gamma_5 \partial/\partial x_0 + \boldsymbol{\sigma} \cdot \nabla]\} \{\tau_{\text{PN}} U + \tau_{\text{NP}} U^*\} \Phi d^3x \\ (2\pi/L^3\epsilon)^{\frac{1}{2}} \hbar c U^*(Q) \{ig\beta\gamma_5 + ip(f/\mu)[- \epsilon\gamma_5 + (\sigma p)]\} u(P),$$

where  $\gamma_5 = -i\alpha_1\alpha_2\alpha_3$   $\boldsymbol{\sigma} = \gamma_5\boldsymbol{\alpha}$ .

The interaction term for the vector meson field is

$$(4\pi)^{\frac{1}{2}} \int \Phi^* \left\{ \begin{array}{l} [g(-U_0 + \boldsymbol{\alpha} \cdot \mathbf{U}) + (f/\kappa)(\mathbf{V}_0 \cdot \boldsymbol{\gamma} + \mathbf{V} \cdot \boldsymbol{\beta} \boldsymbol{\sigma})] \tau_{\text{PN}} \\ + [\text{conjugate complex}] \tau_{\text{NP}} \end{array} \right\} \Phi d^3x,$$

where  $(\mathbf{U}, U_0)$  is the meson vector-field

$$\mathbf{V} = \text{curl } \mathbf{U} \quad \mathbf{V}_0 = -(\partial/\partial x_0)\mathbf{U} - \nabla U_0.$$

Introduce

$$\mathbf{U}(x) = (\hbar c L^{-3})^{\frac{1}{2}} \sum_k (2k_0)^{-\frac{1}{2}} \left\{ (k_0/\kappa) \mathbf{r} U_{3+}(k) + \sum_{i=1,2} \mathbf{e}_i U_{i+}(k) \right\} \exp \{i(kx - k_0 x_0)\}, \\ U_0(x) = (\hbar c L^{-3})^{\frac{1}{2}} \sum_k (2k_0)^{-\frac{1}{2}} (k/\kappa) U_{3+}(k) \exp \{i(kx - k_0 x_0)\},$$

where  $\mathbf{r} = \mathbf{k}/k$ ,  $(\mathbf{e}_i, \mathbf{r}) = 0$ ,  $(\mathbf{e}_1, \mathbf{e}_2) = 0$ ,  $(\mathbf{e}_1, \mathbf{e}_1) = (\mathbf{e}_2, \mathbf{e}_2) = 1$   $\boldsymbol{\gamma} = -i\boldsymbol{\beta}\boldsymbol{\alpha}$ .

This leads to the matrix element

$$(2\pi/L^3\epsilon)^{\frac{1}{2}} \hbar c u^*(Q) \{g[(\epsilon/\mu)(\alpha r) - p/\mu] + \rho f \beta(\alpha r)\} u(P)$$

for longitudinal meson and

$$(2\pi/L^3\epsilon)^{\frac{1}{2}} \hbar c u^*(Q) \{g(\alpha e) + \rho(f/\mu)\beta[\epsilon(\alpha e) + i\sigma(p_\lambda e)]\} u(P)$$

for transverse meson.

The corresponding expressions for the pseudovector case are

$$(4\pi)^{\frac{1}{2}} \int \Phi^* \left\{ \begin{array}{l} [g(-\gamma_5 U_0 + \boldsymbol{\sigma} \cdot \mathbf{U}) + (f/\kappa)(\mathbf{V} \cdot \boldsymbol{\gamma} - \mathbf{V}_0 \cdot \boldsymbol{\beta} \boldsymbol{\sigma})] \tau_{\text{PN}} \\ + [\text{conjugate complex}] \tau_{\text{NP}} \end{array} \right\} \Phi d^3x \\ (2\pi/L^3\epsilon)^{\frac{1}{2}} \hbar c u^*(Q) \{g[(\epsilon/\mu)(\sigma r) - (p/\mu)\gamma_5] - ip\beta(\sigma r)\} u(P) \\ (2\pi/L^3\epsilon)^{\frac{1}{2}} \hbar c u^*(Q) \{g(\sigma e) + \rho(f/\mu)\beta[\alpha(p_\lambda e) - i\epsilon(\sigma e)]\} u(P).$$

These matrix elements will be used to describe the transition

$$M^+(0) \rightarrow m^+(-p) + \gamma(p),$$

where the initial meson is at rest with energy  $\mu_0$ , the final meson has energy  $\epsilon_2$ , momentum  $-\mathbf{p}/c$  and the photon has momentum  $\mathbf{p}/c$ . Conservation of energy requires  $\mu_0 = \epsilon_1 + \epsilon_2 = p + \epsilon_2$ . It is convenient to introduce  $\theta_i = \epsilon_i/\mu_0$  ( $i=1, 2$ ); thus  $1 = \theta_1 + \theta_2$ .

The matrix elements can be summarized as follows:

*Initial Meson:*

$$\begin{aligned} S &: u^*(Q) \{g_0\beta - if_0\} u(P), \\ P_s &: u^*(Q) \{ig_0\beta\gamma_5 - if_0\gamma_5\} u(P), \\ V &: u^*(Q) \{g_0(\alpha e_0) + f_0\beta(\alpha e_0)\} u(P), \\ P_v &: u^*(Q) \{g_0(\sigma e_0) - if_0\beta(\sigma e_0)\} u(P). \end{aligned}$$

*Final Meson:*

$$\begin{aligned}
 S &: u^*(Q)\{g_2\beta + if_2(\mu_0/\mu_2)[\theta_2 + \theta_1(\alpha r)]\}u(P), \\
 P_s &: u^*(Q)\{ig_2\beta\gamma_5 + if_2(\mu_0/\mu_2)\gamma_5[\theta_2 + \theta_1(\alpha r)]\}u(P), \\
 L_v &: u^*(Q)\{-g_2(\mu_0/\mu_2)[\theta_2(\alpha r) + \theta_1] + f_2\beta(\alpha r)\}u(P), \\
 T_v &: u^*(Q)\{g_2(\alpha e_2) - f_2(\mu_0/\mu_2)\beta[\theta_2(\alpha e_2) - i\theta_1\sigma(r_\wedge e_2)]\}u(P), \\
 L_{pv} &: u^*(Q)\{-g_2(\mu_0/\mu_2)\gamma_5[\theta_2(\alpha r) + \theta_1] - if_2\beta(\sigma r)\}u(P), \\
 T_{pv} &: u^*(Q)\{g_2(\sigma e_2) + f_2(\mu_0/\mu_2)\beta[\theta_1\alpha(r_\wedge e_2) + i\theta_2(\sigma e_2)]\}u(P).
 \end{aligned}$$

The matrix element for the emission of a photon by a fermion is  $(\alpha e)$  where  $\mathbf{e}$  is the polarization vector of the photon. In all these expressions the factor  $(2\pi/L^3\epsilon)^{\frac{1}{2}}\hbar c$  has been omitted.

### §3. CALCULATION OF THE MATRIX ELEMENT

A typical way in which the transition by means of virtual creation and annihilation of nucleons can take place, is the following:

<i>Process</i>	<i>Matrix Element</i>
$M^+(0) \rightarrow P^+(q) + N^-(-q)$	$a^*(q)Xb(-q)$
$P^+(q) \rightarrow P^+(q_1) + \gamma(p)$	$a^*(q_1)Ya(q)$
$N^-(-q) + P^+(q_1) \rightarrow m^+(-p)$	$b^*(-q)Za(q_1)$

where  $P^\pm$ ,  $N^\pm$  denotes proton or antiproton, neutron or antineutron and where  $X$  is one of the first group, and  $Z$  one of the second group of expressions listed above, and  $Y = (\alpha e)$ . Conservation of momentum requires

$$\mathbf{q} = \mathbf{q}_1 + \mathbf{p}.$$

The matrix element for the three-stage process is  $n_1/4\epsilon_q^2 d_1$  where

$$\begin{aligned}
 n_1 &= \sum b^*(-q)Za(q_1)a^*(q_1)Ya(q)a^*(q)Xb(-q), \\
 4\epsilon_q^2 d_1 &= (\mu_0 - 2\epsilon_q)(\epsilon_2 - \epsilon_q - \epsilon_{q_1}),
 \end{aligned}$$

$\epsilon_q$  = energy of nucleon with momentum  $\mathbf{q}/c$  and the summation is over the spin states of the nucleons.

The spinors  $a(q)$  and  $b(q)$  have the properties

$$\begin{aligned}
 \sum_{r=1,2} a_\mu^r(q)a_\nu^{r*}(q) &= (1/2\epsilon_q)\{\epsilon_q\delta_{\mu\nu} + (\alpha q)_{\mu\nu} + M\beta_{\mu\nu}\}, \\
 \sum_{r=1,2} b_\mu^r(-q)b_\nu^{r*}(-q) &= (1/2\epsilon_q)\{\epsilon_q\delta_{\mu\nu} - (\alpha q)_{\mu\nu} - M\beta_{\mu\nu}\}.
 \end{aligned}$$

Introduce	$\mathbf{v} = \mathbf{q}/\epsilon_q,$	$\mathbf{z} = M/\epsilon_q,$
	$E = (\alpha v) + \beta z,$	$v^2 + z^2 = 1.$

Thus 
$$n_1 = \frac{1}{8}\text{Sp}Z(1 + E_1)Y(1 + E)X(1 - E).$$

Five more ways in which the decay process can take place are obtained by permuting the three processes involving  $X$ ,  $Y$  and  $Z$ . The quantities  $n_i$  are listed below:

$$\begin{aligned}
 n_1 &= \frac{1}{8}\text{Sp}Z(1 + E_1)Y(1 + E)X(1 - E), \\
 n_2 &= -\frac{1}{8}\text{Sp}Z(1 - E_1)Y(1 + E)X(1 - E), \\
 n_3 &= \frac{1}{8}\text{Sp}Z(1 + E_1)Y(1 - E)X(1 + E), \\
 n_4 &= -\frac{1}{8}\text{Sp}Z(1 - E_1)Y(1 - E)X(1 + E), \\
 n_5 &= -\frac{1}{8}\text{Sp}Z(1 + E_1)Y(1 - E)X(1 - E), \\
 n_6 &= \frac{1}{8}\text{Sp}Z(1 - E_1)Y(1 + E)X(1 + E).
 \end{aligned}$$



The minus signs in processes (2), (4) and (5) result from the commutation properties of the operators  $u$  and  $v$ .

Notice that

$$\begin{aligned}n_2(\mathbf{v}, z, \mathbf{v}_1, z_1) &= -n_1(\mathbf{v}, z, -\mathbf{v}_1, -z_1), \\n_3(\mathbf{v}, z, \mathbf{v}_1, z_1) &= n_1(-\mathbf{v}, -z, \mathbf{v}_1, z_1), \\n_4(\mathbf{v}, z, \mathbf{v}_1, z_1) &= -n_1(-\mathbf{v}, -z, -\mathbf{v}_1, -z_1) \\n_5(\mathbf{v}, z, \mathbf{v}_1, z_1) &= -n_6(-\mathbf{v}, -z, -\mathbf{v}_1, -z_1).\end{aligned}$$

It is therefore only necessary to calculate (say)  $n_1$  and  $n_6$ .

Define

$$x = \frac{\text{mass of initial meson}}{\text{mass of nucleon}}$$

and expand in powers of  $x$

$$\begin{aligned}n_i &= {}^0n_i + x {}^1n_i + \dots, \\d_i &= 1 - x {}^1d_i + \dots\end{aligned}$$

Then

$$n_i/d_i = {}^0n_i + x\{{}^1n_i + {}^0n_i {}^1d_i\} + x^2 \dots$$

The contribution from these six processes is

$$C_1 \dots C_6 = \left(\frac{1}{4}\epsilon_q^2\right) \sum_{i=1}^6 (n_i/d_i).$$

The expansion of the expressions  $d_i$  is carried out as follows:

$$\mathbf{q}_1 = \mathbf{q} - \mathbf{p},$$

or

$$\mathbf{v}_1 = (z_1/z)\mathbf{v} - xz_1\mathbf{l}, \quad \mathbf{l} = \mathbf{p}/\mu_0 = \theta_1\mathbf{r}.$$

Also

$$z_1 = z\{1 - 2xz(lv) + x^2z^2l^2\}^{-\frac{1}{2}}$$

hence

$$\epsilon_{q_1} = M/z_1 = \epsilon_q\{1 - xz(lv) + \frac{1}{2}x^2z^2l^2[1 - rv]^2\} \dots$$

Also

$$\begin{aligned}\epsilon_i &= \mu_0\theta_i \\ &= xz\theta_i\epsilon_q\end{aligned} \quad (i=0, 1, 2; \quad \theta_0=1; \quad \epsilon_0=\mu_0)$$

hence

$$(\epsilon_q + \epsilon_{q_1} - \epsilon_i)^{-1} = (1/2\epsilon_q)\{1 + \frac{1}{2}xz[\theta_i + (lv)] + \dots$$

Finally

$$\begin{aligned}d_1^{-1} &= 4\epsilon_q^2(2\epsilon_q - \mu_0)^{-1}(\epsilon_q + \epsilon_{q_1} - \epsilon_2)^{-1} \\ &= 1 + \frac{1}{2}xz[1 + \theta_2 + (lv)] + \dots\end{aligned} \quad \dots\dots(1)$$

$$\begin{aligned}d_2^{-1} &= 4\epsilon_q^2(2\epsilon_q - \mu_0)^{-1}(\epsilon_q + \epsilon_{q_1} - \epsilon_1)^{-1} \\ &= 1 + \frac{1}{2}xz[1 + \theta_1 + (lv)] + \dots\end{aligned} \quad \dots\dots(2)$$

$$\begin{aligned}d_3^{-1} &= 4\epsilon_q^2(2\epsilon_q + \mu_0)^{-1}(\epsilon_q + \epsilon_{q_1} + \epsilon_1)^{-1} \\ &= 1 + \frac{1}{2}xz[-1 - \theta_1 + (lv)] + \dots\end{aligned} \quad \dots\dots(3)$$

$$\begin{aligned}d_4^{-1} &= 4\epsilon_q^2(2\epsilon_q + \mu_0)^{-1}(\epsilon_q + \epsilon_{q_1} + \epsilon_2)^{-1} \\ &= 1 + \frac{1}{2}xz[-1 - \theta_2 + (lv)] + \dots\end{aligned} \quad \dots\dots(4)$$

$$\begin{aligned}d_5^{-1} &= 4\epsilon_q^2(\epsilon_q + \epsilon_{q_1} + \epsilon_1)^{-1}(\epsilon_q + \epsilon_{q_1} - \epsilon_2)^{-1} \\ &= 1 + \frac{1}{2}xz[-\theta_1 + \theta_2 + 2(lv)] + \dots\end{aligned} \quad \dots\dots(5)$$

$$\begin{aligned}d_6^{-1} &= 4\epsilon_q^2(\epsilon_q + \epsilon_{q_1} + \epsilon_2)^{-1}(\epsilon_q + \epsilon_{q_1} - \epsilon_1)^{-1} \\ &= 1 + \frac{1}{2}xz[\theta_1 - \theta_2 + 2(lv)] + \dots\end{aligned} \quad \dots\dots(6)$$

*Additional Processes.*

Apart from these processes there are other ways in which a charged meson can decay into a lighter charged meson and a photon.

<i>Process</i>	<i>Matrix Element</i>	
$M^+(0) \rightarrow M^+(-p) + \gamma(p)$		} \dots\dots(7)
$M^+(-p) \rightarrow P^+(q_1) + N^-(-q)$	$a^*(q_1)X'b(-q)$	
$P^+(q_1) + N^-(-q) \rightarrow m^+(-p)$	$b^*(-q)Za(q_1)$	

Similar to (7) but with last two processes interchanged. \dots\dots(8)

$0 \rightarrow P^-(-q_1) + N^+(q) + m^+(-p)$	$a^*(q)Zb(-q_1)$	} \dots\dots(9)
$M^+(0) \rightarrow M^+(-p) + \gamma(p)$		
$M^+(-p) + P^-(-q_1) + N^+(q) \rightarrow 0$	$b^*(-q_1)X'a(q)$	

$0 \rightarrow P^-(-q) + N^+(q) + m^+(0)$	$a^*(q)Z'b(-q)$	} \dots\dots(10)
$m^+(0) \rightarrow m^+(-p) + \gamma(p)$		
$M^+(0) + P^-(-q) + N^+(q) \rightarrow 0$	$b^*(-q)Xa(q)$	

$0 \rightarrow P^-(-q) + N^+(q) + m^+(0)$	$a^*(q)Z'b(-q)$	} \dots\dots(11)
$M^+(0) + P^-(-q) + N^+(q) \rightarrow 0$	$b^*(-q)Xa(q)$	
$m^+(0) \rightarrow m^+(-p) + \gamma(p)$		

Similar to (11) but with first two processes interchanged. \dots\dots(12)

The expressions  $X'$ ,  $X$ ,  $Z'$ ,  $Z$  are essentially the same as for processes (1), \dots (6).  $X'$  means  $X$  generalized for a moving meson and  $Z'$  means  $Z$  specialized for a meson at rest.

There are still four more processes by means of which the transition can take place

$0 \rightarrow P^-(-q) + N^+(q) + m^+(-p) + \gamma(p)$	$a^*(q)Z''b(-q)$	} \dots\dots(13)
$M^+(0) + P^-(-q) + N^+(q) \rightarrow 0$	$b^*(-q)Xa(q)$	

$M^+(0) \rightarrow P^+(q) + N^-(-q)$	$a^*(q)Xb(-q)$	} \dots\dots(14)
$P^+(q) + N^-(-q) \rightarrow m^+(-p) + \gamma(p)$	$b^*(-q)Z''a(q)$	

$M^+(0) \rightarrow P^+(q_1) + N^-(-q) + \gamma(p)$	$a^*(q_1)X''b(-q)$	} \dots\dots(15)
$P^+(q_1) + N^-(-q) \rightarrow m^+(-p)$	$b^*(-q)Za(q_1)$	

$0 \rightarrow P^-(-q_1) + N^+(q) + m^+(-p)$	$a^*(q)Zb(-q_1)$	} \dots\dots(16)
$P^-(-q_1) + N^+(q) + M^+(0) \rightarrow \gamma(p)$	$b^*(-q_1)X''a(q)$	

where  $X$  and  $Z$  are the same as for (1) \dots (6), but  $X''$  and  $Z''$  are derived from the interaction term in the Hamiltonian by replacing

$$\begin{aligned} \nabla U & \text{ by } \{\nabla - (ie/\hbar c)\mathbf{A}\}U, \\ \nabla U^* & \text{ by } \{\nabla + (ie/\hbar c)\mathbf{A}\}U^*, \end{aligned}$$

where  $\mathbf{A}$  is the electromagnetic vector potential.

This alteration can only affect the  $f$ -terms and the matrix elements are

$$\begin{aligned} Z_s'' &= ie(f_2/\mu_2)(\alpha e), \\ Z_{ps}'' &= ie(f_2/\mu_2)(\sigma e), \\ Z_{lv}'' &= -e(f_2/\mu_2)(\mu_0/\mu_2)\beta\{\theta_1(\alpha e) + i\theta_2\sigma(e_\Lambda r)\}, \\ Z_{tv}'' &= ie(f_2/\mu_2)\beta\sigma(e_\Lambda e_2), \\ Z_{lpv}'' &= -e(f_2/\mu_2)(\mu_0/\mu_2)\beta\{\theta_2\alpha(e_\Lambda r) - i\theta_1(\sigma e)\}, \\ Z_{tpv}'' &= e(f_2/\mu_2)\beta\alpha(e_\Lambda e_2). \end{aligned}$$

To get  $X''$ , which refers to the absorption of a meson, the only change is the sign and the replacement of  $f_2$  by  $f_0$  etc.

The matrix elements for the individual processes are as follows:

$$\begin{aligned} n_7' &= \frac{1}{4}\text{Sp}X'(1-E)Z(1+E_1), \\ n_8' &= \frac{1}{4}\text{Sp}X'(1+E)Z(1-E_1), \\ n_9' &= \frac{1}{4}\text{Sp}X'(1+E)Z(1-E_1), \\ n_{10}' &= \frac{1}{4}\text{Sp}X(1+E)Z'(1-E), \\ n_{11}' &= \frac{1}{4}\text{Sp}X(1+E)Z'(1-E), \\ n_{12}' &= \frac{1}{4}\text{Sp}X(1-E)Z'(1+E), \\ n_{13}' &= \frac{1}{4}\text{Sp}X(1+E)Z''(1-E), \\ n_{14}' &= \frac{1}{4}\text{Sp}X(1-E)Z''(1+E), \\ n_{15}' &= \frac{1}{4}\text{Sp}X''(1-E)Z(1+E_1), \\ n_{16}' &= \frac{1}{4}\text{Sp}X''(1+E)Z(1-E_1), \end{aligned}$$

where  $n_7' \dots n_{12}'$  must still be multiplied by the matrix element of the process in which a meson emits a photon to get  $n_7 \dots n_{12}$ . Since this matrix element vanishes for a scalar or pseudoscalar meson finally or initially at rest, some of these special cases need not be calculated in these special cases.

The contribution from processes (7), (8) and (9) is

$$C_{789} = (1/2\epsilon_q) \left\{ [1/\mu_0(\theta_3 - \theta_2)][n_7/d_7 + n_8/d_8] + (1/2\epsilon_q)(n_9/d_9) \right\},$$

where  $\theta_3 = (\mu_0^2 + p^2)^{1/2}/\mu_0$   $\theta_2' = \mu_2/\mu_0$

$$\begin{aligned} d_7^{-1} &= 2\epsilon_q(\epsilon_q + \epsilon_{q_1} - \epsilon_2)^{-1} \\ &= 1 + \frac{1}{2}xz[\theta_2 + (lv)] + \dots \end{aligned}$$

$$\begin{aligned} d_8^{-1} &= 2\epsilon_q(\epsilon_q + \epsilon_{q_1} + \theta_3\mu_0)^{-1} \\ &= 1 + \frac{1}{2}xz[-\theta_3 + (lv)] + \dots \end{aligned}$$

$$\begin{aligned} d_9^{-1} &= 4\epsilon_q^2(\epsilon_q + \epsilon_{q_1} + \epsilon_2)^{-1}(\epsilon_q + \epsilon_{q_1} + \theta_3\mu_0)^{-1} \\ &= 1 + \frac{1}{2}xz[-\theta_2 - \theta_3 + 2(lv)] + \dots \end{aligned}$$

Similarly

$$C_{10,11,12} = (1/2\epsilon_q) \left\{ (1/2\epsilon_q)(n_{10}/d_{10}) - [1/\mu_0(1 - \theta_2')][n_{11}/d_{11} + n_{12}/d_{12}] \right\},$$

where  $d_{10}^{-1} = 4\epsilon_q^2(2\epsilon_q + \mu_2)^{-1}(2\epsilon_q + \mu_0)^{-1}$   
 $= 1 + \frac{1}{2}xz(-1 - \theta_2') + \dots$

$$d_{11}^{-1} = 2\epsilon_q(2\epsilon_q + \mu_2)^{-1} = 1 - \frac{1}{2}xz\theta_2' + \dots$$

$$d_{12}^{-1} = 2\epsilon_q(2\epsilon_q - \mu_0)^{-1} = 1 + \frac{1}{2}xz + \dots$$



Similarly  $C_{13,14,15,16} = -(1/2\epsilon_q) \sum_{i=13}^{16} (n_i/d_i),$

where 
$$\begin{aligned} d_{13}^{-1} &= 2\epsilon_q(2\epsilon_q + \mu_0)^{-1} = 1 - \frac{1}{2}xz + \dots \\ d_{14}^{-1} &= 2\epsilon_q(2\epsilon_q - \mu_0)^{-1} = 1 + \frac{1}{2}xz + \dots \\ d_{15}^{-1} &= 2\epsilon_q(\epsilon_q + \epsilon_{q_1} - \epsilon_2)^{-1} = 1 + \frac{1}{2}xz[\theta_2 + (lv)] + \dots \\ d_{16}^{-1} &= 2\epsilon_q(\epsilon_q + \epsilon_{q_1} + \epsilon_2)^{-1} = 1 + \frac{1}{2}xz[-\theta_2 + (lv)] + \dots \end{aligned}$$

The reciprocal of the lifetime of the meson is given by

$$\tau^{-1} = (2\pi/\hbar) |H|^2 \rho$$

where

$$H = (2\pi/L^3)^{3/2} (\hbar c L)^3 \left[ (\epsilon_0 \epsilon_1 \epsilon_2)^{1/2} (2\pi \hbar c)^3 \right] \int d^3 q \{ C_1 \dots C_6 + C_7 \dots C_{12} + C_{13} \dots C_{16} \}$$

and  $\rho$  = density of final states per unit energy.

#### § 4. ADEQUACY OF THE LEADING TERM

The series obtained for  $\Sigma(n_i/d_i)$  by expanding the numerators and denominators in a power series of  $x$  is certainly convergent.

It will be shown that only the leading term is important, even if  $x = \frac{1}{2}$ .

Notice that

$$\mathbf{v}_1(\mathbf{v}, z) = -\mathbf{v}_1(-\mathbf{v}, -z),$$

$$z_1(\mathbf{v}, z) = -z_1(-\mathbf{v}, -z).$$

Anticipate the form

$$n = (z_1/z)A + (1 \pm z_1/z)B + xz_1C,$$

which will be derived in the next section. Suppose the expressions  $X$  and  $Z$  from which  $n$  is derived contain only one type of Dirac matrix like  $\beta(\alpha p)$  and not a linear combination like  $\beta(\alpha p) + \lambda\beta(\sigma k)$ . Then  $A$  and  $B$  contain the same vectors  $\mathbf{v}, \mathbf{e}_i, \dots$  and therefore  $(z_1/z)A$  and  $(1 \pm z_1/z)B$  behave similarly under a change in sign of  $\mathbf{v}$  and  $z$ . From the above this implies also a change in sign of  $\mathbf{v}_1$  and  $z_1$ . Because of the additional factor  $(\alpha r)$  in the spur represented by  $C$ , this expression contains one  $\mathbf{v}$  more (or less) than either  $A$  or  $B$ .

Hence  $n(\mathbf{v}, z) = \pm n(-\mathbf{v}, -z)$ . From the series for  $z_1$  follows that in the expansion

$$n = {}^0n + x^1n + \dots$$

consecutive terms behave differently towards a change in sign of  $\mathbf{v}$ . The same is true for  $d_1^{-1} \pm d_4^{-1}$ . If  $n_1(\mathbf{v}, z) = n_1(-\mathbf{v}, -z)$  then

$$n_4(\mathbf{v}, z) = -n_1(-\mathbf{v}, -z) = -n_1(\mathbf{v}, z),$$

hence  $n_1 d_1^{-1} + n_4 d_4^{-1} = n_1(d_1^{-1} - d_4^{-1})$  which, after integration over the directions of  $\mathbf{v}$ , results in an odd or even series of  $x$ . Closer investigation shows that the second term in the series for  $n_1 d_1^{-1} + n_4 d_4^{-1}$  is smaller than the leading term by about a factor  $\frac{1}{4}x^2 z^2 \theta_1^2 < 4^{-3} z^2$  ( $\theta_1 < \frac{1}{2}, 0 \leq z \leq 1$ ).

The same argument applies to the groups (2, 3), (5, 6), (7, 8, 9), (10, 11, 12), (13, 14, 15, 16). This result holds also for those linear combinations of different types of matrices used in this paper.

*Example.*

Before calculating the matrix element of a particular decay process it is convenient to eliminate  $\mathbf{v}_1$  from the calculation. The equation

$$\mathbf{v}_1 = (z_1/z)\mathbf{v} - xz_1\mathbf{l}$$

is invariant under the various changes in sign of  $\mathbf{v}, z, \mathbf{v}_1$  and  $z_1$ , so that after elimination of  $\mathbf{v}_1$  the calculation of  $n_1$  and  $n_6$  is still sufficient to determine  $n_2, n_3, n_4, n_5$  also.

$$(\alpha v_1) + \beta z_1 = (z_1/z)\{(\alpha v) + \beta z\} - xz_1(\alpha l).$$

Hence  $1 + E_1 = (z_1/z)(1 + E) + 1 - (z_1/z) - xz_1(\alpha l).$

Since  $Y = (\alpha e)$  and  $(1 + E)(\alpha e)(1 + E) = 2(ev)(1 + E)$ , therefore

$$\begin{aligned} n_1 &= \frac{1}{4}(ev)(z_1/z)\text{Sp}Z(1 + E)X(1 - E) \\ &\quad + \frac{1}{8}(1 - z_1/z)\text{Sp}Z(\alpha e)(1 + E)X(1 - E) \\ &\quad - \frac{1}{8}xz_1\text{Sp}Z(\alpha l)(\alpha e)(1 + E)X(1 - E). \end{aligned}$$

Since  $(1 - E)(\alpha e)(1 + E) = 2(\alpha e)(1 + E) - 2(ev)(1 + E)$ ,

therefore 
$$\begin{aligned} n_6 &= -\frac{1}{4}(ev)(z_1/z)\text{Sp}Z(1 + E)X(1 + E) \\ &\quad + \frac{1}{8}(1 + z_1/z)\text{Sp}Z(\alpha e)(1 + E)X(1 + E) \\ &\quad + \frac{1}{8}xz_1\text{Sp}Z(\alpha l)(\alpha e)(1 + E)X(1 + E). \end{aligned}$$

It is evident, from the relationship between  $n_i$  ( $i = 1 \dots 4$ ), that  $\sum_{i=1}^4 n_i = z_1 f(\mathbf{v}, z)$  where  $f(-\mathbf{v}, -z) = f(\mathbf{v}, z)$ . Similarly  $n_5 + n_6 = F(z_1, \mathbf{v}, z)$ , where

$$F(-z_1, -\mathbf{v}, -z) = -F(z, \mathbf{v}, z).$$

Consider now the transition

$$M_V^+(0) \rightarrow m_{ps}^+(-p) + \gamma(p).$$

A vector meson at rest decays into a pseudoscalar meson, momentum  $-\mathbf{p}/c$  and a photon with momentum  $\mathbf{p}/c$ .

To calculate the term in  $eg_0g_2$  put

$$X = (\alpha e_0), \quad Z = i\beta\gamma_5.$$

$$\text{Sp}Z(1 + E)X(1 - E) = 0,$$

$$\text{Sp}Z(\alpha e)(1 + E)X(1 - E) = 0,$$

$$\begin{aligned} \text{Sp}Z(\alpha l)(\alpha e)(1 + E)X(1 - E) &= -2iz\text{Sp}\gamma_5(\alpha l)(\alpha e)(\alpha e_0) \\ &= 8z(e_\lambda e_0)l. \end{aligned}$$

Thus  $n_1 = -xz z_1(e_\lambda e_0)l$  leading to  $-\sum_{i=1}^4 n_i = 0$ .

However  $\sum_{i=1}^4 n_i/d_i = n_1\{d_1^{-1} + d_2^{-1} - d_3^{-1} - d_4^{-1}\} = 3xz n_1$ .

Similarly  $n_6 = 0 = n_5$ . Thus neglecting higher powers of  $x$

$$\sum_{i=1}^6 n_i/d_i = -3x^2(e_\lambda e_0)r\theta_1 z^3.$$

The  $ef_0f_2$ -term was calculated by Finkelstein and is of order  $x^0$  (see Table).

It can easily be seen that the additional processes do not contribute.

$$n'_7 = \frac{1}{4} \text{Sp} X' (1 - E) Z (1 + E_1),$$

where  $X' = (\alpha e'_0)$ ,  $Z = i\beta\gamma_5$ , if in the intermediate state the heavy meson is a transverse one. Because of the  $\gamma_5$  in  $Z$

$$n'_7 = \text{const.} (e'_{0\Lambda} v) v = 0 = n'_8 = n'_9.$$

Similarly if the heavy meson is longitudinal in the intermediate state.

To get  $n_{10}, n_{11}, n_{12}$ , the expressions  $n'_{10}, n'_{11}, n'_{12}$  must be multiplied by a factor which vanishes if the secondary meson is pseudoscalar.

Processes (13) ... (16) only contribute to  $f$ -terms. Thus

$$H = (2\pi/L^3 \mu_0 \epsilon_1 \epsilon_2)^{\frac{1}{2}} x^2 (e_{0\Lambda} e) r \theta_1 (M/4\pi) e g_0 g_2,$$

$$p = 4\pi \mu_0^2 \theta_1^3 L^3 / (2\pi \hbar c)^3,$$

giving

$$\tau^{-1} = \{(e_{0\Lambda} e) r\}^2 \{x^3 \theta_1^4 M / (8\pi^2 \theta_2 \hbar)\} \{e^2 g_0^2 g_2^2 / (\hbar c)^3\}.$$

Summing over the two directions for  $\mathbf{e}$  and averaging over the three directions of  $\mathbf{e}_0$ ,

$$\tau^{-1} = x^3 \theta_1^4 M e^2 g_0^2 g_2^2 / \{12\pi^2 \hbar \theta_2 (\hbar c)^3\} \simeq 10^{12}$$

for the parameters used by Finkelstein.

The picture presented here is however less attractive if it is required to describe the decay of mesons of mass about 900 electron masses.

To get an idea of the order of magnitude in such a case, put  $x = \frac{1}{2}$ ,  $\theta_1 = \frac{1}{4}$ ,  $\theta_2 = \frac{3}{4}$ , giving  $\tau^{-1} = 6 \times 10^{16} g_0^2 g_2^2 / (\hbar c)^2$ . The lifetime  $\tau = 10^{-9}$  sec. would therefore require  $g_0^2 g_2^2 / (\hbar c)^2 \simeq 10^{-8}$ . Since the Berkeley experiments seem to confirm that  $g_0^2 / \hbar c$  is not very small and probably about 1/10, it would follow that  $g_2^2 / \hbar c$  would have to be less than  $10^{-7}$ , which seems incompatible with a reasonable cross section for creation of  $\tau$ -mesons unless some quite new process comes into play.

### Table.

The matrix elements for all choices of initial and final mesons are tabulated below. The scalar, pseudoscalar, vector and pseudovector mesons are denoted by s, ps, v, pv, respectively. Longitudinal and transverse vector mesons are distinguished by lv and tv respectively, similarly for pseudovector mesons. The symbol  $(i, j)$  denotes the group of four matrix elements containing  $g_i g_j$ ,  $g_i f_j$ ,  $f_i g_j$ ,  $f_i f_j$  (in this order) in the decay process where  $i$  is the initial, and  $j$  the final meson. The second column contains the total matrix element for the first six processes, while the contribution from the rest appears in the third column. The entry  $q^2$  in this column denotes a quadratic divergence. The expressions containing a factor  $z^3$  are finite when integrated over  $q$ , but those containing only  $z$  are logarithmic divergent.

For the sake of consistency all divergences will be ignored. This prescription will in some cases require the calculation of new leading terms.



Process	$4\epsilon_q^2 \int C_1 \dots \frac{d\omega}{4\pi}$	$4\epsilon_q^2 \int C_7 \dots \frac{d\omega}{4\pi}$
(s, tpv)	$-(i/3)x^2(e_\Lambda e_2)l\{3+4\theta_1-10\theta_1 z^2\}z^3$ $2x(e_\Lambda e_2)l(\mu_0/\mu_2)\{1-(1+\theta_1)z^2\}z$ $2x(e_\Lambda e_2)lz^3$ $4i(e_\Lambda e_2)l(\mu_0/\mu_2)z$	$2x(e_\Lambda e_2)l\theta_2 z^3$
(s, tv)	$4(ee_2)z^3$ $2x(ee_2)(\mu_0/\mu_2)\{\theta_1+(1-4\theta_1+\theta_1^2)z^2\}z$ $(2i/3)x(ee_2)(\theta_2-\theta_1)(z^2+2)z$ $4i(ee_2)(\epsilon_2/\mu_2)z$	$q^2$ $4i(ee_2)(\mu_0/\mu_2)(\theta_2-\theta_1)z$
(ps, tpv)	$-4i(ee_2)z$ $-2x(ee_2)(\mu_0/\mu_2)\{\theta_1+(1-\theta_1+\theta_1^2)z^2\}z$ $(2i/3)x(ee_2)\{2(1-2\theta_1)+(1+7\theta_1)z^2\}z$ $4(ee_2)(\epsilon_2/\mu_2)z^3$	$q^2$ $-4(ee_2)(\mu_0/\mu_2)\theta_1^2 z^3$
(ps, tv)	$3x^2(e_\Lambda e_2)lz^3$ $2x(e_\Lambda e_2)l(\mu_0/\mu_2)\{1+(1+\theta_2)z^2\}z$ $-4x(e_\Lambda e_2)lz^3$ $-4(e_\Lambda e_2)l(\mu_0/\mu_2)z^3$	$2x(e_\Lambda e_2)l\theta_2 z^3$ $4(e_\Lambda e_2)l(\epsilon_2/\mu_2)z^3$
(v, s)	$4(ee_0)z^3$ $-(2i/3)x(ee_0)(\mu_0/\mu_2)\{2+(1+\theta_1^2)z^2+2\theta_1^2 z^4\}z$ $2x(ee_0)\{-\theta_1+(1+2\theta_1)z^2\}z$ $-4i(ee_0)(\epsilon_2/\mu_2)z$	$2(ee_0)a\theta_1^2\theta_3 z^3$ $q^2$ $x(ee_0)a\theta_1^2\theta_2 z^3$ $-4i(ee_0)(\mu_0/\mu_2)z$
(v, ps)	$-3x^2(e_\Lambda e_0)lz^3$ $2x(e_\Lambda e_0)l(\mu_0/\mu_2)(2+\theta_2)z^3$ $-2x(e_\Lambda e_0)l(1+z^2)z$ $4(e_\Lambda e_0)l(\mu_0/\mu_2)z^3$	$2x(e_\Lambda e_0)l\theta_2 z^3$ $-4(e_\Lambda e_0)l(\epsilon_2/\mu_2)z^3$ *
(v, tv)	$(4/3)x(e_0l)(ee_2)\{2+2z^2-z^4\}z$ $4(e_0l)(ee_2)(\mu_0/\mu_2)z$ $3x^2(e_0l)(ee_2)z^3$ $(2/3)x(e_0l)(ee_2)(\mu_0/\mu_2)\{1+(6-\theta_1)z^2+2\theta_2 z^4\}z$	$q^2$ $2(e_0l)(ee_2)\{-(\mu_0/\mu_2)a(\theta_2-\theta_1)+b\}z$ $2(e_0l)(ee_2)\{a(\theta_1^2-\theta_2\theta_3)+b-2\}z$ $q^2$
(v, lv)	$(2/3)x(ee_0)\theta_1(\mu_0/\mu_2)\{4+(3-\theta_1)z^2+2\theta_2 z^4\}z$ $3x^2(ee_0)\theta_1 z^3$ $4(ee_0)\theta_1(\mu_0/\mu_2)z$ $(2/3)x(ee_0)\theta_1\{1+7z^2-2z^4\}z$	$q^2$ $2(ee_0)\{a(\theta_1^2-\theta_2\theta_3)+b-2(\mu_0^2/\mu_2^2)\}\theta_1$ $2(ee_0)\{a(\theta_1-\theta_2)(\mu_0/\mu_2)+b\}\theta_1 z$ $q^2$
(v, tpv)	$2ix(e_0\Lambda e)e_2(1+\theta_1)z^3$ $4(e_0\Lambda e)e_2(\epsilon_2/\mu_2)z$ $4i(e_0\Lambda e)e_2 z^3$ $(2/3)x(e_0l)(e_2\Lambda e)l(\mu_0/\mu_2)\{1-5z^2-2z^4\}z +$ $(2/3)x(e_0\Lambda e)e_2(\epsilon_2/\mu_2)\{2-\theta_1+(1+4\theta_1)z^2\}z$	$i(e_\Lambda e_2)l(e_0l)a\theta_2 z^3$ $4(e_0\Lambda e)e_2(\mu_0/\mu_2)z$ $2i(e_\Lambda e_2)l(e_0l)a\theta_3 z^3$ $q^2$
(v, lpv)	$2ix(e_\Lambda e_0)r(\mu_0/\mu_2)(1+\theta_1^2)z^3$ $4(e_\Lambda e_0)r z$ $4i(e_\Lambda e_0)r(\epsilon_2/\mu_2)z^3$ $(2/3)x(e_\Lambda e_0)r\{2-\theta_1+(1+4\theta_1)z^2\}z$	$4(e_\Lambda e_0)r(\mu_0\epsilon_2/\mu_2^2)z$ $-4i(e_\Lambda e_0)r\theta_1^2(\mu_0/\mu_2)z^3$ $q^2$

\* This contribution cannot be neglected as Finkelstein suggested. Its inclusion lengthens the lifetime by a factor  $(\epsilon_1/\mu_0)^{-2} \simeq 10$ .

Process	$4\epsilon_q^2 \int C_1 \dots 6 \frac{d\omega}{4\pi}$	$4\epsilon_q^2 \int C_7 \dots 16 \frac{d\omega}{4\pi}$
(pv, s)	$(i/3)x^2(e_\Lambda e_0)l\{(3+4\theta_1)+10\theta_1 z^2\}z^3$ $-2x(e_\Lambda e_0)l\theta_1(\mu_0/\mu_2)z^3$ $2x(e_\Lambda e_0)l(-1-2z^2)z$ $4i(e_\Lambda e_0)l(\mu_0/\mu_2)z$	$2x(e_\Lambda e_0)l\theta_2 z^3$
(pr, ps)	$4i(ee_0)z$ $-(2i/3)z(ee_0)(\mu_0/\mu_2)\{2+(1-9\theta_1+\theta_1^2)x^2+2\theta_1^2 z^4\}z$ $2x(ee_0)\{\theta_1-\theta_2 z^2\}z$ $4(ee_0)(\epsilon_2/\mu_2)z^3$	$2i(ee_0)(\theta_1^2/\theta_2)z$ $q^2$ $-2x(ee_0)a\theta_1^2\theta_2 z^3$ $2(ee_0)(\epsilon_2/\mu_2)a\theta_1^2 z^3$
(pv, tv)	$2ix(e_\Lambda e_0)e_2(2\theta_1-1)z^3$ $4i(e_\Lambda e_0)e_2(\epsilon_2/\mu_2)z^3$ $4(e_\Lambda e_0)e_2 z$ $(2/3)x(e_0 l)(e_\Lambda e_2)l(\mu_0/\mu_2)\{1+4z^2-2z^4\}z+$ $(2/3)x(e_\Lambda e_0)e_2(\epsilon_2/\mu_2)\{2-\theta_1+(1-5\theta_1)z^2\}z$	$-ix(e_\Lambda e_2)l(e_0 l)a\theta_2 z^3$ $2i(e_\Lambda e_2)l(e_0 l)(\epsilon_2/\mu_2)z^3$ $\{-2\theta_2(e_\Lambda e_2)l(e_0 l)+4(e_\Lambda e_0)e_2\theta_2\}z$ $q^2$
(pv, lv)	$2ix(e_\Lambda e_0)r(\mu_0/\mu_2)(1-3\theta_1+\theta_1^2)z^3$ $4i(e_\Lambda e_0)r z^3$ $-4(e_\Lambda e_0)r(\epsilon_2/\mu_2)z$ $(2/3)x(e_\Lambda e_0)r\{-2-\theta_1+(-1+5\theta_1)z^2\}z$	$-4(e_\Lambda e_0)r(\mu_0/\mu_2)(\theta_2-\theta_1)z$ $q^2$
(pv, tpv)	$(2/3)x(ee_2)(e_0 l)\{4-5z^2-2z^4\}z$ $-4i(ee_2)(e_0 l)(\mu_0/\mu_2)z^3$ $-(i/3)x^2(ee_2)(e_0 l)\{3+4\theta_1-10\theta_1 z^2\}z^3$ $(2/3)x(ee_2)(e_0 l)(\mu_0/\mu_2)\{1-(3+\theta_1)z^2+2\theta_2 z^4\}z$	$q^2$ $-2i(ee_2)(e_0 l)(\mu_0/\mu_2)a\theta_1^2 z^3$ $2i(ee_2)(e_0 l)\{a\theta_1^2 z^2-(2/3)(1-2z^2)\}z$ $q^2$
(pv, lpv)	$(2/3)x(ee_0)(\epsilon_1/\mu_2)\{3-\theta_1-5z^2+2\theta_2 z^4\}z$ $+(i/3)x^2(ee_0)\theta_1\{3+4\theta_1-10\theta_1 z^2\}z^3$ $4i(ee_0)\theta_1 z^3$ $+(2/3)x(ee_0)\theta_1\{1-2z^2-2z^4\}z$	$q^2$ $-2i(ee_0)a\theta_1^2 z^3$ $2i(ee_0)a\theta_1^2(\mu_0/\mu_2)z^3$ $q^2$

The notation is as follows:

$\mu_i$ =meson rest energy, where the suffixes 0 and 2 refer to the initial and final mesons respectively.

$\epsilon_2$ =energy of final meson.

$p=e_1$ =energy of photon.

$\mathbf{e}$ =meson polarization vector ( $i=0, 2$ ).

$\mathbf{e}$ =photon polarization vector.

$\mathbf{r}$ =unit propagation vector of photon.

$\theta_1=p/\mu_0$ ,  $\theta_2=\epsilon_2/\mu_0$ ,  $\theta'_2=\mu_2/\mu_0$ ,  $\theta_3=(\mu_0^2+p^2)^{1/2}/\mu_0$ .

$\mathbf{l}=\theta_1\mathbf{r}$ .

$M$ =rest energy of nucleon.

$\epsilon_q=(M^2+q^2)^{1/2}$ .

$\mathbf{q}/c$ =momentum of nucleon in intermediate state.

$x=\mu_0/M$ .

$z=M/\epsilon_q$ .

$a=\{\theta_3(\theta_3-\theta_2)\}^{-1}$ ,  $b=\{\theta'_2(1-\theta'_2)\}^{-1}$ ;  $d^3q=q^2 dq d\omega$ .

## § 5. CONCLUSION

From the table it is clear that for  $x=\frac{1}{2}$  all the matrix elements are roughly of the same order of magnitude. Recalling the result of the example it must be concluded that the decay process  $\tau^+ \rightarrow \pi^+ + \gamma$  makes the  $\tau$ -meson too short-lived to agree even approximately with observation.

The situation is however quite different if both the initial and final mesons have zero spin. In this case the emission of a positron-electron pair or of two photons must be considered. If, in particular, one of the two mesons is scalar and the other pseudoscalar, then the production of a pair is forbidden. A calculation, which will be published in a later paper, of the probability of emitting two photons leads in this case to a lifetime of the order of  $\mathcal{G} \times 10^{-12}$  sec. where  $\mathcal{G}$  is the reciprocal of the product of the dimensionless coupling parameters of the two meson fields. This is no longer in direct disagreement with experimental evidence.

Hence the conclusion is that either  $\tau$ -mesons and  $\pi$ -mesons have spin zero, or the nucleon- $\tau$ -meson interaction is different from that represented by the scheme

$$P \rightarrow N + \tau^+,$$

or the usual perturbation theory is not adequate to describe these processes.

#### ACKNOWLEDGMENTS

It is a pleasure to thank Professor R. E. Peierls for suggesting this investigation and for his advice and criticism.

This work was carried out while the author was holding a scholarship from the University of Stellenbosch, S. Africa.

#### REFERENCES

- FINKELSTEIN, R. J., 1947, *Phys. Rev.*, **72**, 415.  
 KEMMER, N., 1938, *Proc. Roy. Soc. A*, **166**, 127.  
 POWELL, C. F., with others, 1949, *Nature, Lond.*, **163**, 47, 82.



## Excited Electronic Levels in Conjugated Molecules— III: Energy States of Naphthalene\*

By J. JACOBS

Wheatstone Physics Laboratory, King's College, London

*Communicated by C. A. Coulson; MS. received 27th May 1949*

**ABSTRACT.** The electronic states of naphthalene are determined using antisymmetrized molecular orbitals, which are based on wave functions given by the simple molecular orbital theory. This method allows the electronic interaction term to be included explicitly in the Hamiltonian for the system. A clear distinction is made between electronic configurations determined with these wave functions and the actual states of the molecule: states arise from a superposition of configurations of the same symmetry. The ground state becomes considerably stabilized by this configurational interaction, to which even highly excited levels contribute. Calculated energy values for some of the lower transitions agree well with ultra-violet spectral data, as do the newly derived oscillator strengths. A tentative assignment is made regarding the polarization of the electronic transitions in the region of  $30,000\text{--}55,000\text{ cm}^{-1}$ .

### § 1. INTRODUCTION

THERE are two main theories known for the theoretical discussion of molecular structure—the valence bond treatment (Heitler, London, Pauling) and the method of molecular orbitals (Hund, Mulliken). Reasonably good results can be obtained with either method for ground state phenomena; but for the interpretation of ultra-violet spectra—involving electronically excited states in relation to the ground state—both treatments are inadequate. Particularly in the polyacenes the two methods lead to different conclusions, neither of which can be correlated satisfactorily with experimental data. Because of this disagreement it seemed worth while to re-examine the method of molecular orbitals and to extend it; this has been done with reference to the naphthalene molecule.

### § 2. METHOD OF MOLECULAR ORBITALS

Our discussion of the molecular orbital (m.o.) theory falls into three stages: (a) the simplest form in which all electronic repulsion is averaged yields the basic m.o. wave functions and levels; (b) inclusion of the electron repulsion term in the potential energy expression leads to individual configurations; (c) configurational interaction gives the states of the molecule. We reserve the term *state* for the final description of the molecule, whereas any allotment of electrons to the available m.o. levels used in (b) is referred to as a *configuration*.

The first stage deals with the method as developed chiefly by Lennard-Jones and Coulson (1939), who applied it to hydrocarbons. The fundamental assumption is that electronic interaction can be averaged over the whole molecule to give a self-consistent field. This means that the effective Hamiltonian contains one-electron functions only and may be written  $\mathcal{H} = \sum_{\nu} H(\nu)$ , where  $H(\nu)$  is the effective Hamiltonian for electron  $\nu$ . Such an approximation enables us to use one-electron wave functions  $\phi_i$  and to associate with each of them a molecular orbital energy  $\epsilon_i$ . The energy of a configuration of the whole molecule is then simply the sum of the energies  $\epsilon_i$  of the occupied m.o. levels. For convenience only  $\pi$ -electrons are usually considered.

\* For parts I and II see C. A. Coulson, *Proc. Phys. Soc.*, 1948, **60**, 257, and H. C. Longuet-Higgins, *Proc. Phys. Soc.*, 1948, **60**, 270.

Coulson (1948) has published detailed calculations for the polyacenes. As these will be required in our later work (stages (b) and (c) above) it will be necessary to begin by summarizing his results. In these molecules the nuclei are arranged symmetrically with respect to the short and long axes. Calling these the  $y$  and  $z$  axes respectively, we can group the nuclei into sets each of which is symmetrical or antisymmetrical to reflection in the planes perpendicular to the plane of the molecule through the  $y$  and  $z$  axes.

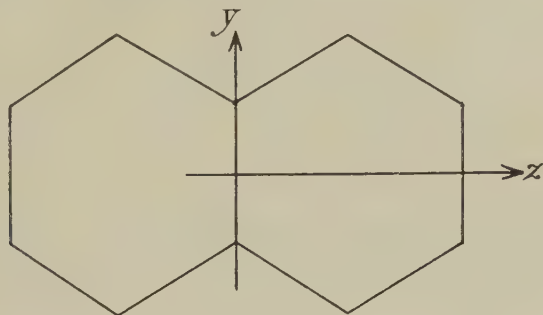


Figure 1.

M.o. wave functions are built up as linear combinations of atomic orbitals at each carbon nucleus  $\phi_i = \sum_r c_r^i \psi_r$ , where  $\phi_i$  = wave function of the  $i$ th m.o.,  $\psi_r$  = atomic  $2p_z$  wave function at carbon atom  $r$ ,  $(c_r^i)^2$  = weight with which  $\psi_r$  enters the  $i$ th m.o. These wave functions themselves must bear the symmetry characteristics of the sets of carbon atoms. Thus four types of wave functions can be written down, which we denote by  $S_z S_y$ ,  $S_z A_y$ ,  $A_z S_y$ ,  $A_z A_y$ , where for example  $S_z$  indicates symmetrical behaviour with respect to reflection in the plane through the  $z$  axis, perpendicular to the plane of the molecule, and  $A_z$  indicates antisymmetrical behaviour with respect to this reflection.

In terms of the effective Hamiltonian  $H(\nu)$  and the normalized m.o. wave functions  $\phi_i$  the energy of a m.o. level is determined by

$$\epsilon_i = \int \phi_i^*(\nu) H(\nu) \phi_i(\nu) d\tau_\nu / \int \phi_i^*(\nu) \phi_i(\nu) d\tau_\nu.$$

Minimizing the energy with respect to the coefficients  $c_r^i$  leads to the secular determinant. Because of the symmetry grouping, the secular determinant factorizes into blocks of these symmetry types called  $P, Q, R, S$  by Coulson. The m.o. energies which are derived as the roots of this determinant are therefore denoted by  $P_1 P_2 P_3, Q_1 Q_2, R_1 R_2 R_3, S_1 S_2$ . Coulson gives a diagram of energy levels which were calculated including the overlap integral of the  $2p_z$  atomic orbitals at adjacent carbon atoms. This diagram shows also relations between the energy groups  $P, Q, R, S$ , and both the symmetry character  $S_z S_y$  etc. and their standard group theory description.

$E_0$  is a Coulomb integral considered constant for all carbon atoms.

In the ground state it is assumed that the five lowest orbitals are each completely filled with  $\pi$ -electrons (each orbital then accommodates two  $\pi$ -electrons according to the Pauli principle); it therefore gives rise to a description  $P_1^2 Q_1^2 R_1^2 P_2^2 S_1^2$ .

Similarly the "first excited configuration"—or, more accurately, the configuration which from this diagram appears to be the first excited one and which arises from the elevation of one electron in m.o.  $S_1$  to the lowest unoccupied one,  $Q_2$ —can be described by  $P_1^2 Q_1^2 R_1^2 P_2^2 S_1 Q_2$ .

To determine the symmetry type to which such a configuration belongs one multiplies the symmetries of the electrons forming it; for the ground state having all m.o.'s doubly filled this gives a totally symmetric configuration. In the "first excited configuration" the symmetry is given by  $S_1 \times Q_2$ , i.e.  $A_z A_y \times S_z A_y$ , i.e.  $A_z$ . A complete table of symmetry types of products of two-electron symmetries is given in Coulson's paper in the more usual notation of group theory first introduced into molecular descriptions by Mulliken (1933).

	<i>P</i>	<i>Q</i>	<i>R</i>	<i>S</i>
<i>P</i>	$A_{1g}$	$B_{1u}$	$B_{2u}$	$B_{3g}$
<i>Q</i>	$B_{1u}$	$A_{1g}$	$B_{3g}$	$B_{2u}$
<i>R</i>	$B_{2u}$	$B_{3g}$	$A_{1g}$	$B_{1u}$
<i>S</i>	$B_{3g}$	$B_{2u}$	$B_{1u}$	$A_{1g}$

An electronic transition from the ground state is spectrally allowed if the product of the electron symmetries in the excited state behaves like a  $y$  or  $z$  vector

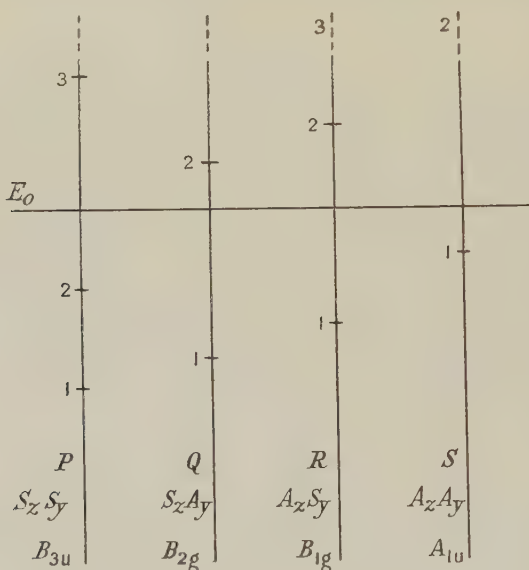


Figure 2.

(symmetry  $A_z$  or  $A_y$  respectively), the direction in which the electric moment vector changes during the excitation, which must be in the plane of the molecule. Above, we deduced  $\bar{y}$  for the first transition; Coulson's results for higher transitions are given in Table 1 together with values for excitation energies.

Table 1. Naphthalene Energies (Coulson's Results)

Symmetry of excited configuration.	$B_{2u}$	$B_{1u}$	$B_{3g}$	$B_{1u}$	$A_{1g}$	$B_{2u}$	$A_{1g}$
Excitation energy in terms of $\gamma$	1.267	1.532	1.715	1.868	1.884	2.133	2.316
Polarization	$y$	$z$	F	$z$	F	$y$	F

F=forbidden.

In this Table  $\gamma$  is a resonance integral between neighbouring carbon atoms and has a value of 3-4 ev.



In all polyacenes the lowest transition appears to be of  $A_{1g} \rightarrow B_{2u}$  type, i.e. polarized in the  $y$  direction. This result is in direct contrast to valence bond calculations (Craig, in course of publication) which predict  $z$  polarization for the first allowed band in each case.

One limitation of this m.o. method is that no account is taken of electron spin so that the calculated energies of excited configurations are really averages of the corresponding energies for singlet and triplet configurations. The averaging of electron repulsion uniformly over the whole molecule is a further approximation that cannot be justified. Particularly for some excited levels the calculations give electronic charge distributions that are not at all even, so that the potential field for each electron is certainly not equivalent at all atoms of the carbon framework.

### § 3. EXPLICIT INTRODUCTION OF ELECTRON REPULSION

Our first step towards a refinement of this simple method is to include electronic repulsion explicitly in the Hamiltonian of the system with the m.o. wave functions obtained above as basis. This necessitates introducing antisymmetrized determinantal wave functions, as was done by Goeppert-Mayer and Sklar (1938) for benzene.

Let the normalized wave functions for the simple m.o. be  $\phi_i = \sum_r c_r^i \psi_r$ . Then the wave function for the configuration is, in the first approximation,  $\Psi_j = N \Pi_i \phi_i$ , where  $i$  is taken over occupied m.o.'s and  $N$  is a normalizing constant.

Instead of these, the wave functions of the type used by Goeppert-Mayer and Sklar for a configuration  $j$  of the molecule are

$$\Psi_j = N \begin{vmatrix} \phi_1(1) \alpha(1) & & & \\ & \phi_1(2) \beta(2) & & \\ & & \ddots & \\ & & & \phi_i(n) \beta(n) \end{vmatrix},$$

where  $n$  electrons occupy m.o.'s  $1, \dots, i$ .  $\alpha(1)$ ,  $\beta(1)$  define the spin function of electron 1 as  $\alpha$ ,  $\beta$  respectively, and  $N$  is a normalizing constant. This can be written in the form

$$\Psi_j = N \sum_P (-1)^P \Pi_i P \phi_i(\mu) \alpha(\mu) \phi_i(\nu) \beta(\nu),$$

where  $P$  is the permutation operator permuting electrons over all available  $\phi_i \alpha$ ,  $\phi_i \beta$  and  $\mu$ ,  $\nu$  represent electrons.

Including the term  $\sum_{\mu, \nu} e^2 / r_{\mu\nu}$  ( $e$  = electronic charge,  $r_{\mu\nu}$  = distance between electrons  $\mu$ ,  $\nu$ ) in the Hamiltonian in their investigation of benzene, these authors obtain fair agreement with experiment. However, all integrals except those for nearest neighbours are neglected and three-or-more centre integrals are omitted altogether (some numerical errors also occur in their integrals (Griffing 1947, Parr and Crawford 1948)). London (1945) has carried out similar calculations for diphenyl and concludes that some of the three-centre integrals may be quite important; they would certainly destroy the good agreement with spectral data for benzene (but see Parr and Crawford). Goeppert-Mayer and Sklar (1938) treat configurations calculated with these antisymmetrized wave functions  $\Psi_j$  as giving the energies of the actual states of the molecule and compare the resulting energy

differences with those observed in the spectrum. The only interactions between configurations which they consider arise from the special degeneracies of benzene that have no parallel in the higher -acenes. However, we find this to be an inadequate description of the energies, and further interactions between some of the calculated configurations can arise in the following way.

#### § 4. CONFIGURATIONAL INTERACTION

Let the wave function  $\Psi_j$  define the electronic configuration  $j$  of the molecule; then the symmetry type of the configuration can be determined from the product of the symmetries of the m.o. wave functions  $\phi$  which form  $\Psi_j$ . Since several such configurations may belong to the same symmetry class (e.g. configurations in which the m.o.'s are each completely filled are all totally symmetric) the possibility of interaction between them must be conceded. Configurations belonging to different symmetry classes or of different multiplicity cannot interact with one another. Parr and Crawford (1948) find in their calculations for ethylene that the configuration in which both  $\pi$ -electrons are excited gives rise to considerable interaction with the lowest configuration, stabilizing it by about 1.3 ev.

This concept of configurational interaction finds confirmation in some recent work carried out in this laboratory on the hydrogen molecule (Coulson and Fischer 1949). For this molecule more accurate values can be obtained as fewer assumptions and approximations have to be made in energy computations. As for the  $\pi$ -electrons in ethylene, there are only two totally symmetric configurations. It is found that even at equilibrium internuclear distance some degree of mixing takes place, which increases for greater nuclear separations. Only after taking configurational interaction into account does the ground state appear as the lowest state of all, with the singly excited state falling below the doubly excited one for all internuclear separations.

The fact that configurational interaction exists indicates that the anti-symmetrized wave functions  $\Psi_j$  are not by themselves suitable for describing the molecule. If we consider a linear combination of  $\Psi_j$ 's including a sufficiently large number of terms we should approximate to the true wave function of a state (Longuet-Higgins 1948). Our procedure is therefore to carry out energy calculations using antisymmetrized wave functions and to obtain the excited configurations and their symmetries. We then allow configurational interaction to take place among the lower levels in the same symmetry class. This third step in the calculations we consider essential as it leads to a sequence of energy levels differing significantly from that obtained in stage two of our method. Only the lower levels in each symmetry class are considered for convenience in computation, although theoretically all levels in one class should be included.

#### § 5. METHOD AND RESULTS FOR NAPHTHALENE

The true Hamiltonian for the system of  $\pi$ -electrons is

$$\mathcal{H} = \sum_{\nu=1}^{10} H(\nu) + \sum_{\nu=1}^{10} T(\nu) + \sum_{\nu < \mu} \frac{e^2}{r_{\nu\mu}},$$

where  $T(\nu)$  is the kinetic energy term for electron  $\nu$  and  $H(\nu)$  is the potential energy of electron  $\nu$  in a field of molecular framework when each C atom is stripped

of its  $\pi$ -electron. This  $H(\nu)$  differs from that introduced in § 1 (first stage of m.o. theory): the earlier  $H(\nu)$  included a term arising from electronic averaging, not found in the present  $H(\nu)$ .

We take  $H(\nu) = \sum_{k=1}^{10} H_k^c(\nu)$  = a sum of contributions from each carbon atom  $k$  which has lost its  $\pi$ -electron. This may be written

$$H_k(\nu) = H_k^c(\nu) - e^2 \int \frac{|\psi_k^{(\lambda)}|^2}{r_{\nu\lambda}} d\tau_\lambda,$$

where  $H_k^c(\nu)$  is the field acting on electron  $\nu$  due to neutral carbon atom  $k$ . We further assume that the potential field around each carbon atom is the same (so that the form of  $H_k^c$  is independent of  $k$ )—an approximation here, but true in the case of benzene, where Goeppert-Mayer and Sklar introduced this substitution.

The wave function for the ground configuration is

$$\Psi_0 = (10!)^{-\frac{1}{2}} \sum_P (-1)^P P \phi_1(1)\alpha(1)\phi_1(2)\beta(2) \dots \phi_5(9)\alpha(9)\phi_5(10)\beta(10),$$

where  $P, \phi, \alpha, \beta$  are defined as above, and its energy is

$$\int \Psi_0^* \mathcal{H} \Psi_0 d\tau,$$

with corresponding expressions for other energies and with functions which are all real. It is found that all energy integrals can be given in terms of three series of expressions,  $\epsilon, \gamma, \delta$ , defined by

$$\begin{aligned} \epsilon_i &= \text{energy of } i\text{th molecular orbital level} \\ &= \int \phi_i^*(\nu) [T(\nu) + H(\nu)] \phi_i(\nu) d\tau_\nu \\ \gamma_{ll'} &= \iint \phi_l^*(\nu) \phi_{l'}^*(\mu) \frac{e^2}{r_{\mu\nu}} \phi_l(\nu) \phi_{l'}(\mu) d\tau_\mu d\tau_\nu \\ \delta_{ll'} &= \iint \phi_l^*(\nu) \phi_{l'}^*(\mu) \frac{e^2}{r_{\mu\nu}} \phi_{l'}(\nu) \phi_l(\mu) d\tau_\mu d\tau_\nu. \end{aligned}$$

Let us use  ${}^r E_n^{pq}$  to denote an energy level of multiplicity  $r$  for which  $n$  electrons have been raised and the m.o. levels concerned with the excitation are  $p \rightarrow q$ .  $n=0$  will represent the ground configuration,  $n=1$  singly excited configurations which alone are usually considered in m.o. calculations. But doubly excited configurations ( $n=2$ ) are also important as they have the symmetry of the ground state and so may give rise to configurational interaction with it. Using the simple diagram of Coulson's paper (Figure 2) and labelling the m.o. levels in order of magnitude, we expect the following excitations to be significant for low-energy differences.

The relation between the notation in Figure 2 and the present enumeration of energy levels is:  $P_1, Q_1, R_1, P_2, S_1, Q_2, R_2$  are equal to 1, 2, 3, 4, 5, 6, 7 respectively;  $p \rightarrow q = 5 \rightarrow 6, 4 \rightarrow 6, 3 \rightarrow 6, 5 \rightarrow 7, 4 \rightarrow 7, \dots$  all of which have been evaluated below.



In terms of the molecular integrals  $\epsilon$ ,  $\gamma$ ,  $\delta$  the energies can be expressed as

$$\begin{aligned}
 {}^1E_0 &= 2(\epsilon_1 + \epsilon_2 + \epsilon_3 + \epsilon_4 + \epsilon_5) + (\gamma_{11} + \gamma_{22} + \gamma_{33} + \gamma_{44} + \gamma_{55}) \\
 &\quad + 4(\gamma_{12} + \gamma_{13} + \gamma_{14} + \gamma_{15} + \gamma_{23} + \gamma_{24} + \gamma_{25} + \gamma_{34} + \gamma_{35} + \gamma_{45}) \\
 &\quad - 2(\delta_{12} + \delta_{13} + \delta_{14} + \delta_{15} + \delta_{23} + \delta_{24} + \delta_{25} + \delta_{34} + \delta_{35} + \delta_{45}), \\
 {}^1E_1^{56} &= 2(\epsilon_1 + \epsilon_2 + \epsilon_3 + \epsilon_4) + (\epsilon_5 + \epsilon_6) + (\gamma_{11} + \gamma_{22} + \gamma_{33} + \gamma_{44} + \gamma_{56}) \\
 &\quad + 4(\gamma_{12} + \gamma_{13} + \gamma_{14} + \gamma_{23} + \gamma_{24} + \gamma_{34}) + 2(\gamma_{15} + \gamma_{16} + \gamma_{25} + \gamma_{26} \\
 &\quad + \gamma_{35} + \gamma_{36} + \gamma_{45} + \gamma_{46}) + \delta_{56} - 2(\delta_{12} + \delta_{13} + \delta_{14} + \delta_{23} + \delta_{24} + \delta_{34}) \\
 &\quad - (\delta_{15} + \delta_{16} + \delta_{25} + \delta_{26} + \delta_{35} + \delta_{36} + \delta_{45} + \delta_{46}), \\
 {}^1E_2^{56} &= 2(\epsilon_1 + \epsilon_2 + \epsilon_3 + \epsilon_4 + \epsilon_6) + (\gamma_{11} + \gamma_{22} + \gamma_{33} + \gamma_{44} + \gamma_{66}) \\
 &\quad + 4(\gamma_{12} + \gamma_{13} + \gamma_{14} + \gamma_{16} + \gamma_{23} + \gamma_{24} + \gamma_{26} + \gamma_{34} + \gamma_{36} + \gamma_{46}) \\
 &\quad - 2(\delta_{12} + \delta_{13} + \delta_{14} + \delta_{16} + \delta_{23} + \delta_{24} + \delta_{26} + \delta_{34} + \delta_{36} + \delta_{46}).
 \end{aligned}$$

Similar expressions for other energies are easily written down, and in particular for the singlet triplet separations one obtains, for example,

$${}^1E_1^{56} - {}^3E_1^{56} = 2\delta_{56}.$$

Changing now to integrals over atomic orbitals, we neglect three-or-more centre integrals and introduce the notation of Goeppert-Mayer and Sklar.

$$A = (rr, rr) = \int \psi_r(1)\psi_r(2) \frac{e^2}{r_{12}} \psi_r(1)\psi_r(2) d\tau,$$

$$B = (rr, ss) = \int \psi_r(1)\psi_s(2) \frac{e^2}{r_{12}} \psi_r(1)\psi_s(2) d\tau,$$

$$C = (rs, ss) = \int \psi_r(1)\psi_s(2) \frac{e^2}{r_{12}} \psi_s(1)\psi_s(2) d\tau,$$

$$D = (rs, rs) = \int \psi_r(1)\psi_r(2) \frac{e^2}{r_{12}} \psi_s(1)\psi_s(2) d\tau,$$

$$Q = (H_r^c, ss) = - \int \psi_s(1)H_r^c(1)\psi_s(1) d\tau,$$

$$R = (H_r^c, rs) = - \int \psi_r(1)H_r^c(1)\psi_s(1) d\tau.$$

Let  $W_{2p}$  = energy of a  $\pi$ -electron in a neutral carbon atom so that

$$[T(\nu) + H_j(\nu)]\psi_j(\nu) = W_{2p}\psi_j(\nu),$$

and let the molecular orbital wave functions  $\phi$  be expanded as

$$\phi_l = \sum_r c_r \psi_r, \quad \phi_{l'} = \sum_r d_r \psi_r,$$

in which  $\psi_r$  is the hydrogen-like  $2p_z$  orbital at carbon atom  $r$ , and  $(c_r)^2$ ,  $(d_r)^2$  are the weights with which it enters the m.o.'s  $\phi_l$ ,  $\phi_{l'}$  respectively. With this notation the following expressions are obtained:

$$\begin{aligned}
 \gamma_{ll'} &= A \sum_r c_r^2 d_r^2 + \sum B_{rs} (c_r^2 d_s^2 + c_s^2 d_r^2) + 2 \sum C_{rs} (c_r d_s + c_s d_r) (c_r d_r + c_s d_s) + 4 \sum D_{rs} c_r c_s d_r d_s, \\
 \delta_{ll'} &= A \sum_r c_r^2 d_r^2 + 2 \sum B_{rs} c_r c_s d_r d_s + 2 \sum C_{rs} (c_r d_s + c_s d_r) (c_r d_r + c_s d_s) + \sum D_{rs} (c_r d_s + c_s d_r)^2, \\
 \epsilon_l &= W_{2p} - 2 \sum (R_{rs} + C_{rs}) c_r c_s - \sum (Q_{rs} + B_{rs}) (c_r^2 + c_s^2).
 \end{aligned}$$

At this stage the following approximations and assumptions are made:

In the atomic  $2p\pi$  functions which are of the form  $r \sin \theta e^{-Zr/2}$  (in the usual notation) the screening constant  $Z$  is taken as 3.18 throughout. The C—C bond-length is taken as 1.39 Å. everywhere, an approximation allowing the naphthalene molecule to consist of two hexagons with the dimensions of benzene. In the evaluation of the integrals  $C$ ,  $D$ ,  $Q$ ,  $R$  only contributions from neighbouring atoms  $r$ ,  $s$  are taken into account, those for non-nearest neighbours being neglected, whereas integrals of type  $B$  (i.e. simple Coulomb terms for the atomic charge clouds on two distant atoms) are taken for all pairs of atoms as  $B$  decreases but slowly with distance between  $r$  and  $s$ . Corrected values for these integrals are used as given by Parr and Crawford (1948), with some extrapolation in type  $B$  integrals. Possible variations of the screening constant  $Z$  and the C—C distance

Table 2

(1)	(2)	(3)	(4)	(5)	(1)	(2)	(3)	(4)	(5)
		0.0	$^1A_{1g}$	Ground state	$^1E_1^{26}$	6.7876			
		0.9840	$^3B_{2u}$	$T$	$^1E_2^{56}$	6.8617			
		1.1015	$^3B_{1u}$	$T$			6.8683	$^1A_{1g}$	$F$
$^3E_1^{56}$	3.1687				$^1E_1^{56}$	6.9349			
		3.2219	$^3B_{2u}$	$T$	$^1E_1^{46}$	7.0614			
$^3E_1^{57}$	3.4648				$^1E_2^{57}$	7.1400			
		3.5210	$^3B_{1u}$	$T$	$^1E_1^{47}$	7.2582			
		3.5624	$^3A_{1g}$	$T$			7.2643	$^1B_{2u}$	$Y$
		3.6214	$^1B_{1u}$	$Z$	$^1E_1^{16}$	7.4488			
		3.6503	$^1B_{2u}$	$Y$	$^1E_1^{17}$	7.5898			
$^3E_1^{26}$	3.6660						7.9080	$^3B_{2u}$	$T$
$^3E_1^{47}$	3.7441						8.5309	$^3B_{1u}$	$T$
$^1E_0$	4.0657						8.6198	$^1A_{1g}$	$F$
$^3E_1^{46}$	4.5572				$^3E_1^{36}$	8.8152	8.8152	$^3B_{3g}$	$T$
$^3E_1^{16}$	4.9513				$^1E_1^{37}$	9.1620			
		4.9873	$^1A_{1g}$	$F$	$^1E_2^{46}$	9.6411			
$^3E_1^{17}$	5.2010						9.9329	$^1A_{1g}$	$F$
$^3E_1^{37}$	5.2936						10.6308	$^1B_{1u}$	$Z$
		5.3972	$^3A_{1g}$	$T$			10.8683	$^1B_{2u}$	$Y$
$^1E_1^{57}$	6.4304				$^1E_1^{36}$	12.3728	12.3728	$^1B_{3g}$	$F$
		6.6883	$^1B_{1u}$	$Z$			13.2497	$^1A_{1g}$	$F$

(1) Description of configuration; (2) Energy (ev.) of configuration : zero at  $-4.0657$ ; (3) Energy (ev.) of state : interaction taken into account; (4) Symmetry; (5) Spectral activity.  $T$ , triplet;  $Z$ ,  $z$ -polarized;  $Y$ ,  $y$ -polarized;  $F$ , forbidden.

in excited states are neglected. In the wave functions overlap up to two C—C bond distances is included.

Using the wave functions  $\phi$  obtained by Coulson's method as basis for the antisymmetrized wave functions  $\Psi$ , we determine configurational energies which are recorded in column (2) of Table 2. Finally, resonance among configurations of the same symmetry is allowed for as described below, the results being shown in column (3).

There are six configurations (which are shown in column (1)) of  $^1A_{1g}$  type whose wave functions can be denoted by  $\Psi_{1,2,\dots}$ . To find the energies of the corresponding states of the molecule we take linear combinations of these,

$$\chi = \sum_{r=1}^6 c_r \Psi_r$$

and minimize the energy calculated from the  $\chi$  with respect to the coefficients  $c_r$ . Such configurational interaction should in principle take place in any symmetry class for all configurations within it. We have here considered it for the six lowest configurations of  $^1A_{1g}$  symmetry and for the three lowest ones in each of the following classes respectively:  $^1B_{1u}$ ,  $^3B_{1u}$ ,  $^1B_{2u}$ ,  $^3B_{2u}$ ,  $^3A_{1g}$  (two levels only). ('Lower' or 'higher' means here as given by calculations of method (a), § 2.) In the  $^1A_{1g}$  configurations this resonance is most pronounced, and it therefore seemed best to include levels up to about 6 ev. above the ground one, assuming that the influence of any higher energies on the ground state would be negligible. In the remaining symmetry types we assume that interactions of the lowest three configurations in each case will suffice as an indication of the effect. But care must be taken to include a sufficient number of configurations in each symmetry group: the differences between taking two or three levels into consideration (in  $^1B_{1u}$  and  $^1B_{2u}$  classes) are considerable both as regards energy separations and calculated oscillator strengths. The values in column (3) must therefore not be taken as final, for inclusion of still higher levels will lower these energies a little further. In so far as these results are valid, therefore, the calculated energy levels must correspond to observed bands at somewhat lower energies.

#### § 6. DISCUSSION

The energy values in column (2) (i.e. of the separate configurations) differ from those found by Coulson both in magnitude and in the order in which they arise because of the corrected Hamiltonian that has included electronic repulsion explicitly. But this improved Hamiltonian leads to the unlikely result that it is energetically sometimes easier to raise two electrons than one, for the  $^1E_2^{56}$  level just precedes the level  $^1E_1^{56}$ . That levels like  $^1E_1^{56}$ ,  $^1E_2^{56}$  should fall fairly close is inherent in our procedure. We start with the simple (Coulson's) molecular orbitals which give levels  $E_1^{56}$ ,  $E_2^{56}$  well separated; we then combine the wave functions  $\phi$  with spin factors  $\alpha$ ,  $\beta$  which separate the singly excited level into a triplet and a singlet level as in the diagram, bringing  $^1E_1^{56}$  near to  $^1E_2^{56}$ , which itself is unaffected by spin.



Only at the third stage—resonance among configurations of the same symmetry—do we reach the final arrangement of states. This resonance is strongest among  $^1A_{1g}$  levels and is particularly effective in lowering the ground level (by about 4.1 ev.). Since spectral term values depend on energy differences with the ground state it is essential to perform calculations like those that lead to column (3) before a comparison with experiment can be attempted.

In Table 3 we give a list of weights ( $c_r^2$ ) to indicate the degree of mixing of configurations in the lowest two states of  $^1A_{1g}$ ,  $^1B_{1u}$ ,  $^1B_{2u}$  symmetry respectively. In this table configurational wave functions are listed in the order in which the corresponding levels occur on an energy scale (column (2), Table 2). The most important conclusion we reach is that this order is not always an indication of the importance of a level in its resonance effect. Judging by the  $^1A_{1g}$  results it is approximately true that the lowest configuration ( $^1E_0$ ) is most important in the



ground state, while the second and third configurations are the chief contributors to the first excited  ${}^1A_{1g}$  state. On the other hand, in  ${}^1B_{1u}$  and  ${}^1B_{2u}$  states the order of configurations is not even approximately in accord with the weights of the wave functions belonging to the final states.

Table 3  
Weights of Configurations in States

${}^1A_{1g}$ configurational wave function	$\Psi_0$	$\Psi_1^{26}$	$\Psi_2^{56}$	$\Psi_2^{57}$	$\Psi_1^{37}$	$\Psi_2^{46}$	
$c_r^2$ in ground state	0.668	0.087	0.017	0.063	0.155	0.009	
$c_r^2$ in 1st excited state	0.001	0.474	0.480	0.009	0.032	0.004	
${}^1B_{1u}$ configurational wave function	$\left. \begin{array}{l} \Psi_1^{57} \quad \Psi_1^{46} \quad \Psi_1^{16} \end{array} \right\}$			${}^1B_{2u}$ configurational wave function $\left. \begin{array}{l} \Psi_1^{56} \quad \Psi_1^{47} \quad \Psi_1^{17} \end{array} \right\}$			
$c_r^2$ in 1st state	0.133	0.499	0.368	$c_r^2$ in 1st state	0.096	0.485	0.419
$c_r^2$ in 2nd state	0.829	0.018	0.153	$c_r^2$ in 2nd state	0.899	0.031	0.070

Returning to Table 2 column (2), we observe that the ground level configuration does not appear as that of lowest energy, for several triplet configurations fall below it: apparently the triplets form a cluster of configurations preceding a group of singlet ones. This may arise in part from too wide a singlet-triplet separation met with in m.o. calculations; the placing of triplets relative to singlets is, however, considered less significant than the order of singlet states alone. It is, indeed, this sequence of states which is perhaps the most unexpected feature of our results. In Coulson's method the sequence of transitions to singlet levels is in the following order

$${}^1E_1^{56}(Y) \quad {}^1E_1^{46}(Z) \quad {}^1E_1^{36}(F) \quad {}^1E_1^{57}(Z) \quad {}^1E_1^{26}(F) \quad {}^1E_1^{47}(Y),$$

whereas now the first of all singlet levels is  $z$ -polarized, very closely followed by a  $y$ -polarized one. The next transition is again long-axis polarized. For comparison we quote the results of valence bond calculations obtained by Craig where the lowest transitions in terms of polarizations are (i) forbidden, (ii)  $z$ -polarized, (iii)  $y$ -polarized. Although this agrees with our determination that a  $z$ -polarized transition occurs energetically below a  $y$ -polarized one, the two predictions do not necessarily support one another. According to our present calculations the first two bands are so close that they could not be detected easily as two distinct bands in the spectrum. Our second  ${}^1B_{1u}$  state (i.e. the third allowed transition, again  $z$ -polarized) should be attributed to the second observed band. This new sequence of singlet levels then gives fairly satisfactory agreement with Kasha's experimental results (in course of publication). He interprets the spectrum of naphthalene as consisting of the 33,100  $\text{cm}^{-1}$  weakly allowed transition preceded by a separate forbidden one at 31,060  $\text{cm}^{-1}$ . These are followed (in order of increasing excitation energy) by the strongly allowed 45,000  $\text{cm}^{-1}$  band; a further weakly allowed band appears at 52,500  $\text{cm}^{-1}$ . Numerically our results for the lowest allowed transition agree fairly closely with the observed values, experiment giving about 4 ev. while we calculate 3.6 ev. Energy values for higher excited states are less reliable but should be attributed to bands at energies rather lower than the calculated ones. The uncertainty about the lowest forbidden transition persists, however; several triplet states

fall immediately below our lowest allowed band, whereas the first excited  $^1A_{1g}$  state (to which such a forbidden transition might well have been attributed) occurs 1.4 ev. above the first allowed transition.

A further test of the value of our present extension of the simple molecular orbital treatment is afforded by a comparison of observed and computed oscillator strengths. The intensity of absorption depends on the transition moment  $Q$  associated with that transition, and Mulliken's (Mulliken and Rieke 1941) theoretical formula for determining oscillator strengths is used:

$$f_{\text{theor.}} = 1.085 \times 10^{11} \nu Q^2,$$

where  $\nu$  is the frequency of absorption in  $\text{cm}^{-1}$ ,  $Q$  is in cm. The transition moment  $Q$  is calculated from the integral

$$Q = \int \chi_l^*(\mathbf{r}) \chi_k d\tau.$$

Here  $\mathbf{r}$  is the displacement vector of the electron;  $\chi_l, \chi_k$  are the wave functions of the states  $l, k$  between which the excitation takes place.

A comparison with experimental values is given below.

Table 4. Oscillator Strengths

$f_{\text{obs.}}$	0.18	1.7	0.20?	$f_{\text{theor.}} (a)$	0.52 (y)	1.109 (z)	1.306 (z)
$\nu_{\text{obs.}} \times 10^{-3} \text{ (cm}^{-1}\text{)}$	33	45	52	$\nu_{\text{theor.}} \times 10^{-3} \text{ (cm}^{-1}\text{)}$	29	30	54      59
				$f_{\text{theor.}} (c)$	0.22 (z)	0.36 (y)	1.49 (z)      0.033 (y)

In this Table (a), (c) refer to the first and last of the three stages of m.o. theory described in § 2, so that  $f(a)$  is calculated from the simple m.o. wave functions  $\phi$  using frequencies of the observed spectrum, while  $f(c)$  is determined from wave functions  $\chi$  belonging to the states of the molecule with frequencies corresponding to calculated energy separations.

These new oscillator strengths represent some improvement over those of the simple form of m.o. theory. Although in the m.o. method the calculations for higher states are less reliable than for lower excited states, the new  $f$  values do reproduce the great difference in intensities of the 33,000, 45,000, 52,000  $\text{cm}^{-1}$  bands in the naphthalene spectrum.

A further interpretation emerges from the calculated oscillator strengths  $f(c)$ ; the 33,000  $\text{cm}^{-1}$  band might be attributed to a  $z$ - and a  $y$ -polarized transition nearly overlapping one another. This conclusion differs from results of both the simple m.o. theory and of valence bond theory, but it is not altogether in disagreement with experiment. In 1944 Prikhotoiko measured the absorption spectrum of naphthalene crystals at low temperatures in polarized light and found both  $z$ - and  $y$ -polarized lines present in the region 29,000–33,000  $\text{cm}^{-1}$ . Nor does a vibrational analysis of this spectral region exclude the possibility of two distinct sequences of lines which might belong to two separate electronic transitions. This dual character in the vibrational lines persists even on substitution by methyl groups.

To summarize: we consider the value of the present investigations to be two-fold. Firstly, they show how unreliable the results of the simple m.o. method are when applied to problems involving excited states; at the same time they

point the way to an improvement which lies in taking electronic interaction into account explicitly together with configurational interaction. However, the calculations become rather long and the new method is probably too laborious to be of use for more complicated molecules. Secondly, in so far as these new calculations have a physical meaning, they suggest a new interpretation of the ultra-violet spectrum of naphthalene. The 'first' allowed observed band may consist of two bands of different polarity almost coinciding with one another. The 'second' strong band (having its peak around  $45,000\text{ cm}^{-1}$ ) is then to be correlated with the next  $z$ -polarized transition. The polarity of this band thus agrees with the results of the simple m.o. method, but it is now attributed to the next higher state of that symmetry. For the lowest forbidden transition the symmetry remains uncertain from these calculations.

#### ACKNOWLEDGMENTS

The writer wishes to thank Prof. C. A. Coulson for suggesting this problem and for the great interest he has taken in this work, and Dr. D. P. Craig for many helpful discussions. A grant from the Department of Scientific and Industrial Research, which enabled this work to be carried out, is also acknowledged.

#### REFERENCES

- COULSON, C. A., 1948, *Proc. Phys. Soc.*, **60**, 257.  
 COULSON, C. A., and FISCHER, I., 1949, *Phil. Mag.*, **40**, 386.  
 GOEPPERT-MAYER, M., and SKLAR, A. L., 1938, *J. Chem. Phys.*, **6**, 645.  
 GRIFFING, V., 1947, *J. Chem. Phys.*, **15**, 421.  
 LENNARD-JONES, J. E., and COULSON, C. A., 1939, *T.F.S.*, **35**, 811.  
 LONDON, A., 1945, *J. Chem. Phys.*, **13**, 396.  
 LONGUET-HIGGINS, H. C., 1948, *Proc. Phys. Soc.*, **60**, 270.  
 MULLIKEN, R. S., 1933, *Phys. Rev.*, **43**, 279.  
 MULLIKEN, R. S., and RIEKE, C. A., 1941, *Rep. Prog. Phys.*, **8**, 231 (London: Physical Society.)  
 PARR, R. G., and CRAWFORD, B. L., 1948, *J. Chem. Phys.*, **16**, 526.  
 PRIKHOTKO, A., 1944, *J. Phys. U.S.S.R.*, **8**, 257.



## A New Technique for the Spectroscopic Examination of Flames at Normal Pressures

By H. G. WOLFARD AND W. G. PARKER

Royal Aircraft Establishment, Farnborough

*MS. received 7th June 1949; read on 11th March 1949*

**ABSTRACT.** Up to the present spectroscopic studies of flames supported on a tube have been limited by the geometry of the flame. Thus the important reaction zone presents a three-dimensional problem in which it is impossible to locate the emitters exactly. Moreover this zone is so thin in premixed gas flames that intermediate products cannot be determined from absorption studies. To overcome these difficulties the authors have constructed a burner with a two-dimensional diffusion flame in which the reaction zone at ordinary pressures is 5–10 mm. thick and has an optical depth of 5 cm. or more. With this flame many of the reacting molecules can be located through either their emission or absorption spectra or both. The value of the new technique in the elucidation of combustion processes is demonstrated with reference to  $\text{NH}_3\text{-O}_2$  and  $\text{H}_2\text{-O}_2$  flames, and mention is made of its application to hydrocarbon flames.

### § 1. INTRODUCTION

THE application of spectroscopy to combustion has been widely practised and has provided much of the existing evidence on the subject. It is well known, however, that there are a number of serious limitations in the methods employed, particularly from the structure of the flame. In a Bunsen flame for example, the most interesting reactions occur in the narrow inner cone and not in the large volume of interconal gas above it. The thickness of the inner cone, however, is usually less than 0.1 mm. and it is extremely difficult to study the detail. Moreover, it presents a three-dimensional problem in which it is virtually impossible to decide on the precise location of the emitters. The optical depth of the inner cone is insufficient for absorption studies and this too is a great drawback because absorption spectra can give quantitative as well as qualitative information on the molecules and atoms involved. Spectroscopic evidence is thus limited to overall observations such as the emission of  $\text{C}_2$  and CH bands in the inner cone of hydrocarbon flames or to the emission and absorption of OH radicals in the interconal gases.

Some of these difficulties have been partially overcome by Gaydon and Wolfhard (1948) who used premixed flat flames. Normally a premixed gas flame will strike back when the mass flow is reduced below a critical value and this occurs before the cone has flattened out. Under carefully controlled conditions, with small gas flows which approached the limiting value for self propagation, Wolfhard (1943) found it possible to obtain a flat flame above the burner at any pressure. At 1 atmosphere, however, these flames are very small and require a burner of about 1 mm. diameter. At low pressures (2–20 mm. Hg) the burner diameter may be increased to about 50 mm. and the reaction zone has a thickness of more than 10 mm. depending on the mixture strength. Emission spectra can be observed in different parts of the flame and thus the relative positions of the various emitters may be obtained. At reduced pressures the flat flames are too thin optically for absorption work and it has only been possible to detect OH radicals in absorption using very high resolving power.

Egerton and Powling (1948) have recently developed a large flat premixed gas flame at atmospheric pressure by having a uniform gas flow across the burner, thereby eliminating the usual parabolic velocity distribution which leads to conical flames. The inner cone of the flame is normally very thin but widens for very slow and rich flames. The method is very promising especially for the detection of radicals in the zones before and after the main reaction.

Apart from the last example it may be said that neither premixed gas nor diffusion flames examined hitherto allow full use of absorption spectroscopy. The primary requirements for this are a broad reaction zone with good optical depth for absorption work. These requirements have been met at normal pressure in a diffusion flame of unusual design which is described in this paper.

It should perhaps be pointed out that the chemical reactions in diffusion flames may be different from those in a premixed gas flame. Nevertheless an attempt to understand these reactions is fully justified by the great technical importance of diffusion flames. Apart from calculations on the height and shape of such flames by Burke and Schumann (1928) little fundamental work has been done hitherto.

## §2. DESCRIPTION OF NEW TECHNIQUE

Diffusion flames burning with oxygen have a reaction zone up to 1 cm. in thickness depending on the height of the flame. This zone can be obtained in a more convenient form by using a flat burner in lieu of the usual cylindrical pipe.

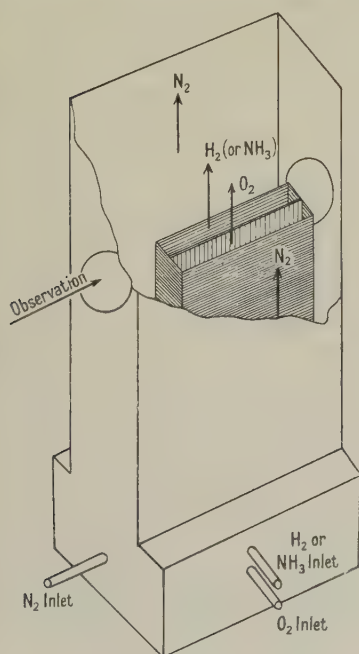


Figure 1. Burner.

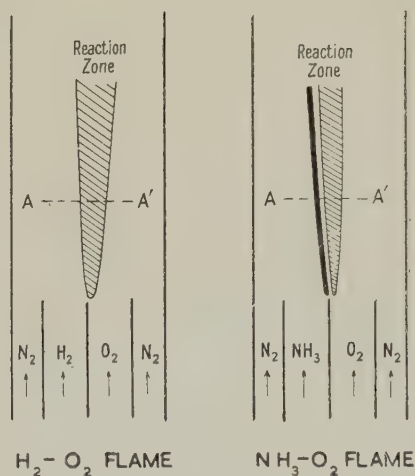


Figure 2. End view of flame.  
Spectroscopic examination made across the reaction zone at A-A'.

Figure 1 shows the design of the burner. The fuel gas and oxygen issue with equal velocities of about 20 cm/sec. from parallel rectangular tubes (5 cm.  $\times$  0.7 cm.) which have one long side in common. The gases rise vertically and diffuse into each other in a laminar flow on account of the low Reynolds number.

On ignition burning takes place at the interface and a flat diffusion flame is obtained which presents a two-dimensional problem, rather similar to the premixed flat flames described in §1. The flame front is kept very steady by stabilizing it with a surrounding stream of nitrogen which flows up the outer jacket. The optical depth of the flame is the length of the interface and is arbitrarily fixed by the burner dimensions; in the investigation described here it was 5 cm. This depth at ordinary pressure is sufficient for absorption studies. Quartz windows are suitably sited in the outer jacket.

This burner has not been used so far for a detailed study of combustion problems, but an assessment of its potential usefulness has been made by finding out what bands can be detected in absorption and emission and the location of these bands in the reaction zone.

Combustion occurs where the fuel and oxygen are in contact at the interface. Figure 2 shows an end view of a  $\text{H}_2\text{-O}_2$  and an  $\text{NH}_3\text{-O}_2$  flame. The reaction zone is thin at first but broadens higher up the flame. The combustion products, viz.  $\text{H}_2\text{O}$  or  $\text{H}_2\text{O}$  and  $\text{N}_2$ , etc., are formed in the reaction zone and diffuse outwards on both sides whereas the oxygen and the hydrogen (or ammonia) diffuse towards the reaction zone and maintain combustion. The reaction zone of the hydrogen flame emits in the visible region a fairly uniform blue continuum similar to that experienced with a premixed  $\text{H}_2\text{-O}_2$  flame, whereas the reaction zone of the  $\text{NH}_3\text{-O}_2$  flame is clearly divided into two parts. On the ammonia side a narrow plane of yellow radiation can be seen, which is due to the ammonia  $\alpha$ -bands; moving across the flame towards the right this is followed by a dark space and then by a fairly thick plane of blue continuum on the oxygen side. The flames are not exactly vertical even when the velocities of both gases are equal, because the diffusion rates of the fuel and oxygen are different. The position of the gas interface in the burner has therefore no relation to any point in the reaction zone above the burner.

A spectroscopic study in emission was made by projecting an image of the end view of the flame (12 mm. above the burner and corresponding to the line AA' in Figure 2), on to the slit of a spectrograph by means of a quartz-fluorite achromatic lens, the aperture being chosen so that the different layers in the flame did not overlap appreciably. For absorption work an image of a carbon arc or a hydrogen discharge lamp was focused on to the flame. This image and the flame were then focused on the slit of the spectrograph. Since the most information about the reactants would be derived in the horizontal direction AA' across the interface and not in a vertical direction parallel to the interface, the images on the spectrograph were made to fall across the slit either by the use of a  $90^\circ$  quartz prism or by putting the spectrograph on its side. Two hairs were placed across the image of the flame on the slit, and cast line shadows over the whole wavelength region of the spectra. These lines served to locate the source of the bands in the flame. A Hilger medium quartz spectrograph was used for most of the investigation.

### § 3. THE HYDROGEN-OXYGEN FLAME

The use of a  $\text{H}_2\text{-O}_2$  flame in this assessment is limited because hydrogen cannot be detected in absorption with a quartz spectrograph. The reaction is less complicated than the hydrocarbon reaction, or even the ammonia flame, and it seemed a simple application for the new technique. The results are shown



graphically in Figure 3. The hydrogen diffuses from the left and the oxygen from the right. The abscissa represents the horizontal distance (in millimetres) in the flame 12 mm. above the burner mouth. The ordinate on the right is a rough qualitative measure of the strength of the bands estimated from the negatives. No attempt has yet been made to measure the intensities accurately for calculating the absolute concentration of the molecules. The absorption bands of the OH radical extend over approximately 9 mm. and the emission bands are symmetrically located over the greater part of this distance. The ordinate on the left is a temperature scale. Temperature measurements in the reaction zone were made by the Na line-reversal method. A thin wire coated with sodium chloride was inserted into the flame below the point of measurement. This coloured only the small and relevant part of the flame and eliminated risk of self-reversal. The anode of a carbon arc was used as light source together with a rotating sector to reduce the effective temperature. The results are shown by the top line of

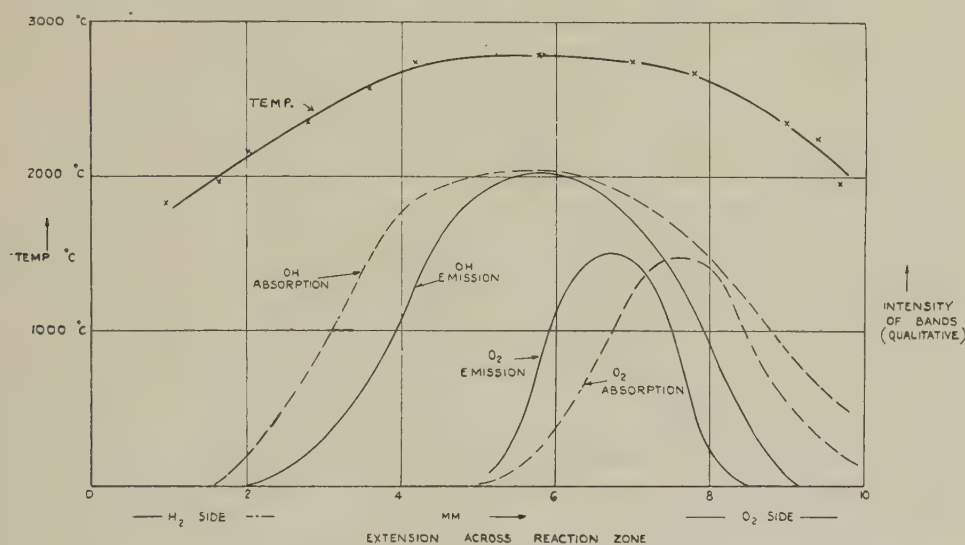


Figure 3.  $\text{H}_2$ - $\text{O}_2$  flat diffusion flame.

Figure 3. The temperature attained a rather flat maximum at  $2,800^\circ\text{C}$ . This agrees very closely with the calculated value for a stoichiometric mixture of  $\text{H}_2$  and  $\text{O}_2$ , allowing for dissociation but not for external heat losses. It appears therefore that diffusion flames are quite as hot as premixed flames.

Comparing the temperature and OH measurements, the latter cease in emission at about  $2,100^\circ\text{C}$ . (though this depends to some extent on the sensitivity of the measurements). The OH absorption extends slightly further on both sides. By using the OH bands for temperature measurements by reversal, instead of the Na lines, the values obtained agreed within the limits of error with the sodium reversal temperature, and proved that in the  $\text{H}_2$ - $\text{O}_2$  diffusion flame the electronic excitation of molecules and atoms is thermal even in the reaction zone. This is believed to be the case in the premixed flame of  $\text{H}_2$ - $\text{O}_2$  also but certainly not in premixed flames of hydrocarbons with oxygen.

Oxygen is normally transparent in the ultra-violet, but hot oxygen absorbs because higher vibrational levels are excited which permit a transition to the upper electronic state above  $2,000\text{ \AA}$ . At  $1,000^\circ\text{C}$ . the absorption has already

spread to 2400 Å. and is readily observed. The spectrum contains a vast number of lines which do not form definite heads, and a satisfactory analysis has not been achieved up to the present. The existence of these lines however provides a means of detecting the oxygen in the flame. On the outside of the flame where the temperature is only moderate the absorption by oxygen is a complicated function of the temperature, but in the reaction zone where the temperature is above 2,000° C. the absorption must give at least a qualitative indication as to where the  $O_2$  is used up. These results for the  $H_2-O_2$  flame are also shown in Figure 3. Just beyond the point of maximum temperature the  $O_2$  concentration had fallen to a value where absorption could no longer be detected.

The height of these excited vibrational levels is interesting. The  $O_2$  absorption bands in the flame can be followed up to about 2600 Å. This corresponds to a vibrational energy of about 33 kcal. The reaction  $H + O_2 \rightarrow OH + O$  which can be regarded as an important step in the  $H_2-O_2$  reaction is normally endothermic (16 kcal.), but if this high vibrational energy of the  $O_2$  is available it may be exothermic. At least one metastable  $O_2$  level ( ${}^1\Delta_g$ ) is lower than 33 kcal. and may therefore be partially excited and play an important role in combustion. It seems to be a characteristic of the diffusion flame that the reactants only meet after they have nearly reached the theoretical flame temperature in contrast to the premixed flames where they are continuously in contact and begin to react at the ignition point (800–1,000° C.). The oxygen molecules emit as well as absorb, and the emission is shifted towards higher temperature compared with the absorption. Figure 4 (see Plate) shows an actual spectrum which gives in emission the (0,1) OH band, and the (0,14) and (0,15)  $O_2$  bands. It is noticeable that both  $O_2$  bands and OH bands do not occur at the same position in the flame. The existence of the Schumann–Runge  $O_2$  bands in emission in the flame was rather unexpected since it is very difficult to obtain them in a discharge tube because the potential energy curves of the excited and unexcited states are relatively displaced. In a diffusion flame where the  $O_2$  has high vibrational levels in the ground state it is easier to excite the upper state in accordance with the Frank–Condon principle.

The  $HO_2$  radical could not be detected either in absorption or in emission. The radical is supposed to play an important part in combustion and Minkoff (1947) has calculated that its spectrum should lie around 2900 Å. It has not been reported so far.

In some reaction schemes  $H_2O_2$  has been suggested as an intermediate product and Egerton and Minkoff (1947) found appreciable amounts in an  $H_2-O_2$  flame at low pressure.  $H_2O_2$  has a continuous absorption which is not very strong in the quartz ultra-violet and does not make a very sensitive test. Since no continuum was detected down to 2100 Å., however, it may be said that the  $H_2O_2$  concentration was less than 0.2% of the total pressure.

By a similar reasoning the partial pressure of ozone must be smaller than 0.006% since ozone absorbs quite strongly near 2500 Å., but this continuum was not observed.

#### §4. THE AMMONIA-OXYGEN FLAME

The experimental arrangement for the ammonia flame was in every way similar to that of the  $H_2-O_2$  flame. The ammonia system has an advantage over hydrogen in that the fuel can be observed in absorption. At room temperature  $NH_3$  begins to absorb at 2254 Å. and after a few diffuse bands the absorption becomes a continuum towards the vacuum ultra-violet. The effect of temperature

on this absorption was studied separately in a quartz cell 5 cm. long which was filled with ammonia gas and inserted in a furnace. The length of the optical path was thus similar to that of the flame. As the temperature was raised new band heads appeared and at  $1,000^{\circ}\text{C}$ . these bands had spread up to  $2440\text{ \AA}$ ., the whole absorption becoming more continuous in appearance. Figure 5 (see Plate) shows how the absorption by ammonia in the cell varied with temperatures between  $20^{\circ}\text{C}$ . and  $800^{\circ}\text{C}$ ., and Figure 6 shows the ammonia absorption observed in the flat diffusion flame. As the ammonia approaches the reaction zone the bands near  $2200\text{ \AA}$ . become stronger and later continuous, then they suddenly cease. Figure 7 shows again in graphical form the results for the  $\text{NH}_3\text{--O}_2$  flame of all the absorption and emission spectra observed in a horizontal traverse of the flame 12 mm. above the burner mouth. The height of the curves is again only a qualitative indication of the strength of the bands. The ammonia diffuses

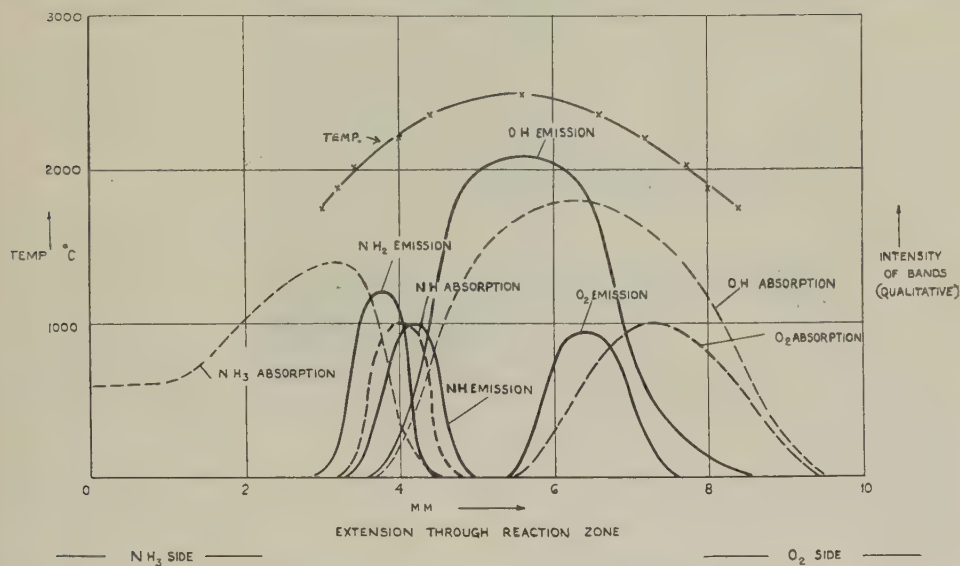


Figure 7.  $\text{NH}_3\text{--O}_2$  flat diffusion flame.

from left to right and the oxygen in the opposite direction. The ammonia is apparently unaffected until about the 1.0 mm. point on the abscissa then the bands increase in strength due to the increasing temperatures and reach a maximum at 3.2 mm. At 4.8 mm. the  $\text{NH}_3$  disappears completely. At the point of maximum decline in the  $\text{NH}_3$  absorption, however, the ammonia  $\alpha$ -bands appear in emission and these bands are usually attributed to  $\text{NH}_2$  radicals. The maximum of these bands is at 3.8 mm. At 4.0 mm. the maximum of the  $\text{NH}$  bands appears in absorption and the emission bands of this are strongest at 4.2 mm., the shift being due to the higher temperature in this direction. In this way the whole course of the dehydrogenation of the  $\text{NH}_3$  in the flame can be followed.

$\text{NH}$  has been detected in absorption by Frank and Reichard (1936) who decomposed pure  $\text{NH}_3$  at  $2,000^{\circ}\text{C}$ .  $\text{NH}_2$  could not be found in absorption possibly because of the small dispersion of the quartz spectrograph in the visible region, and possibly also the multi-line nature of the band renders it difficult to find it in absorption. These bands are discussed again later. The  $\text{NH}$  band at  $3360\text{ \AA}$ . is much easier to find because the Q branch forms a strong head and the band looks like a strong line.



O<sub>2</sub> was again detected in absorption and spreads from the right (Figure 7) up to 5.4 mm. Since the ammonia spreading from the left has completely disappeared at 4.8 mm. (see above) it appears that the ammonia and oxygen never come in contact and the whole reaction goes via the intermediate products. The relevant positions of the two bands can be seen in Figure 6.

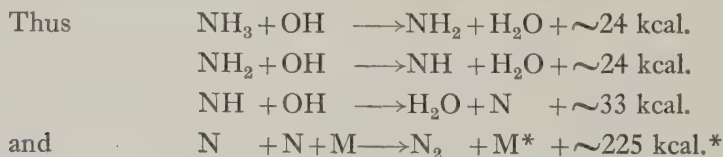
O<sub>2</sub> in emission is again displaced relative to the absorption on account of the temperature gradient in the flame.

OH is the most prominent feature in the spectra, either emission or absorption. It commences near 3.6 mm. and goes far over to the oxygen side (Figure 7).

The temperature of the ammonia flame is plotted in Figure 7 (with reference to the ordinate on the left) from sodium line-reversal measurements. The maximum temperature was found to be very close to the theoretical temperature for a stoichiometric mixture. The fall on either side of the maximum is similar. OH reversal temperature measurements agreed with the Na line results and it was again concluded that the electronic excitation of the OH and Na is purely thermal in the NH<sub>3</sub>-O<sub>2</sub> flame as in the H<sub>2</sub>-O<sub>2</sub> diffusion flame. Even the NH bands may be used to obtain the reversal temperature in the position where they appear and the measurement made with them was 2,200° c. at 4.1 mm. (Figure 7) in agreement with the other values. Figure 8 shows the position of the NH band compared with OH on the plate.

Returning to the problem of the NH<sub>2</sub> bands, the following rather sensitive test was applied. The NH<sub>2</sub> radiation is the only strongly visible radiation and occurs in a narrow vertical plane less than 1 mm. thick; by holding a piece of white paper across the end of the flame and looking at the outside of the paper one should see an equally illuminated field except directly opposite the extension of the luminous plane. Here if absorption is appreciable a vertical shadow will occur on the paper. No such shadow was obtained however. This supports the view that the stationary concentration of NH<sub>2</sub> radicals is very small and that the NH<sub>2</sub> decompose very quickly. The strength of the emission is not exceptional in view of the fact that the temperature at that point is about 2,100° c.

Several additional facts can be gleaned from the analysis. For example, the strongest visible radiation comes from a point some distance from the position of maximum temperature where the reaction rate is highest. Also on the ammonia side the OH in absorption ceases at about 2,100° c., whereas on the O<sub>2</sub> side it is still very strong at that temperature. This may be due to the lower partial pressure of OH in water vapour than in the H<sub>2</sub>O-O<sub>2</sub> mixtures, but it is rather striking that the OH ceases just where the NH<sub>3</sub> dehydrogenation begins. It may be an important dehydrogenation process, though it is unlikely to be the only one, otherwise the temperature distribution in the flame should be somewhat different. This may be shown by assuming that the OH does all the dehydrogenation since it is more exothermic in reaction with NH<sub>3</sub>, NH<sub>2</sub> and NH than the H or O atoms.



\* The symbols M and M\* are the usual convention for denoting collision with a third body to take away energy of recombination N+N.

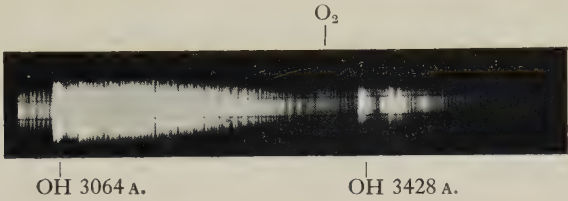


Figure 4.

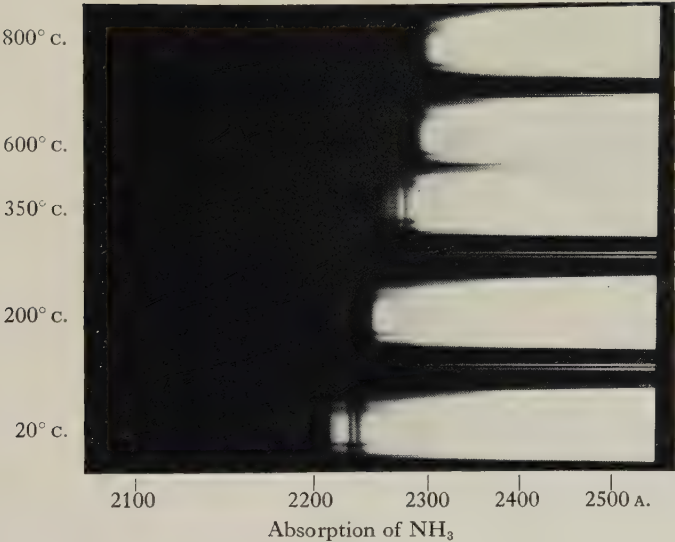


Figure 5.

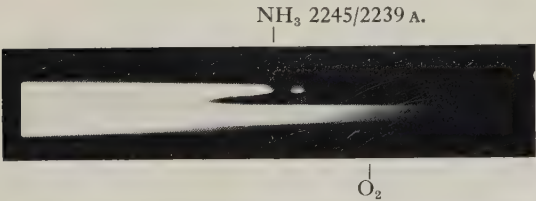


Figure 6.

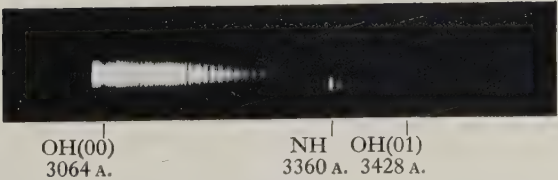


Figure 8.





Hence a very big release of energy would occur at the point of dehydrogenation which does not accord with the temperature plot of the flame. It seems more likely that the product of dehydrogenation is mostly  $\text{H}_2$  and not  $\text{H}_2\text{O}$  and that the  $\text{H}_2$  is subsequently burnt with oxygen and provides the greatest heat release of the reaction at about 5.6 mm. (Figure 7).

A fuller investigation could be made with this technique and more quantitative data obtained from the band strengths would greatly help in completely elucidating the reaction mechanisms.

## § 5. HYDROCARBON FLAMES

Although no extensive work has yet been done with hydrocarbon flames, a few preliminary tests with methane-oxygen flames in this burner are worth recording. On the  $\text{CH}_4$  side of the burner there was a narrow plane of strong luminosity due to radiant soot particles and on the  $\text{O}_2$  side a weak blue continuum which was probably due to recombination of electrons and ions. These two vertical planes, visible to the naked eye, were apparently separated by a thin dark space. Figure 9 gives some of the results graphically represented as before.

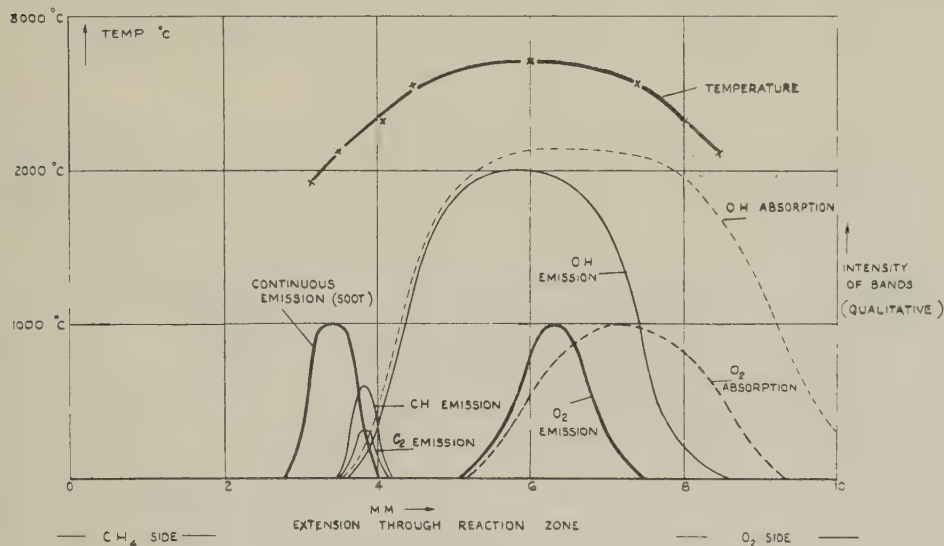


Figure 9:  $\text{CH}_4\text{-O}_2$  flat diffusion flame.

The  $\text{CH}_4$  diffuses from the left and the  $\text{O}_2$  from the right; the distances in the flame are marked in millimetres on the abscissa. The visible continuous radiation (from carbon particles) extends from 2.8 to 4.0 mm. and the OH in absorption and emission just reaches the carbon region. The OH bands are again much stronger on the  $\text{O}_2$  side than at the corresponding temperatures on the  $\text{CH}_4$  side. The maximum temperature (by Na line-reversal method) is close to the theoretical. It is also interesting to note that  $\text{O}_2$  does not reach the luminous zone and the carbon particles cannot therefore burn in oxygen but probably react with OH or  $\text{H}_2\text{O}$ . The region of greatest heat release is at 6.0 mm. and it seems very probable that this is due to combustion of  $\text{H}_2\text{-O}_2$  and perhaps  $\text{CO-O}_2$ .

The information which this preliminary work gives relevant to carbon formation may be indicated; a discussion of this complex phenomenon will be presented

elsewhere. It is commonly supposed that carbon particles in the flame are formed by condensation of  $C_2$  molecules or even C atoms which are sometimes observed in emission from premixed flames. This theory is quite untenable for the type of flame examined here because the  $C_2$  is not observed prior to the zone of carbon particles, i.e. on the fuel side of the luminous zone (Figure 9). Rather weak  $C_2$  bands occur together with CH bands on the oxygen side of the zone.

#### §6. CONCLUDING REMARKS

It is hoped that sufficient evidence has been presented to show the potential value of the flat flame technique in the application of spectroscopy to diffusion flames. Very full information can be obtained in this way with fuels which absorb light. For the study of hydrocarbon flames other than aromatic flames it may be necessary to use the near vacuum ultra-violet region, but this does not present very great difficulties. Nitrogenous fuels and many other combustible inorganic compounds such as compounds of sulphur can be very fully examined. The behaviour of fuel additives can be investigated and so also can the action of any promoters or inhibitors which give absorption spectra. The problem of carbon formation has already been mentioned and the technique of the flat diffusion flame is at present being used in this connection by the authors.

#### ACKNOWLEDGMENT

The authors are indebted to the Chief Scientist, Ministry of Supply, and to the Controller, H.M. Stationery Office, for permission to publish this communication.

#### REFERENCES

- BURKE, S. P., and SCHUMANN, T. E. W., 1928, *Industr. Engng. Chem.*, **20**, 998.  
EGERTON, A. C., and MINKOFF, G. T., 1947, *Proc. Roy. Soc. A*, **191**, 185.  
EGERTON, A. C., and POWLING, T., 1948, *Colloquium on Combustion* (Paris).  
FRANK, H. H., and REICHARD, H., 1936, *Naturwissenschaften*, **24**, 171.  
GAYDON, A. G., and WOLFHARD, H. G., 1948, *Proc. Roy. Soc. A*, **194**, 169.  
MINKOFF, G. T., 1947, *The Labile Molecule*, Discussion of the Faraday Society, No. 2, p. 151.  
WOLFHARD, H. G., 1943, *Z. techn. Phys.*, **24**, 206.

## Dielectric Changes in Phosphors containing more than One Activator

By G. F. J. GARLICK AND A. F. GIBSON \*

Physics Department, The University, Birmingham

*MS. received 18th May 1949*

**ABSTRACT.** It is well known that some luminescent materials, notably zinc sulphide, show marked changes in dielectric constant and dielectric loss when excited. Recent work by the authors has established that the changes are due to the filling of electron traps, which have large effective diameter and high polarizability.

The present paper describes measurements of the dielectric changes in phosphors containing two or more luminescence activators. Assuming that the dielectric changes are due to electron trapping, it is possible to derive information regarding the nature of electron traps and in particular their apparent association with the luminescence centres. The results support the contention that the introduction of the activating impurity into phosphors produces trapping states for excited electrons and that each trap forms part of a complex which includes the luminescence centre.

### § 1. INTRODUCTION

RECENT studies of the extent to which retrapping occurs in conventional phosphors show that it is a negligible process when the electrons are ejected from the traps by thermal energy only (Garlick and Gibson 1948). This result cannot be reconciled with the conventional model of a luminescent material used by Randall and Wilkins (1945) and other authors. It was suggested, therefore, that each luminescence centre has one electron trap associated with it, the two together forming a closed system from which the excited electron did not normally escape. This view was supported by the experiments described by Garlick (1948) and by Garlick and Gibson (1949). Garlick showed that the introduction of impurities modified the trap distribution in the phosphor specimen. This was illustrated by the production of new peaks, due to the introduction of specific impurities, in the thermoluminescence curve. Garlick also showed that the thermoluminescence curves of phosphors containing two activators could be resolved into 'colour peaks', that is, the colour of the emission at a peak of the thermal curve glow depended upon the particular group of traps being emptied. The colour changes during thermoluminescence might be explained by migration of positive holes and electrons between different types of luminescence centres, as postulated in a recent theory due to Klasens *et al.* (Klasens, Ramsden and Chow Quantie 1948, Klasens and Wise 1948). However, this explanation is unlikely in many cases as the following experiment shows. If a phosphor with more than one type of luminescence centre is excited by radiation of suitable wavelength then it is possible to excite one type of centre only. The resulting thermoluminescence curve obtained after such excitation, using suitable optical filters, may be the same as that after excitation affecting both types of centre, provided that the same optical filters are used to select emission from the same luminescence centres. If this is so, then it is unlikely that any interchange of electrons or

\* Now at T.R.E., Malvern.



positive holes occurs between the different centres. In effect, such a result supports the hypothesis mentioned above (Garlick and Gibson 1948) that retrapping of electrons does not occur in conventional phosphors, such as the zinc sulphides.

Work on the increase in dielectric constant and loss which occurs in zinc sulphide on excitation (Garlick and Gibson 1947) has shown that the increase is due to the filling of electron traps. The present studies, described below, contain further evidence from dielectric measurements to show that electron traps and luminescence centres are closely associated. In particular, the effects of field frequency, temperature, exciting intensity and time of excitation have been studied. It has been shown that the dielectric constant change per filled trap is exponentially dependent on temperature, the exponent varying from phosphor to phosphor. The dependence on field frequency is typical of a dipole system having a relaxation time of about  $10^{-7}$  second. The latter figure also varies among phosphor specimens of different constitution.

It was noticed during the work on dielectric effects that both the relaxation time and the temperature exponent of the polarizability were, to a first approximation, determined by the nature of the activating impurity. The lattice structure (cubic or hexagonal), the constitution of the bulk material (i.e. ZnS or mixed ZnS-CdS) and other parameters were of secondary importance. This suggested that the activating impurity producing the traps largely determined the dielectric properties of the traps.

## § 2. EXPERIMENTAL RESULTS

Garlick (1948) used the phosphor  $\text{CaWO}_4\text{-U}$  as an example of a doubly activated material and gave the thermoluminescence curves of the material, using optical filters to select emission from the different types of luminescence centre.

The same phosphor will be used as an example of the characteristics of the dielectric changes occurring when phosphors containing more than one activator are excited.

### (i) *The Variation of the Dielectric Changes with Applied Field Frequency*

Measurements have been made by the methods described previously (Garlick and Gibson 1947) and over the same frequency range (75 kc/s. to 20 Mc/s.). In a singly activated phosphor the relaxation time  $\tau$  is single valued or nearly so, anomalous dispersion of simple form occurring at about 2 Mc/s. In a doubly activated phosphor, however, it is clear from inspection of the dispersion curve that there are two regions of anomalous dispersion and hence two values of the relaxation time. If the values are sufficiently different it is quite simple to treat the two dispersion regions separately and apply to each region the formula

$$\frac{\Delta\epsilon_0 - \Delta\epsilon}{\Delta\epsilon - \Delta\epsilon_\infty} = \omega^2\tau^2 \quad \dots\dots(1)$$

given as equation (8) by Garlick and Gibson (1947)\*. In Figure 1 the factor on the left-hand side of equation (1) is plotted against the square of the field frequency for the two dispersion regions considered separately. The slopes of the two lines

\*  $\Delta\epsilon$  is the change in the real part of the complex dielectric constant at the given field frequency, while  $\Delta\epsilon_0$  and  $\Delta\epsilon_\infty$  are its values at zero and optical frequencies respectively.

give the two values of the relaxation time. The values obtained are  $\tau_1 = 31 \times 10^{-8}$  second,  $\tau_2 = 5.3 \times 10^{-8}$  second. Measurement of the variation in loss factor change  $\Delta\epsilon''$ , given by (Garlick and Gibson 1947)

$$\Delta\epsilon'' = \frac{(\Delta\epsilon_0 - \Delta\epsilon_\infty)\omega\tau}{0.9 \times 10^{12}(1 + \omega^2\tau)^2}, \quad \dots\dots(2)$$

shows that this factor has two frequency maxima corresponding to the two relaxation times already noted. As  $\Delta\epsilon''$  is a maximum when  $\omega\tau = 1$ , values of  $\tau$  may be obtained. For the specimen of uranium activated calcium tungstate used they are  $\tau_1 = 23 \times 10^{-8}$  second and  $\tau_2 = 4.0 \times 10^{-8}$  second. The agreement with those deduced from the dispersion curve is as good as can be expected.

In view of the results discussed above it seems reasonable to suppose that two different types of electron trap exist in this and similar materials. Each type of trap can be associated with one or other of the two types of luminescent centre in the material. In the above case of  $\text{CaWO}_4\text{-U}$  we may talk loosely of 'WO<sub>4</sub> traps' and 'U traps'. It will be clear from the thermoluminescence curve given by Garlick (1948) that 'U traps' are deeper than 'WO<sub>4</sub> traps'.

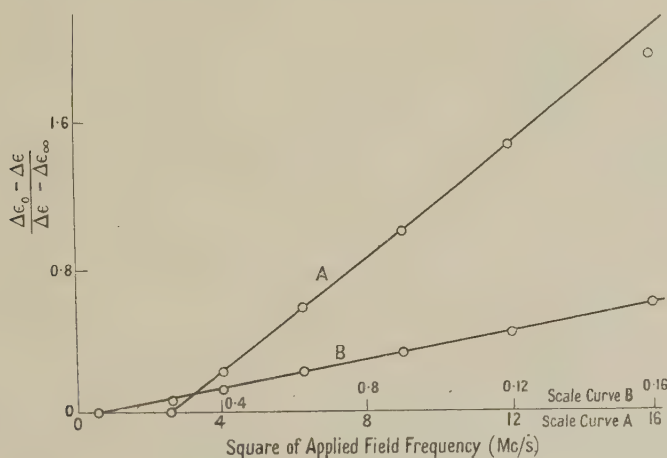


Figure 1. Variation of dielectric constant change with applied field frequency for a  $\text{CaWO}_4\text{-U}$  phosphor. Curves plotted on assumption that phosphor has two types of polarizable centres, as explained in text. A: 'WO<sub>4</sub> traps'; B: 'U traps'.

It is now important to ascribe the two values of  $\tau$  obtained by experiment to the 'WO<sub>4</sub>' and 'U traps' respectively. One method is to determine the reciprocal of  $\tau$  ( $=s$ , Garlick and Gibson 1947) for the two types of trap by luminescence measurements. This can be done by the method due to Randall and Wilkins (1945), but high accuracy cannot be expected. Experiment indicates that the large value of  $\tau$  is associated with the deeper 'U traps'. This result was confirmed by a second method. If the decay of the dielectric constant change after cessation of excitation is measured at frequencies of the order of 5 Mc/s., the decay rate is fast, but becomes slower as the applied field frequency is reduced to a low value ( $\sim 500$  kc/s.). At high frequencies the dipoles of small  $\tau$  are operative, and hence the smaller value of  $\tau$  must be associated with the shallower (in this case WO<sub>4</sub>) traps.

In general, therefore, traps associated with given centres have a relaxation time  $\tau$  peculiar to the impurity involved. Some typical results for zinc sulphide phosphors are summarized in the following table.

Phosphor	$\tau$ (seconds $\times 10^8$ )		
	Zn traps	Cu traps	Mn traps
ZnS-Zn	35	—	—
ZnS-Zn-Cu	34	17	—
ZnS-Zn-Cu-Mn (1)	46	19	2.5
ZnS-Zn-Cu-Mn (2)	36	15	2.4

(ii) *The Variation of the Dielectric Changes during Thermoluminescence*

Measurements of the changes in dielectric constant and loss which occur during the emission of thermoluminescence have been made by methods already described (Garlick and Gibson 1947). The results obtained for doubly activated phosphors may be treated in the way described in the same paper. Ignoring the slow variation in polarizability with trap depth, the magnitude of the dielectric

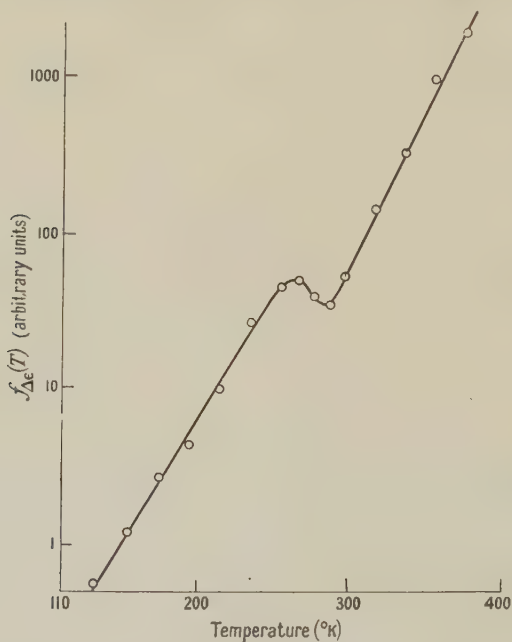


Figure 2. Temperature function  $f_{\Delta\epsilon}(T)$  for the dielectric constant change in a  $\text{CaWO}_4\text{-U}$  phosphor derived from measurements of dielectric changes during thermoluminescence.

constant change at any temperature  $T$  divided by the total number of filled traps remaining at that temperature is taken as a measure of the polarizability of the filled traps. Denoting the polarizability as  $f_{\Delta\epsilon}(T)$ , it was shown by Garlick and Gibson (1947) that

$$f_{\Delta\epsilon}(T) = \text{const.} \exp(\alpha T) \quad \dots\dots(2)$$

where  $\alpha$  is a constant.

The variation of  $f_{\Delta\epsilon}(T)$  with temperature for a doubly activated material ( $\text{CaWO}_4\text{-U}$ ) is shown in Figure 2,  $f_{\Delta\epsilon}(T)$  being plotted logarithmically. The



simple linear relation expected is not obtained, a marked inflection occurring at about 280°K. At about this temperature the emission changes from blue ( $\text{WO}_4$  emission centres) to green (U emission centres). Apparently equation (2) is obeyed while 'WO<sub>4</sub> traps' predominate and while 'U traps' predominate, the inflection occurring intermediately.

This result is explicable if it is assumed that the polarizabilities of 'WO<sub>4</sub>' and 'U traps' are different. As there is a drop in the polarizability-temperature curve at the inflection, it is clear that the polarizability of 'WO<sub>4</sub> traps' ( $P_{\text{WO}_4}$ ) is greater than the polarizability of 'U traps' ( $P_{\text{U}}$ ). The ratio  $P_{\text{WO}_4}/P_{\text{U}}$  can be found by extrapolating both curves to 0°K. and is

$$P_{\text{WO}_4}/P_{\text{U}} = 3.4. \quad \dots\dots(3)$$

It will be clear that such a difference in polarizability will influence the decay of the dielectric constant change at room temperature, making the initial portion relatively faster. This is, in fact, observed.

A difference in apparent polarizabilities of 'WO<sub>4</sub>' and 'U traps' is bound to arise, due to the difference in  $\tau$  value for each kind of trap. As the value of the constant  $\alpha$  obtained from Figure 2 is almost the same for each kind of trap (indicated by the fact that the two linear parts of the curve in Figure 2 are nearly parallel), it is likely that the difference in the values of  $\alpha$  determines the difference in polarizability. The ratio of the apparent polarizabilities may be calculated from equation (1) as  $\omega$ ,  $\Delta\epsilon_0$ ,  $\Delta\epsilon_\infty$ , and  $\tau$  are known. It is found that, at the measurement frequency of 2.7 Mc/s.,

$$P_{\text{WO}_4}/P_{\text{U}} = 3. \quad \dots\dots(4)$$

Agreement with the other experimental value above is better than might be expected.

### § 3. DISCUSSION AND CONCLUSION

Measurements of the increases in dielectric constant and loss of simple phosphors when excited suggest that the increases are due to the filling of electron traps (Garlick and Gibson 1947). If this result is assumed, dielectric measurements may be used to obtain more information on the nature of electron traps.

The study of the dielectric changes occurring in doubly or triply activated materials shows that the theory already developed (Garlick and Gibson 1947) can only be extended to cover such materials if fuller assumptions are made. It is necessary to assume that the introduction of the impurity centres gives rise to the formation of electron traps, and further, that some measurable parameters of the filled traps are determined by the nature of the impurity. This hypothesis has been suggested in previous work (Garlick and Gibson 1948, Garlick 1948), the measurable parameter concerned there being the depth of the electron traps. In the present case the parameter measured was relaxation time  $\tau$  of the filled electron traps.

The relaxation time of such a dipole system is related to the diameter and other fundamental properties of the electron trap. The relation between  $\tau$  and the nature of the activating impurity thus gives further evidence in favour of the view that the impurity ion forms the electron trap, possibly by distortion of the local lattice.

## ACKNOWLEDGMENTS

We wish to thank Professor M. L. E. Oliphant for the provision of facilities for this work and the Ministry of Supply (D.C.D.) for permission for one of us (A.F.G.) to remain in this laboratory for the completion of this work.

## REFERENCES

- GARLICK, G. F. J., 1948, *Solid Luminescent Materials* (New York: John Wiley), paper 5.  
 GARLICK, G. F. J., and GIBSON, A. F., 1947, *Proc. Roy. Soc. A*, **188**, 485; 1948, *Proc. Phys. Soc.*, **60**, 574; 1949, *J. Opt. Soc. Amer.* (in the press).  
 KLASENS, H. A., RAMSDEN, W., and CHOW QUANTIE, 1948, *J. Opt. Soc. Amer.*, **38**, 60.  
 KLASENS, H. A., and WISE, M. E., 1948, *J. Opt. Soc. Amer.*, **38**, 226.  
 RANDALL, J. T., and WILKINS, M. H. F., 1945, *Proc. Roy. Soc. A*, **184**, 366.

## Eigenfunctions following from Sommerfeld's Polynomial Method

BY A. RUBINOWICZ

Institute of Theoretical Mechanics, University of Warsaw

MS. received 7th June 1949

**ABSTRACT.** The eigenfunctions following from Sommerfeld's polynomial method were determined in the general case. They are products of a convergence factor  $E$  and a polynomial  $P$  given by a hypergeometric series. The form of  $E$  depends upon whether  $P$  is expressible by the ordinary or the confluent hypergeometric series.

SOMMERFELD'S polynomial method (Sommerfeld 1939) for the solution of the eigenvalue problems of the quantum theory is applicable only to a limited group of such problems. It supposes that the eigenfunctions  $f(x)$  are expressible in the form of a product of two functions  $f(x) = E(x)P(x)$ .

$P(x)$  is a polynomial fulfilling a linear differential equation of the second order of the form

$$x^2(A_2 + B_2x^h) \frac{d^2P}{dx^2} + 2x(A_1 + B_1x^h) \frac{dP}{dx} + (A_0 + B_0x^h)P = 0, \quad \dots\dots(1)$$

where  $A_i, B_i$  are constants ( $A_2 \neq 0$ ) and  $h$  is a positive integer.

The factor  $E(x)$  however is responsible for the convergence of the normalization integral and the fulfilment of boundary conditions. In a paper published elsewhere (Rubinowicz 1949) it is proved that  $E(x)$  can appear only in two forms, corresponding to  $B_2 \neq 0$  and  $B_2 = 0$ , provided that  $A_2 \neq 0$ . If the differential equation of the eigenvalue problem has the form

$$\frac{d}{dx} \left( p \frac{df}{dx} \right) - qf + \lambda \rho f = 0,$$

then we have

(I) in the case  $B_2 \neq 0$ ,

$$E = p^{-\frac{1}{2}} x^{A_1/A_2} (A_2 + B_2 x^h)^{(1/h)(B_1/B_2 - A_1/A_2)}; \quad \dots\dots(2a)$$

(II) in the case  $B_2 = 0$ ,

$$E = p^{-\frac{1}{2}} x^{A_1/A_2} \exp \{ (1/h)(B_1/A_2)x^h \}. \quad \dots\dots(2b)$$

Since the differential equation of the polynomial (1) is reducible to the hypergeometric differential equation (cf. Riemann-Weber 1901, p. 11) we can now write down the eigenfunctions for all cases accessible to Sommerfeld's polynomial method. For this purpose we must transform equation (1) into the hypergeometric differential equation. Writing

$$y = x^h \quad \dots\dots(3)$$

and

$$P = y^\mu \phi(y), \quad \dots\dots(4)$$

we obtain the differential equation

$$y^2(p_2 + q_2y) \frac{d^2\phi}{dy^2} + y(p_1 + q_1y) \frac{d\phi}{dy} + (p_0 + q_0y)\phi = 0. \quad \dots\dots(5)$$

Here

$$\left. \begin{aligned} p_2 = n_2, \quad p_1 = n_1 + 2\mu n_2, \quad p_0 = n_0 + \mu n_1 + \mu(\mu - 1)n_2, \\ q_2 = m_2, \quad q_1 = m_1 + 2\mu m_2, \quad q_0 = m_0 + \mu m_1 + \mu(\mu - 1)m_2, \end{aligned} \right\} \dots\dots(6a)$$

where

$$\left. \begin{aligned} n_2 = h^2 A_2, \quad n_1 = h\{2A_1 + (h-1)A_2\}, \quad n_0 = A_0, \\ m_2 = h^2 B_2, \quad m_1 = h\{2B_1 + (h-1)B_2\}, \quad m_0 = B_0. \end{aligned} \right\} \dots\dots(6b)$$

Determining  $\mu$  in such a way that  $p_0$  vanishes, that is, from (6a) and (6b), so that

$$\mu h(\mu h - 1)A_2 + 2\mu h A_1 + A_0 = 0,$$

and introducing a new independent variable

$$z = -\frac{q_2}{p_2}y = -\frac{B_2}{A_2}x^h, \quad \dots\dots(7)$$

we get in place of (5) the hypergeometric differential equation

$$z(1-z) \frac{d^2\phi}{dz^2} + \{\gamma - (\alpha + \beta + 1)z\} \frac{d\phi}{dz} - \alpha\beta\phi = 0. \quad \dots\dots(8a)$$

The constants  $\alpha, \beta, \gamma$  are here given according to (6a) and (6b) by the equations

$$\alpha + \beta + 1 = \frac{q_1}{q_2} = \frac{m_1}{m_2} + 2\mu = \frac{1}{h} \left( 2\frac{B_1}{B_2} - 1 \right) + 2\mu + 1, \quad \dots\dots(9a)$$

$$\alpha\beta = \frac{q_0}{q_2} = \frac{m_0}{m_2} + \mu \frac{m_1}{m_2} + \mu(\mu - 1) = \frac{1}{h^2 B_2} \{ \mu h(\mu h - 1)B_2 + 2\mu h B_1 + B_0 \}, \quad \dots\dots(9b)$$

$$\gamma = \frac{p_1}{p_2} = \frac{n_1}{n_2} + 2\mu = \frac{1}{h} \left( 2\frac{A_1}{A_2} - 1 \right) + 2\mu + 1. \quad \dots\dots(9c)$$

From (9a) and (9b) we obtain for  $\xi = \alpha$  or  $\xi = \beta$  the equation

$$(\mu h - \xi h)(\mu h - \xi h - 1)B_2 + 2(\mu h - \xi h)B_1 + B_0 = 0, \quad \dots\dots(10)$$

which is identical with Sommerfeld's condition for the breaking off of the power series.

The function  $\phi$  which is a solution of the hypergeometric differential equation (8a) is given by

$$\phi = F(\alpha, \beta, \gamma, z) = F[\alpha, \beta, \gamma, -(B_2/A_2)x^h], \quad \dots\dots(11)$$



so that from (3), (4) and (11) we obtain for the polynomial  $P$  the expression

$$P(x) = x^{\mu h} F[\alpha, \beta, \gamma, -(B_2/A_2)x^h]. \quad \dots\dots(12a)$$

In order that  $P(x)$  may be a polynomial,  $\alpha$  (or  $\beta$ ) must be a negative integer.

But we must remark that our transformation (7) can be used only in the case where  $B_2 \neq 0$ , and is inapplicable if  $B_2 = 0$ .

In this second case we have to apply the substitution

$$z = -\frac{2}{h} \frac{B_1}{A_2} x^h,$$

which transforms the differential equation (1) into

$$z \frac{d^2 \phi}{dz^2} + (\gamma - z) \frac{d\phi}{dz} - \alpha \phi = 0. \quad \dots\dots(8b)$$

The constant  $\gamma$  is here determined by (9c), whereas  $\alpha$  is given according to (10) by

$$\alpha = \frac{1}{2h} \frac{B_0}{B_1} + \mu.$$

(8b) is the differential equation of the confluent hypergeometric function  $F_1(\alpha, \gamma, z)$ . A solution of Sommerfeld's differential equation (1) is therefore in case (II) given by

$$P(x) = x^{\mu h} F_1\left(\alpha, \gamma, -\frac{2}{h} \frac{B_0}{B_1} x^h\right). \quad \dots\dots(12b)$$

We are now able to write down the complete eigenfunctions  $f(x) = E(x)P(x)$ . We get

(I) in the case  $B_2 \neq 0$  from equations (2a), (9a) and (12a),

$$f(x) = p^{-\frac{1}{2}} \xi^{1/2} \xi^{\gamma-1/2} (1+\xi)^{(\alpha+\beta-\gamma+1)/2} F(\alpha, \beta, \gamma, -\xi) \quad \text{where} \quad \xi = (B_2/A_2)x^h;$$

(II) in the case  $B_2 = 0$  from equations (2b), (9c) and (12b),

$$f(x) = p^{-\frac{1}{2}} \zeta^{1/2} \zeta^{\gamma-1/2} e^{\zeta/2} F_1(\alpha, \gamma, -\zeta) \quad \text{where} \quad \zeta = \frac{2}{h} \frac{B_1}{A_2} x^h.$$

The constants  $\alpha$  or  $\beta$  are here negative integers.

Using these expressions we can determine immediately the eigenfunctions in all cases accessible to Sommerfeld's polynomial method. For this purpose we must know the values of  $A_i$ ,  $B_i$  and  $h$ , which enable us to calculate the constants  $\alpha$ ,  $\beta$ ,  $\gamma$  with the aid of the formulae given in this paper. For all special cases we have dealt with in our former paper (Rubinowicz 1949) the values of  $A_i$ ,  $B_i$  and  $h$  can be found there.

#### REFERENCES

- RIEMANN, B., and WEBER, H., 1901, *Die partiellen Differentialgleichungen der mathematischen Physik*, 4th edition, Vol. II (Braunschweig: Vieweg und Sohn).  
 RUBINOWICZ, A., 1949, *Proc. K. Ned. Akad. Wet. Amst.*, **52**, 351.  
 SOMMERFELD, A., 1939, *Atombau und Spektrallinien*, Vol. II (Braunschweig: Vieweg und Sohn), p. 716.

## LETTERS TO THE EDITOR

### Origin of Low-Energy Electron Lines in the $\beta$ -spectrum of $^{198}\text{Au}$

The low-energy part of the  $\beta$ -spectrum of  $^{198}\text{Au}$  was investigated, using the  $254^\circ\text{-radial}$  electrostatic field spectroscopy that has been constructed in this laboratory. Several samples made from pure precipitated gold and also from gold foil were irradiated in the Harwell pile. It was found in all cases that two fairly intense conversion electron lines appear in the spectrum, one at energy 44 kev. and the other at 58 kev. Interpreted as due to internal conversion in gold in K and L shells respectively, they would correspond to  $\gamma$ -ray energies of 0.125 mev. and 0.072 mev. The intensity of these lines was observed over five days and the half-life was found to be of the order of three days.

The conversion-electron peak at 58 kev., which is broad, and due to 0.072 mev. radiation, is in agreement with the observation of Jnanananda (1946), but there is a lack of agreement among observers about  $\gamma$ -rays from  $^{198}\text{Au}$ , other than the well-known one at 0.4 mev. Electron lines due to  $\gamma$ -rays of very nearly the same energies as above have been reported by Valley (1941) and Helmholtz (1942) for  $^{197}\text{Hg}$ , which decays by K-capture to  $^{197}\text{Au}$ , the  $\gamma$ -rays, which are highly converted, being due to transitions from the excited states of  $^{197}\text{Au}$  to the ground state. It is suggested, therefore, that these conversion lines and the corresponding  $\gamma$ -rays are to be associated not with the slow-neutron induced activity,  $^{198}\text{Au}$ , but with the activity induced by fast neutrons during irradiation, giving  $^{197}\text{Pt}$  by (n, p) reaction. Thus,  $^{197}\text{Au} \xrightarrow{(n, p)} ^{197}\text{Pt} \xrightarrow{\beta^-} ^{197}\text{Au}$ . Excited  $^{197}\text{Au}$  produced by the  $\beta$ -decay of  $^{197}\text{Pt}$  would, on transition to the ground level, emit the same  $\gamma$ -rays, highly converted in gold, as are found in the K-capture decay of  $^{197}\text{Hg}$ .

Krishnan and Nahum (1941), who produced  $^{197}\text{Pt}$  by (d, p) reaction on platinum, found that the 2.8 day isotope, as studied by absorption methods, emits strong discrete groups of low-energy electrons of secondary origin, the maximum energy being 0.120 mev. Assuming K, L and M internal conversion in gold to be taking place, this would correspond to a  $\gamma$ -ray energy of 0.124 mev., in good agreement with the energy of the  $\gamma$  ray reported above. They also found evidence for a softer  $\gamma$  ray from  $^{197}\text{Pt}$  and give the energy as 0.075 mev., which again is in close agreement with the other  $\gamma$ -ray energy mentioned above. The half-life for this isotope,  $^{197}\text{Pt}$ , as given by McMillan *et al.* (1937) and Krishnan and Nahum (1941) is of the order of three days, which was also the value found for the decay of these conversion-electron lines.

A long strip of gold foil, made into a small tight roll, was then irradiated at Harwell, so that the inner portion of the coil would be shielded from resonance neutrons, which produce the  $^{198}\text{Au}$  activity. Measurement of the strength of  $^{198}\text{Au}$  activity as indicated by the 0.4 mev.  $\gamma$ -ray from equal areas of the shielded and unshielded portions of the foil showed that the unshielded portion was substantially stronger than the shielded one, as is to be expected. On the other hand, the intensity of the conversion-electron lines, relative to that of the continuous  $\beta$ -ray background of  $^{198}\text{Au}$ , was greater in the spectrum of the shielded foil. This further strengthens the suggestion that the activity responsible for these  $\gamma$ -rays and the conversion lines is induced in gold by fast neutrons and is not the  $^{198}\text{Au}$  activity.

A fuller account of this and other investigations of conversion lines from some other isotopes and also of the electrostatic  $\beta$ -ray spectroscopy used for this purpose will be given at a later date.

The author is very grateful to Professor P. B. Moon for his continued interest and guidance. He also wishes to thank Dr. D. M. Millest, with whom he collaborated in the design and construction of the  $\beta$ -ray spectroscopy, and the Government of India for a State Scholarship.

Physics Department, The University,  
Edgbaston, Birmingham, 15.  
18th September 1949.

B. V. THOSAR.

HELMHOLTZ, A. C., 1942, *Phys. Rev.*, **61**, 204.

JNANANANDA, S., 1946, *Phys. Rev.*, **70**, 812.

KRISHNAN, R. S., and NAHUM, E. A., 1941, *Proc. Camb. Phil. Soc.*, **37**, 422.

McMILLAN, E., KAMEN, M., and RUBEN, S., 1937, *Phys. Rev.*, **52**, 375.

VALLEY, G. E., 1941, *Phys. Rev.*, **60**, 167.

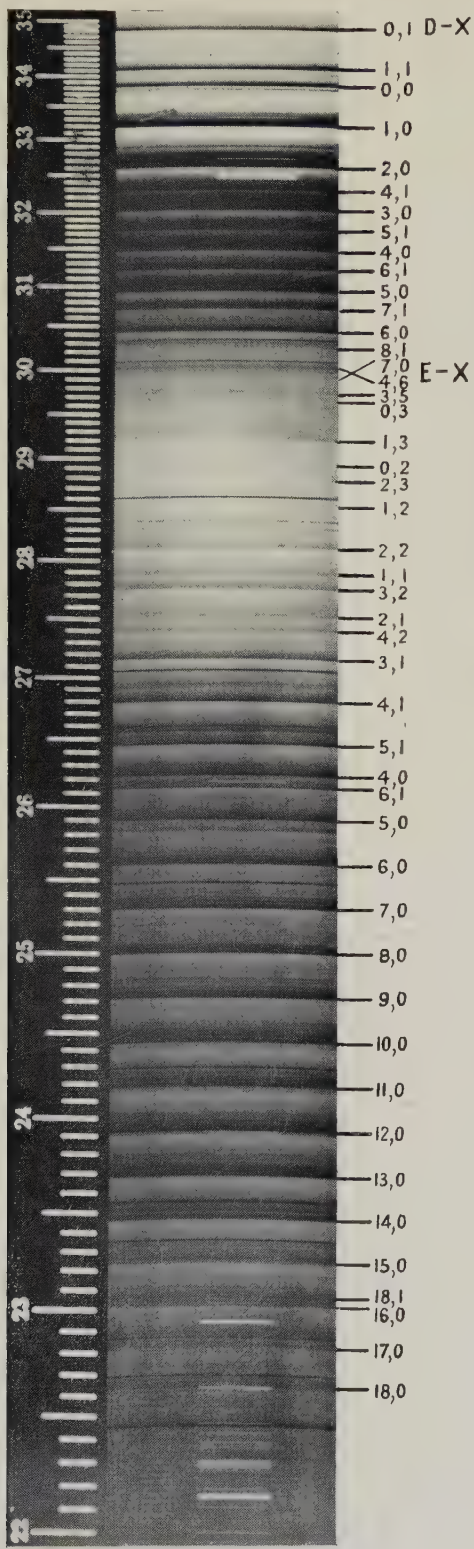
# The Ultra-Violet Absorption Spectrum of SnO

In the course of other work, we have recently obtained low-dispersion spectrograms of the absorption by SnO in the range 2040–3500 Å. (see Plate). Two band-systems are known in this region: the less refrangible system, D–X, studied especially by Connolly (1933), and the E–X system, first obtained by Loomis and Watson (1934) in emission. The absorption plates add little to our knowledge of the D–X system, but about twenty new

## The E–X System of SnO

v'	(42059.5)			
	v'' →			
19				
18	44170.3 358.0	43351.9 351.4	804.9	42547.0
17	43812.3 387.3	43000.5 (382.9)	811.8	
16	43425.0 394.5	(42617.6) (402.2)	(807.4)	
15	43030.5 412.9	42215.4 409.4	815.1	
14	42617.6 415.0	41806.0 418.6	811.6	
13	42202.6 426.6	41387.4 430.3	815.2	(39773.5)
12	41776.0 440.5	40957.1	818.9	
11	41335.5 440.6	(39706.7)		
10	40894.9 448.3			
9	40446.6 454.3	38823.9 455.6		
8	39992.3 464.4	38368.3 460.7		
7	39527.9 470.7	38714.0 468.7	813.9	37907.6 799.6
6	39057.2 471.7	38245.3 472.1	811.9	
5	38585.5 477.5	37773.2 480.0	812.3	35373.6
4	38108.0 479.1	37293.2 485.1	814.8	(34118.7) (487.1)
3	37628.9 489.5	36808.1 485.2	820.8	(33801.1) (485.5)
2	37139.4 495.8	36322.9 497.6	809.6	35684.8
1	36643.6	35825.3	808.4	35513.3 496.4
0			804.6	34710.5 494.0
			806.7	33921.2 495.3
			801.7	33425.9 503.4
			802.8	(32647.2) (505.8)
			800.4	32922.5
			791.3	32141.4
			781.1	
			789.3	
			790.6	
			800.4	
			802.8	
			804.6	
			806.7	
			808.4	
			810.8	
			812.3	
			814.8	
			816.5	
			818.9	
			820.8	
			822.3	
			824.8	
			826.3	
			828.8	
			830.3	
			832.8	
			834.3	
			836.8	
			838.3	
			840.8	
			842.3	
			844.8	
			846.3	
			848.8	
			850.3	
			852.8	
			854.3	
			856.8	
			858.3	
			860.8	
			862.3	
			864.8	
			866.3	
			868.8	
			870.3	
			872.8	
			874.3	
			876.8	
			878.3	
			880.8	
			882.3	
			884.8	
			886.3	
			888.8	
			890.3	
			892.8	
			894.3	
			896.8	
			898.3	
			900.8	
			902.3	
			904.8	
			906.3	
			908.8	
			910.3	
			912.8	
			914.3	
			916.8	
			918.3	
			920.8	
			922.3	
			924.8	
			926.3	
			928.8	
			930.3	
			932.8	
			934.3	
			936.8	
			938.3	
			940.8	
			942.3	
			944.8	
			946.3	
			948.8	
			950.3	
			952.8	
			954.3	
			956.8	
			958.3	
			960.8	
			962.3	
			964.8	
			966.3	
			968.8	
			970.3	
			972.8	
			974.3	
			976.8	
			978.3	
			980.8	
			982.3	
			984.8	
			986.3	
			988.8	
			990.3	
			992.8	
			994.3	
			996.8	
			998.3	
			1000.8	





Bands of the D-X and E-X systems of SnO photographed in absorption on Hilger small quartz prism spectrograph : Ilford Q.1 plate.  
Temperature c. 1,400° C., effective path-length c. 25 cm.



bands have been assigned to the E-X system. Apart from the necessity of raising their  $v'$ -values by one unit, the vibrational analysis of Loomis and Watson is unchanged, and the main effect of our measurements, which are summarized in the Table, is to provide more information about the course of the upper-state vibrational levels. (The new values of  $\Delta G'$  are also more consistent than those of Loomis and Watson: the reason seems to be that for the vibrational analysis of a band-system of a molecule which gives an irresolvable complex of isotopic heads it is a positive advantage to use not too high dispersion.)

In attempting to derive an expression for  $G_v'$ , we used the values of  $G_v''$  given by Jevons (1938):  $G_v'' = 822.4(v'' + \frac{1}{2}) - 3.73(v'' + \frac{1}{2})^2$ . No simple expression for  $G_v'$  was however found to fit the levels over the whole range, but up to  $v' = 17$  the equation

$$G' = 508.0(v' + \frac{1}{2}) - 2.9(v' + \frac{1}{2})^2 - 5 \times 10^{-5}(v' + \frac{1}{2})^5$$

is reasonably satisfactory. With this,  $\nu_0 = 36,295 \text{ cm}^{-1}$ .

The sharp drop in the vibrational interval beginning at  $v' = 18$  seems to be real and suggests that this point is not far from a dissociation limit. Graphical extrapolation gives  $D_0' \sim 1.2 \text{ ev.}$ , corresponding to a dissociation limit  $5.6_g \text{ ev.}$  above  $v'' = 0$ . This value of  $D_0'$  agrees fairly well with that suggested earlier by analogy with SnSe (Vago and Barrow 1946). Linear extrapolation of the ground-state vibrational intervals leads to  $D_0'' = 5.6 \text{ ev.}$ , so it is possible that both states dissociate into the same atomic products.

Band-systems of SnO are also expected at shorter wavelengths than the E-X system. On some of our plates weak red-degraded bands are to be seen with heads at about 2037, 2050, 2054, 2069, 2073, 2084, 2102, 2117 and 2132 Å. These may belong to a new system, but we have so far been unable to get pictures on which the bands are sufficiently well defined for accurate measurement.

To complete the outline of the absorption spectrum of this molecule—so far as it is known at present—it may be mentioned that, contrary to statements in the literature (e.g. Sharma 1944), the stronger bands of the B and C systems (Pearse and Gaydon 1941) are also observed in absorption (Mrs. R. E. Richards, unpublished work): the vibrational analysis of these bands is however still uncertain.

Physical Chemistry Laboratory,  
Oxford.  
21st August 1949.

B. EISLER.  
R. F. BARROW.

CONNELLY, F. C., 1933, *Proc. Phys. Soc.*, **45**, 780.

JEVONS, W., 1938, *Proc. Phys. Soc.*, **50**, 910.

LOOMIS, F. W., and WATSON, T. F., 1934, *Phys. Rev.*, **45**, 805.

PEARSE, R. W. B., and GAYDON, A. G., 1941, *Identification of Molecular Spectra* (London: Chapman and Hall).

SHARMA, D., 1944, *Proc. Nat. Acad. Sci. India*, **14A**, 133.

VAGO, E. E., and BARROW, R. F., 1946, *Proc. Phys. Soc.*, **58**, 707.

## X-Ray Line Broadening in Metals

It is the author's belief that the diverse opinions of different workers on the explanation of x-ray line broadening in metals can be reconciled in terms of the hypothesis of Dehlinger and Kochendorfer (1939 a, b) and Kochendorfer (1944) that both particle size and stress effects are presented simultaneously. The theoretical work of Bragg (1942, 1949) gives mathematical support to the hypothesis.

In the limiting case of pure particle size broadening the line breadth  $\beta_P$  is related to the effective particle size  $\epsilon$ , the x-ray wavelength  $\lambda$  and the Bragg angle  $\theta$  by the equation (Jones 1938)

$$\beta_P = \frac{\lambda}{\epsilon \cos \theta}.$$

For pure stress broadening the breadth  $\beta_S$  is related to the effective strain  $\eta$  (Stokes and Wilson 1944) and the Bragg angle by the equation

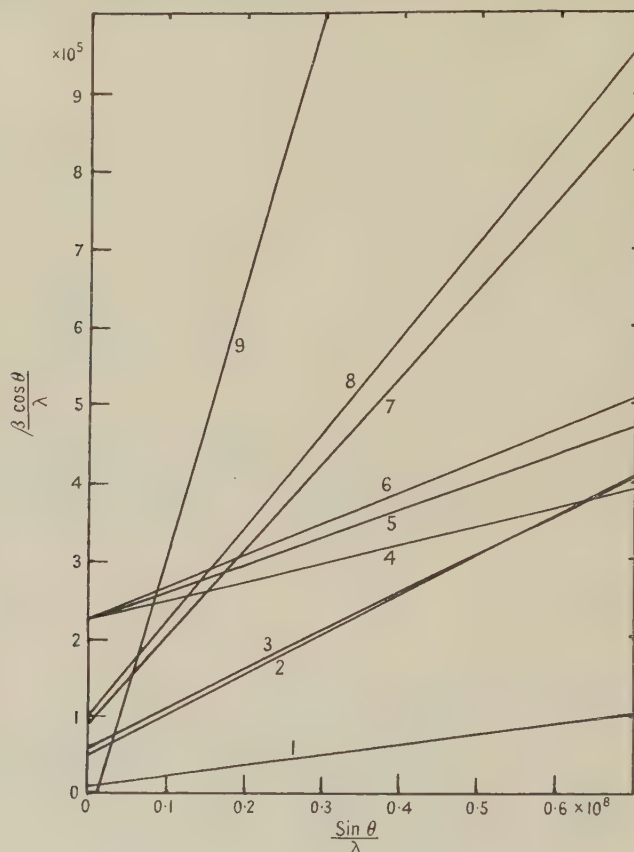
$$\beta_S = \eta \tan \theta.$$



If both types of broadening are present, the resultant line breadth  $\beta$  should be obtained by compounding the component lines as discussed by Jones (1938), Shull (1946) and Stokes (1948), but it has been shown by Wood and Rachinger (1949) that for a commonly occurring line shape the breadths are additive, i.e.  $\beta = \beta_P + \beta_S$ . In this case we may write

$$\frac{\beta \cos \theta}{\lambda} = \frac{1}{\epsilon} + \eta \frac{\sin \theta}{\lambda}.$$

In a distorted lattice the effective particle size  $\epsilon$  must be interpreted as a measure of the volume of regions in the lattice which diffract coherently. In anisotropic metals the strain



Summary of line broadening measurements.

- Key : 1. Aluminium filings, CuK $\alpha$ , Hall and Williamson (unpublished measurements).  
 2. Copper filings, ZnK $\alpha$ , Brindley (1939).  
 3. Copper filings, CuK $\alpha$ , Stokes, Pascoe and Lipson (1943).  
 4. Copper sheet, 20% reduction, CuK $\alpha$ , Dehlinger and Kochendorfer (1939).  
 5. Copper sheet, 60% reduction, CuK $\alpha$ , Dehlinger and Kochendorfer (1939).  
 6. Copper sheet, 99.5% reduction, CuK $\alpha$ , Dehlinger and Kochendorfer (1939).  
 7. Rhodium filings, CuK $\alpha$ , Brindley (1938).  
 8. Rhodium filings, ZnK $\alpha$ , Brindley (1938).  
 9. Martensite rod, FeK $\alpha$ , Wheeler and Jaswon (1947).

distribution is not the same for different crystallographic planes, and a relationship of the type

$$\frac{\beta \cos \theta}{\lambda} = \frac{1}{\epsilon} + \frac{2\sigma}{E_{hkl}} \frac{\sin \theta}{\lambda}$$

is frequently a better representation of the experimental breadths. In this equation  $E_{hkl}$  is the value of Young's modulus for the direction perpendicular to the planes  $\{hkl\}$  and  $\sigma$  is the Laue breadth of the stress distribution function, which is assumed to be independent of direction.

The accurate determination of the value of  $\epsilon$  from these equations is difficult, since the intercept which defines it depends largely on the breadths of lines for which  $\sin \theta/\lambda$  is small. Metals rarely diffract at very low angles, and for such lines the total broadening is small and difficult to measure accurately. A number of published results have been analysed in this way and the best straight lines shown in the diagram determined by the method of least squares. It will be seen that the slopes of the lines (i.e. the stress effects) increase progressively from soft to hard metals. The intercepts are all positive with the exception of that for martensite, and a very small error in the steep slope of the graph would account for this physically unreal result. The mean value of all intercepts corresponds to  $\epsilon=10^{-5}$  cm. Owing to the uncertainties of the analysis no more than the order of magnitude of this quantity can be regarded as significant. This is about the same as that determined by Wood and Rachinger (1949) by a different method. The physical significance of this value may be understood from the theory of dislocations. There is abundant evidence (Taylor 1934, Brown 1941, Koehler 1941, Cottrell and Churchman 1949) suggesting that the maximum density of dislocations in most cold-worked metals corresponds to an average distance between dislocation lines of about  $10^{-6}$  cm. The coherently diffracting regions of the lattice ought to have an effective particle size rather greater than this, since the dislocation lines are thought to be long compared with their separation. This suggestion agrees well with the experimental values, and it seems that direct calculations of line broadening based on the dislocation model should lead to a much clearer understanding of the problem.

Department of Metallurgy,  
University of Birmingham.  
30th August 1949.

W. H. HALL.

BRAGG, W. L., 1942, *Nature, Lond.*, **149**, 511; 1949, *Proc. Camb. Phil. Soc.*, **45**, 125.  
BRINDLEY, G. W., 1938, *Proc. Phys. Soc.*, **50**, 501; 1939, *Ibid.*, **51**, 432.  
BROWN, W. F., 1941, *Phys. Rev.*, **60**, 139.  
COTTRELL, A. H., and CHURCHMAN, A. T., 1949, *J. Iron and Steel Inst.*, **162**, 271.  
DEHLINGER, U., and KOCHENDORFER, A., 1939 a, *Z. Metallkde.*, **31**, 231; 1939 b, *Z. Kristallogr. A.*, **101**, 134.  
JONES, F. W., 1938, *Proc. Roy. Soc. A*, **166**, 16.  
KOCHENDORFER, A., 1944, *Z. Kristallogr. A*, **105**, 393.  
KOEHLER, J. S., 1941, *Phys. Rev.*, **60**, 397.  
SHULL, C. G., 1946, *Phys. Rev.*, **70**, 679.  
STOKES, A. R., 1948, *Proc. Phys. Soc.*, **61**, 382.  
STOKES, A. R., PASCOE, K. J., and LIPSON, H., 1943, *Nature, Lond.*, **151**, 137.  
STOKES, A. R., and WILSON, A. J. C., 1944, *Proc. Phys. Soc.*, **56**, 174.  
TAYLOR, G. I., 1934, *Proc. Roy. Soc. A*, **145**, 362.  
WHEELER, J. A., and JASWON, M. A., 1947, *J. Iron and Steel Inst.*, **157**, 161.  
WOOD, W. A., and RACHINGER, W. A., 1949, *J. Inst. Metals*, **75**, 571.

## Magnetic Viscosity in Mn-Zn Ferrite

In a previous paper (Street and Woolley 1949), referred to below as I, a theory of magnetic viscosity, based on activation energy concepts, has been given. The relation between the rate of increase of the intensity of magnetization of a specimen and the time of observation (equation (9) of I), is

$$\frac{dI}{dt} = \frac{\bar{i}p k T}{t} [\exp(-\lambda_0 t) - \exp(-Ct)],$$

where the symbols have the meanings given in I. The general solution of this expression is

$$\Delta I = \bar{i}p k T \left[ Ei(-\lambda_0 t) - Ei(-Ct) + \frac{E_0}{kT} \right], \quad \dots \dots (1)$$

$\Delta I$  being zero at time  $t=0$ .

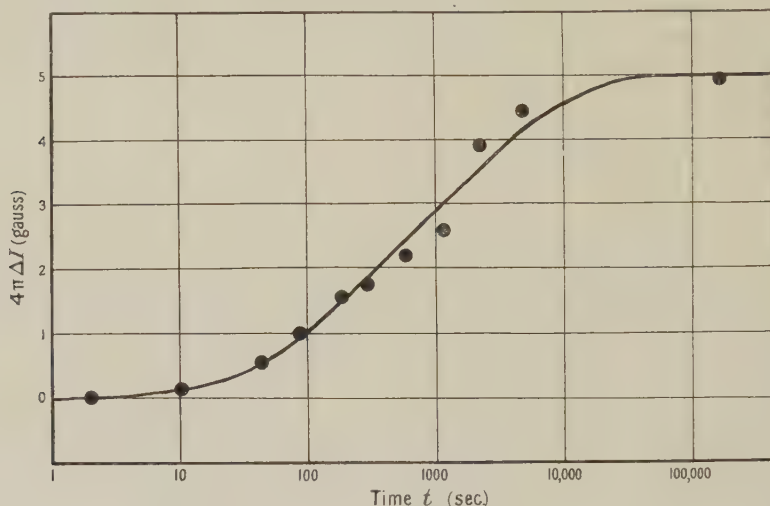
In I it was found that only a limited range of  $t$  need be considered, viz. for values of  $t$  from  $t > t_c$ , where  $Ei(-Ct_c) \ll Ei(-\lambda_0 t_c)$ , to  $t < t_0$ , where  $\lambda_0 t_0 \ll 1$ . Over this range (1) reduces to

$$\Delta I = \bar{i} p k T \log t + \text{constant}. \quad \dots\dots (2)$$

The results of experiments made on magnetic viscosity in alnico satisfied this simplified equation (2). However, in those cases where observations are extended over time periods greater than the limits detailed above, it is necessary to use the exact form given in equation (1). A convenient test of the expression is provided by considering the experimental results for magnetic viscosity in Mn-Zn ferrite (Snoek 1947). The numerical values of the constants of equation (1) were chosen to fit Snoek's experimental results, and the equation obtained was

$$\Delta B = 0.875[Ei(-5.4 \times 10^{-5}t) - Ei(-1.64 \times 10^{-2}t) + 5.72], \quad \dots\dots (3)$$

where  $\Delta B$  is the difference between the value of the magnetic induction of the specimen at any time  $t$  seconds and that at  $t=0$ . A plot of equation (3) and Snoek's experimental results are shown in the Figure, and it will be seen that satisfactory agreement is obtained.



Magnetic viscosity in Mn-Zn ferrite.

The full line is calculated from equation (3). ● Experimental points obtained by Snoek (1947).

The curve of best fit as drawn by Snoek is almost identical with the theoretical curve of equation (3).

From the numerical equation, the following quantitative results may be obtained:

$$E_0/kT = 5.72; \quad C = 1.64 \times 10^{-2} \text{ sec}^{-1}; \quad 4\pi\bar{i}p kT = 0.875.$$

Thus, if it is assumed that  $T = 290^\circ \text{K}$ , then the upper value of the activation energy,  $E_0$ , is appropriate to a temperature of  $1,660^\circ \text{K}$ , and  $\bar{i}p = 1.72 \times 10^{12}$  gauss/erg. This value of  $E_0$  is very much smaller than the activation energy suggested by Snoek, viz.  $10,000^\circ \text{K}$ .

Equation (1) is of the same general form as that obtained by Becker and Döring (1939) in their treatment of magnetic viscosity as the analogue of dielectric after-effect. However, the importance of equation (1) lies in the fact that the constants involved are expressed in terms of quantities which are characteristic of the domain processes which lead to magnetic viscosity. Thus, although it is fairly certain that the domain processes are different for soft iron, Mn-Zn ferrite and alnico, it is of interest to compare the available values of the various constants of these three materials, assuming relation (1) to hold in each case:

	Fe*	Mn-Zn ferrite	Alnico
$C \text{ (sec}^{-1}\text{)}$	$2 \times 10^{14}$	$1.6 \times 10^{-2}$	—
$\bar{i}p \text{ (gauss erg}^{-1}\text{)}$	$2.6 \times 10^{13}$	$1.7 \times 10^{12}$	$3.6 \times 10^{14}$
$E_0/k \text{ (}^\circ \text{K.)}$	10,300	1,660	15,000 (estimate)

\* From analysis of results obtained by Richter (1937) using soft iron at  $55^\circ \text{C}$ .



Snoek considers that the phenomena of magnetic viscosity and time decrease of permeability are two different aspects of identical domain processes. It follows therefore that the activation energy theory of magnetic viscosity given in I should account satisfactorily for time decrease of permeability. From preliminary experimental results using alnico specimens, it appears that the theoretical predictions are confirmed. It is hoped to publish further details of this work at a later date.

The University, Nottingham.  
12th September 1949.

R. STREET.  
J. C. WOOLLEY.

- BECKER, R., and DÖRING, W., 1939, *Ferromagnetismus* (Berlin: Springer), p. 247 ff.  
RICHTER, G., 1937, *Ann. Phys., Lpz.*, **29**, 605.  
SNOEK, J. L., 1947, *New Developments in Ferromagnetic Materials* (Amsterdam: Elsevier), p. 55.  
STREET, R., and WOOLLEY, J. C., 1949, *Proc. Phys. Soc. A*, **62**, 562.

## REVIEWS OF BOOKS

*Scientific Foundations of Vacuum Technique*, by SAUL DUSHMAN. Pp. xi + 882.  
First Edition. (New York: John Wiley; London: Chapman and Hall, 1949). 90s.

The introduction of Gaede's mercury diffusion pump marked the commencement of great advances in high-vacuum technique. A new industry—vacuum technology—has grown up, and a small-scale laboratory operation has been transformed within the past forty years into an industrial one, carried out on a scale that would have been almost inconceivable in the minds of the early workers in the field. Speed, and greater speed, is demanded for the exhaustion of all types of electronic equipment, cyclotrons, betatrons, etc., and for vacuum distillation, dehydration and the evaporation of metals and other substances. These higher speeds have been attained by paying more attention to jet design in pumps.

Only a few books have been written on the subject, and the first one to appear was that written by Dr. Dushman in 1922. The recent rapid advances have more than justified the present volume, which workers in this field have required for some time. In spite of its 882 pages, and of the fact that it contains a reference to the researches of practically every investigator in high-vacuum technique, it is no mere encyclopaedia, no catalogue of methods and results, but contains the theory which is so essential if successful operations are to be understood and appreciated. It is not only a complete revision of the earlier work, but it includes a very considerable amount of new material. The diagrams are numerous and good, and a useful feature is the copious references to original papers.

The opening chapters deal with the kinetic theory of gases and their flow through tubes and orifices, features which play important parts in high-vacuum work and which considerably affect pumping speeds. The treatment of mechanical and vapour pumps is interesting and explicit. The rôles of diffusion and condensation are discussed, and the extreme importance of jet design is fully explained. Alexander's modern type of pump is described and reasons are given why all vapour pumps do not function as diffusion ones—a conclusion which agrees with Langmuir's view on their operation. Manometers receive full treatment and the various indispensable leak detectors are included. Then follows a description of other methods whereby gases may be removed from vessels, such as the sorption of gases and vapours by solids, and in particular by activated charcoal, silicates, cellulose and metals. Diffusion through the latter and degassing problems are also fully discussed. The chapter on chemical and electrical clean-up of gases at low pressures gives a comprehensive survey of the clean-up of gases by evaporated metals, technical getters, incandescent filaments, cold and hot cathode discharges, and the production of extremely low pressures in sealed-off devices. The later chapters deal with vapour pressures, rates of evaporation and dissociation pressures—including useful information on vacuum distillation—and the deposition of films.

The book is a complete treatment of the subject, one which should be in the hands of every worker in the fields of physics, engineering and chemistry.

F. H. NEWMAN.

*Thermocinétique*, by PIERRE VERNOTTE. Pp. xxi + 459. Publications Scientifiques et Techniques du Ministère de l'Air. (Paris: Service de Documentation et d'Information Technique de l'Aéronautique, 1949.) No price.

Monsieur Vernotte is a well-known writer on thermal subjects, and those familiar with his work are aware that he does not blindly follow convention without asking the reasons for it. In this book, which deals with the subject that is sometimes described as Heat Transfer, he opens his challenge to tradition by objecting to the traditional names, and selecting eventually that of thermokinetics, so that, between them, thermokinetics and thermodynamics cover the main part of the subject of Heat.

After this, and before we begin on the main subject, we find a stimulating discussion of the question whether the unit of heat is indeed a unit of energy, and whether, therefore, many of us are right in saying that the erg or joule is the proper unit for heat quantities; the author thinks it is not, though it may be used for convenience.

The main part of the book deals with conduction, convection and radiation. In dealing with the first of these, Vernotte sets up the differential equation in the usual way, with a perfectly correct warning that it is only strictly applicable if the thermal constants do not vary with temperature. He claims also that the passage from a difference between two first derivatives to a second derivative is not really valid, though he accepts it in practice. The reviewer confesses to an inability to understand the grounds on which the objection is based.

Having set up the equation, he solves a number of problems; these are well chosen for their illustrative value or for practical use, but they do not illustrate as many methods as might perhaps have been expected in a book of this size. There is no reference to the value of conjugate function methods in two-dimensional problems, nor of the Laplace transform.

Convection is interestingly treated, and the main laws of radiation are brought out.

Altogether, as mentioned earlier, the value of the book is as a stimulus to our own thinking, rather than as a compendium of methods or results, but for its actual purpose it is an extremely successful effort.

J. H. A.

## CORRIGENDUM

"The Physical Basis of Life", by J. D. BERNAL (*Proc. Phys. Soc. A*, 1949, **62**, 537).

Page 540, last clause of footnote \*, viz.: "and secondly, they must originate and develop out of some pre-existing system, or, in plain English, they must work and they must have got there in the first place" *should occur* in the text immediately after the words "dynamic stability" (line 22).

## CONTENTS FOR SECTION B

	PAGE
Prof. E. N. DA C. ANDRADE and Mr. A. J. KENNEDY. An Automatic Recording Apparatus for the Study of Flow and Recovery in Metals . . . . .	669
Dr. H. KOLSKY. An Investigation of the Mechanical Properties of Materials at very High Rates of Loading . . . . .	676
Dr. K. W. HILLIER. A Method of Measuring some Dynamic Elastic Constants and its Application to the Study of High Polymers . . . . .	701
Prof. L. C. MARTIN. The Theory of the Microscope—IV : The Boundary-Wave Theory of Image Formation . . . . .	713
Mr. W. WEINSTEIN. Wave-front Aberrations of Oblique Pencils in a Symmetrical Optical System : Refraction and Transfer Formulae . . . . .	726
Mr. T. S. MOSS. The Temperature Variation of the Long-Wave Limit of Infra-Red Photoconductivity in Lead Sulphide and Similar Substances . . . . .	741
Reviews of Books . . . . .	749
Contents for Section A . . . . .	750
Abstracts for Section A . . . . .	751
Corrigendum . . . . .	752

---

## ABSTRACTS FOR SECTION B

*An Automatic Recording Apparatus for the Study of Flow and Recovery in Metals,*  
by E. N. DA C. ANDRADE and A. J. KENNEDY.

**ABSTRACT.** An apparatus is described which records continuously on photographic paper the extension-against-time curve of a metal wire creeping under stress. The length and time scales are recorded on the paper at the same time as the extension, so that deformation of the paper during development and drying does not affect the accuracy of the record, which allows an extension of up to 10 cm. to be read to within 0.02 mm. The apparatus also automatically removes and restores, repeatedly if desired, the load at times which can be set before the start of the experiment.

*An Investigation of the Mechanical Properties of Materials at very High Rates of Loading,* by H. KOLSKY.

**ABSTRACT.** A method of determining the stress-strain relation of materials when stresses are applied for times of the order of 20 microseconds is described. The apparatus employed was a modification of the Hopkinson pressure bar, and detonators were used to produce large transient stresses. Thin specimens of rubbers, plastics and metals were investigated and the compressions produced were as high as 20% with the softer materials. It was found that whilst Perspex recovered almost as soon as the stress was removed, rubbers and polythene showed delayed recovery, and copper and lead showed irrecoverable flow. The phenomenon of delayed recovery is discussed in terms of the theory of mechanical relaxation and *memory* effects in the material.



*A Method of Measuring some Dynamic Elastic Constants and its Application to the Study of High Polymers*, by K. W. HILLIER.

**ABSTRACT.** The preliminary work on the measurement of velocity of propagation and attenuation of longitudinal sound oscillations in high polymer filaments already described by Hillier and Kolsky has been continued. It was concluded in that paper that temperature control would be advantageous, and that by varying the temperature and the frequency of oscillations more useful information could be acquired. An apparatus is described whereby the velocity of the propagation and attenuation of longitudinal oscillations throughout the range  $0^{\circ}$  to  $50^{\circ}$  C. and 500 c/s. to 30 kc/s. can be measured. The results obtained with one material, polythene, are discussed in terms of several theories of the elasticity of high polymers, and the constants of the several equations considered are calculated from the data.

*The Theory of the Microscope—IV: The Boundary-Wave Theory of Image Formation*, by L. C. MARTIN.

**ABSTRACT.** The theory of boundary waves (Young, Rubinowicz, and others) is developed for the two-dimensional case and applied to discuss image formation for small apertures, obstacles and phase-retarding laminae. The theoretical predictions are illustrated by diffraction photographs. It is hoped thus to contribute towards a fuller understanding of microscope images for bright-field, dark-field and phase-contrast conditions.

*Wave-front Aberrations of Oblique Pencils in a Symmetrical Optical System: Refraction and Transfer Formulae*, by W. WEINSTEIN.

**ABSTRACT.** The wave-front aberrations which occur in a pencil traversing a symmetrical optical system at a finite field angle are defined in a new way. Refraction and transfer formulae are derived for all the aberration coefficients up to and including those depending on the fourth power of the aperture of the pencil.

*The Temperature Variation of the Long-Wave Limit of Infra-Red Photoconductivity in Lead Sulphide and Similar Substances*, by T. S. MOSS.

**ABSTRACT.** Measurements have been carried out on the spectral distribution of the photoconductive effect in layers of lead sulphide, selenide and telluride, at temperatures ranging from room temperature to that of liquid hydrogen. It is shown that cooling has a marked effect on the long-wave limit of sensitivity, which increases by as much as two microns on cooling with liquid hydrogen.

Brief descriptions of spectral measurements on these materials have already been published by the author. It is shown that depopulation of energy levels due to thermal activation of electrons is not responsible for the shift of spectral sensitivity. The suggestion is made that the shift may be related to the variation of dielectric constant with temperature.



## PHYSICAL SOCIETY SPECIALIST GROUPS

## OPTICAL GROUP

The Physical Society Optical Group exists to foster interest in and development of all branches of optical science. To this end, among other activities, it holds meetings about five times a year to discuss subjects covering all aspects of the theory and practice of optics, according to the papers offered.

## COLOUR GROUP

The Physical Society Colour Group exists to provide an opportunity for the very varied types of worker engaged on colour problems to meet and to discuss the scientific and technical aspects of their work. Five or six meetings for lectures and discussions are normally held each year, and reprints of papers are circulated to members when available. A certain amount of committee work is undertaken, and reports on Defective Colour Vision (1946) and on Colour Terminology (1948) have already been published.

## LOW TEMPERATURE GROUP

The Low Temperature Group was formed to provide an opportunity for the various groups of people concerned with low temperatures—physicists, chemists, engineers, etc.—to meet and become familiar with each other's problems. The Group seeks to encourage investigations in the low temperature field and to assist in the correlation and publication of data.

## ACOUSTICS GROUP

The Acoustics Group was formed to meet the long felt need for a focus of acoustical studies in Great Britain. The scope includes the physiological, architectural, psychological, and musical aspects of acoustics as well as the fundamental physical studies on intensity, transmission and absorption of sound. The Group achieves its object by holding discussion meetings, by the circulation of reprints and by arranging symposia on selected acoustical topics.

*Further information may be obtained from the Offices of the Society :*

1 LOWTHER GARDENS, PRINCE CONSORT ROAD, LONDON S.W. 7.

## BULLETIN ANALYTIQUE

## Publication of the Centre National de la Recherche Scientifique, France

The *Bulletin Analytique* is an abstracting journal which appears monthly in two parts, Part I covering scientific and technical papers in the mathematical, chemical and physical sciences and their applications, Part II the biological sciences.

The *Bulletin*, which started on a modest scale in 1940 with an average of 10,000 abstracts per part, now averages 35 to 40,000 abstracts per part. The abstracts summarize briefly papers in scientific and technical periodicals received in Paris from all over the world and cover the majority of the more important journals in the world scientific press. The scope of the *Bulletin* is constantly being enlarged to include a wider selection of periodicals.

The *Bulletin* thus provides a valuable reference book both for the laboratory and for the individual research worker who wishes to keep in touch with advances in subjects bordering on his own.

A specially interesting feature of the *Bulletin* is the microfilm service. A microfilm is made of each article as it is abstracted and negative microfilm copies or prints from microfilm can be purchased from the editors.

The subscription rates for Great Britain are 4,000 frs. (£5) per annum for each part. Subscriptions can also be taken out to individual sections of the *Bulletin* as follows :

	frs.	
Pure and Applied Mathematics—Mathematics—Mechanics	550	14/6
Astronomy—Astrophysics—Geophysics .. .. .	700	18/-
General Physics—Thermodynamics—Heat—Optics—Electricity and Magnetism .. .. .	900	22/6
Atomic Physics—Structure of Matter .. .. .	325	8/6
General Chemistry—Physical Chemistry .. .. .	325	8/6
Inorganic Chemistry—Organic Chemistry—Applied Chemistry—Metallurgy .. .. .	1,800	45/-
Engineering Sciences .. .. .	1,200	30/-
Mineralogy—Petrography—Geology—Paleontology .. .. .	550	14/6
Biochemistry—Biophysics—Pharmacology .. .. .	900	22/6
Microbiology—Virus and Phages .. .. .	600	15/6
Animal Biology—Genetics—Plant Biology .. .. .	1,800	45/-
Agriculture—Nutrition and the Food Industries .. .. .	550	14/6

Subscriptions can be paid directly to the editors : Centre National de la Recherche Scientifique, 18, rue Pierre-Curie, Paris 5ème. (Compte-chèque-postal 2,500-42, Paris), or through Messrs. H. K. Lewis & Co. Ltd., 136, Gower Street, London W.C. 1.



*The*  
**PHILOSOPHICAL  
MAGAZINE**

(First Published 1798)

*A Journal of  
Theoretical Experimental  
and Applied Physics*

EDITOR :

**PROFESSOR N. F. MOTT,**  
M.A., F.R.S.

EDITORIAL BOARD :

**SIR LAWRENCE BRAGG,**  
O.B.E., M.C., M.A., D.Sc., F.R.S.

**ALLAN FERGUSON,**  
M.A., D.Sc.

**SIR GEORGE THOMSON,**  
M.A., D.Sc., F.R.S.

**PROFESSOR A. M. TYNDALL,**  
D.Sc., F.R.S.

ANNUAL SUBSCRIPTION

**£5 2s. 6d.**

OR

**10s. 6d.**

EACH MONTH  
POST-FREE

Contents for November 1949

**Dr. E. P. WOHLFARTH** on "The Magnetic Properties of Nickel-Cobalt and Related Alloys".

**Mr. S. T. MA** on "The Vacuum Polarization in the Positron Theory".

**Dr. S. R. KHASTGIR, F.N.I., & Mr. R. ROY, M.Sc.,** on "The Study of the Wave-forms of Atmospherics".

**Mr. M. G. TROCHERIS** on "Electrodynamics in a Rotating Frame of Reference".

**Mr. E. R. RAE, M.A.,** on "The Internal Pair Creation in  $\text{Na}^{24}$ ".

**Messrs. E. CORINALDESI & G. FIELD** on "The Scattering of Pseudoscalar Charged Mesons by Nucleons.—I".

**Messrs. C. A. COULSON & H. C. LONGUET-HIGGINS:** "Notes on the Validity and Application of the Method of Molecular Orbitals".

BOOK REVIEWS.



Established 150 Years

**TAYLOR & FRANCIS LTD., Red Lion Court, Fleet St., LONDON, E.C.4**

Printed by TAYLOR AND FRANCIS, LTD., Red Lion Court, Fleet Street, London E.C.4